การออกซิไดซ์อะนิลีนด้วยไททาเนียมไดออกไซด์ที่ถูกกระตุ้นโดยแสงในช่วงคลื่นที่มองเห็นได้

นางสาว อมรรัตน์ เจวประเสริฐพันธุ์

วิทยานิพนธ์นี้เป็นส่วนหนึ่งของการศึกษาตามหลักสูตรปริญญาวิทยาศาสตรมหาบัณฑิต
สาขาวิชาการจัดการสิ่งแวดล้อม (สหสาขาวิชา)
บัณฑิตวิทยาลัย จุฬาลงกรณ์มหาวิทยาลัย
ปีการศึกษา 2551

ANILINE OXIDATION BY TITANIUM DIOXIDE ACTIVATED BY VISIBLE LIGHT

Miss Amornrat Jevprasesphant

A Thesis Submitted in Partial Fulfillment of the Requirements
for the Degree of Master of Science Program in Environmental Managament
(Interdisciplinary Program)
Graduate School
Chulalongkorn University
Academic Year 2008

Thesis Title	ANILINE OXIDATION BY TITANIUM DIOXIDE ACTIVATED BY VISIBLE LIGHT
By	Miss Amornrat Jevprasesphant
Field of Study	Environmental Management
Advisor	Associate Professor Jin Anotai, Ph.D.
Co-Advisor	Professor Ming-Chun Lu, Ph.D.

Accepted by the Graduate School, Chulalongkorn University in Partial Fulfillment of the Requirements for the Master's Degree

.....Dean of the Graduate School
(Associate Professor Pornpote Piumsomboon,Ph.D.)

THESIS COMMITTEE

.....Chairman
(Assistant Professor Manaskorn Rachakornkij, Ph.D.)

..... Advisor
(Associate Professor Jin Anotai, Ph.D.)

..... Co-Advisor
(Professor Ming-Chun Lu, Ph.D.)

.....Examiner
(Assistant Professor Khemarath Osathaphan, Ph.D.)

.....External Examiner
(Assistant Professor Mallika Panyakapo, Ph.D.)

อมรรัตน์ เจวประเสริฐพันธุ์ : การออกซิไดซ์อะนิลีนด้วยไททาเนียมไดออกไซด์ที่ถูกกระตุ้นโดยแสงในช่วงคลื่นที่มองเห็นได้. (ANILINE OXIDATION BY TITANIUM DIOXIDE ACTIVATED BY VISIBLE LIGHT) อ.ที่ปรึกษาวิทยานิพนธ์หลัก : รศ. ดร. จินต์ อโณทัย, อ.ที่ปรึกษาวิทยานิพนธ์ร่วม : Prof. Ming-Chun Lu, Ph.D., 80 หน้า.

ไททาเนียมไดออกไซด์โฟโตคะตะลิสต์ถูกสังเคราะห์ขึ้นโดยกระบวนการโซล-เจลที่มีกรดเป็นสารคะตะลิสต์และไททาเนียมบิวทอกไซด์เป็นสารตั้งต้น ไททาเนียมไดออกไซด์ที่สังเคราะห์ได้นี้สามารถตอบสนองต่อแสงในช่วงที่มองเห็นได้และมีโครงสร้างส่วนใหญ่ในรูปของอนาเทส ปัจจัยต่างๆ รวมทั้งชนิดของแอลกอฮอล์ ชนิดของกรด อุณหภูมิที่ใช้ในการสังเคราะห์ ความยาวคลื่นแสง และพีเอชได้ถูกศึกษาถึงผลกระทบที่เกิดขึ้นต่อการสังเคราะห์ไททาเนียมไดออกไซด์โดยใช้อะนิลีนเป็นสารเป้าหมายภายใต้สภาวะสารละลายแขวนลอย หลอดแอลอีดีถูกใช้เป็นต้นกำเนิดแสงในช่วงที่มองเห็น (ฟ้า, เขียว, เหลือง และแดง) ไททาเนียมไดออกไซด์ที่สังเคราะห์ขึ้นสามารถทำปฏิกิริยาโฟโตคะตะไลติกได้โดยการกระตุ้นด้วยแสงสีฟ้า ในขณะที่ไททาเนียมไดอกไซด์ที่ผลิตขึ้นเพื่อการค้าไม่สามารถถูกกระตุ้นภายใต้เงื่อนไขดังกล่าว โดยแสงสีฟ้าสามารถกระตุ้นได้ดีที่สุดตามด้วยแสงสีเหลือง, สีเขียว และสีแดงตามลำดับ ซึ่งสอดคล้องกับสเปกตัมในการดูดกลืนแสงที่วัดได้ เมื่อความเข้มข้นของอนิลีนเพิ่มขึ้นจาก 0.047 เป็น 0.80 มิลลิโมลาร์ ประสิทธิภาพในการย่อยสลายของอะนิลีนภายใต้การกระตุ้นด้วยแสงเป็นเวลา 4 ชั่วโมง กับ 1 กรัมต่อลิตรของไททาเนียมไดออกไซด์ลดลงจากร้อยละ 72 เป็น 18 อัตราการเกิดปฏิกิริยาสามารถอธิบายโดยสมการที่ไม่ใช่เส้นตรงลำดับที่สองซึ่งสอดคล้องกับทฤษฎีของแลงเมียร์-ฮินเชลวูด โดยค่าคงที่สมดุลในการดูดซับเท่ากับ 15.89 ต่อมิลลิโมลาร์ และค่าคงที่ของปฏิกิริยาลำดับที่สองเท่ากับ 9.96×10^{-4} ต่อมิลลิโมลาร์ต่อนาที สำหรับการทดลองในช่วงพีเอชระหว่าง 4-10 พบว่าพีเอชที่เหมาะสมสำหรับปฏิกิริยาโฟโตคะตะไลซิสของอะนิลีน คือที่พีเอช 7

สาขาวิชา การจัดการสิ่งแวดล้อม ลายมือชื่อนิสิต อมรรัตน์ เจวประเสริฐพันธ์

ปีการศึกษา 2551 ลายมือชื่ออ.ที่ปรึกษาวิทยานิพนธ์หลัก

ลายมือชื่ออ.ที่ปรึกษาวิทยานิพนธ์ร่วม

5087559320 : MAJOR ENVIRONMENTAL MANAGEMENT
KEYWORDS : TITANIUM DIOXIDE / PHOTOCATALYSIS / VISIBLE LIGHT / ANILINE / LEDs

AMORNRAT JEVPRASESPHANT : ANILINE OXIDATION BY TITANIUM DIOXIDE ACTIVATED BY VISIBLE LIGHT. ADVISOR : ASSOC. PROF. JIN ANOTAI, Ph.D., CO-ADVISOR : PROF. MING-CHUN LU, Ph.D., 80 pp.

Photocatalytic titanium dioxide (TiO_2) was synthesized by using an acid-catalyzed sol-gel process with titanium n-butoxide as the precursor. This synthetic TiO_2 responded to the visible light and its crystal structure was dominated by anatase. Several factors including the alcohol/acid type, calcinations temperature, light wavelength, and pH were examined for their impacts on the photocatalytic activity of the synthetic TiO_2 by using aniline as a target compound in aqueous suspension solution under visible light irradiation by using light-emitting diodes (blue, green, yellow, or red light). Photocatalytic activity of the synthetic TiO_2 under blue light illumination was detected whereas no photoreaction was observed for the commercial Degussa P-25 TiO_2 under the similar conditions. In addition, this photo-activity was more pronouncing under the blue than green, yellow, and red light, respectively, which was corresponding very well with its adsorption spectrum. As the initial concentration of aniline increased from 0.047 to 0.80 mM, the degradation efficiency of aniline for 4-hour irradiation with 1 g L^{-1} TiO_2 decreased from 72 to 18%. The reaction rate was sufficiently explained by a non-linear second-order rate expression according to the Langmuir-Hinshelwood kinetic model. The value of the adsorption equilibrium constant was 15.89 mM^{-1} and the second-order rate constant was 9.96 x 10^{-4} mM^{-1} min^{-1}. Between pH 4 to 10, the optimum pH for the photocatalysis of aniline was 7.

Field of Study : Environmental Management Student's Signature Amornrat Jevprasesphant

Academic Year : 2008 Advisor's Signature

Co-Advisor's Signature Ming-Chun Lu

ACKNOWLEDGEMENTS

I would like to express my sincere thanks to my advisor Assoc. Prof. Dr. Jin Anotai and my Co-advisor Prof. Dr. Ming-Chun Lu for their invaluable advice, guidance, support, and encouragement throughout the course of this study. Their comments and suggestions are very valuable and also broaden my perspective in the practical applications.

Special thanks go to the committee members, Asst. Prof. Dr. Manaskorn Rachakornkij, Asst. Prof. Dr. Khemarath Osathaphan, and Asst. Prof. Dr. Mallika Panyakapo for their helpful and valuable comments that significantly enhanced the quality of this work. I should also like to thank the Department of Environmental Resources Management, Chia-Nan University of Pharmacy and Science in Tainan of Taiwan and the Department of Environment engineering, King Mongkut's University of Technology Thonburi in Bangkok of Thailand for providing the worth opportunity for me to do my great research.

I also wish to thank my friends and others who have shared experiences throughout my studying period and made my research much more enjoyable. Very special thanks to my family for love and encouraging.

Finally I would like to thank the National Center of Excellence for Environmental and Hazardous Waste Management, Chulalongkorn University for its financial support.

CONTENTS

	Page
ABSTRACT IN THAI.....	iv
ABSTRACT IN ENGLISH…….	v
ACKNOWLEDGEMENTS…….	vi
CONTENTS…….	vii
LIST OF TABLES……...	ix
LIST OF FIGURES…….	x
LIST OF ABBREVIATIONS……..	xii
CHAPTER I INTRODUCTION……	1
1.1 Objective……	1
1.2 Scopes of the Study……...	2
1.3 Obtained Results……	2
CHAPTER II THEORIES AND LITERATURE REVIEWS……...	3
2.1 Theoretical Backgrounds……..……	3
2.1.1 Advanced Oxidation Processes……	3
2.1.2 Photolysis…….	3
2.1.3 Photocatalysis……...	4
2.1.4 Property of TiO_2……	6
2.1.5 Sol-Gel Process……	7
2.1.6 Point of Zero Charge……	9
2.1.7 Property of Aniline……...	9
2.1.8 Light-Emitting Diodes…….	12
2.1.9 Langmuir-Hinshelwood Expression…….	13
2.1.10 Application of TiO_2 in Fields Practices……...	14
2.2 Literature Reviews……..	15
2.2.1 Oxidative Degradation of Pollutant by AOPs……..	15
2.2.2 Oxidative Degradation of Pollutant by TiO_2/UV…….	15
2.2.3 Oxidative Degradation of Pollutant by TiO_2/Solar Light….	17
2.2.4 Oxidative Degradation of Pollutant by TiO_2/Visible Light..	18
2.2.5 Adsorption of Pollutant onto TiO_2 Surface……..	18
CHAPTER III METHODOLOGY…….	19
3.1 Materials and Chemicals……	19
3.1.1 Chemicals……	19
3.1.2 Reactor…….	19
3.2 Experimental Procedures……	19
3.2.1 Photocatalyst Synthesis……	19
3.2.2 Photoreactivity Investigation……...	19
3.3 Experimental Scenarios……..	23
3.3.1 Scenarios for Preliminary Study…….	23
3.3.2 Scenarios for Modification of TiO_2 Synthesis…….	24
3.3.3 Photo-Reactivity Investigation……	24
3.3.4 Photo-Catalytic Study…….	26

Page
3.4 Analytical Methods……. 26
3.4.1 Measurement of Aniline…….. 26
3.4.2 Identification Crystalline Structure……. 26
3.4.3 Point of Zero Charge Analysis…… 27
3.4.4 Spectrum Analysis……... 27
3.4.5 Surface Area Analysis……. 27
3.4.6 Particle Size Analysis…….. 27
3.4.7 Soluble Ion Analysis…… 27

CHAPTER IV RESULTS AND DISCUSSION...…….. 28
4.1 Preliminary Study……... 28
4.1.1 Comparison between Commercial P-25 and Synthetic TiO_2 28
4.1.2 Effect of Light Wavelength on TiO_2 Photo-Activity……..... 31
4.1.3 Aniline Adsorption Equilibrium……... 33
4.2 Modification of TiO_2 Synthesis…….. 33
4.2.1 Effect of Alcohol and Acid Types…...…….. 33
4.2.2 Effect of Calcinations Temperature…….. 33
4.3 Photo-Reactivity Investigation…… 37
4.3.1 Determination of Optimum Light Configuration…….. 37
4.4 Photo-Catalytic Study 39
4.1.1 Effect of pH……... 39
4.4.2 Kinetics Determination……. 42
4.5 Application of TiO_2/Visible Light in Water Treatment…….. 46

CHAPTER V CONCLUSIONS……. 47
5.1 Conclusions…… 47
5.2 Recommendations for Further Studies…… 47

REFERENCES…… 48

APPENDICES……. 50
APPENDIX A Experimental Setup…….. 51
APPENDIX B Experimental Data…… 54
APPENDIX C Experimental Figures……..... 70

BIOGRAPHY…….. 80

LIST OF TABLES

Table		page
2.1	Comparison between rutile and anatase……...	7
2.2	Forms of TiO_2……...	7
2.3	Properties of aniline……..	11
3.1	Scenario for the effect of light wavelength……..	23
3.2	Scenario for the comparison of commercial TiO_2 and synthetic TiO_2.	24
3.3	Scenario for aniline adsorption characterization……..	24
3.4	Scenario for the effect of alcohol and acid types…….	24
3.5	Scenario for the effect of calcinations temperature……..	25
3.6	Scenario for the effect of light distance……	25
3.7	Scenario for the effect of light power……...	25
3.8	Scenario for the effect of light position……	25
3.9	Scenario for the effect of pH…….	26
3.10	Scenario for the effect of aniline concentration……	26
4.1	Comparison between synthetic TiO_2 and commercial TiO_2……	30
4.2	Comparison the particle size distribution between synthetic TiO_2 and commercial TiO_2 in differential phase…….	30
4.3	Apparent second-order rate constants (k_{app}) of the photodegradation of aniline at different initial concentration……...	44

LIST OF FIGURES

Figure		page
2.1	The mechanism of heterogeneous photocatalysis…….	5
2.2	Crystalline structures of TiO_2…….....	6
2.3	Sol-Gel technologies…….....	8
2.4	Characteristic of surface charge and the point of zero charge...……...	9
2.5	Chemical structure of aniline……	10
2.6	Synthesis of aniline……...	12
2.7	Reaction pathways for mineralization of aniline by $OH^{\bullet}$…….	12
2.8	Connecting of LEDs……..	13
2.9	Appearance of LEDs…….	13
3.1	Schematic batch reactor for photocatalytic study…….	20
3.2	Reactor setup…….	20
3.3	TiO_2 synthetic scheme……...	21
3.4	Analytical scheme for point of zero charge……..	22
3.5	Visible-light-activated titanium dioxide photocatalyst…….	22
3.6	Experiment scheme for photoreactivity investigation……...	23
4.1	Effect of light and synthetic TiO_2 on the removal of aniline……	29
4.2	Effect of light and commercial P-25 on the removal of aniline……	29
4.3	Comparison between synthetic TiO_2 and Commercial P-25 on the photocatalysis of aniline……	30
4.4	UV-vis adsorption spectra of synthetic TiO_2 and Commercial P-25..	31
4.5	XRD patterns of synthetic TiO_2 and Commercial P-25……	32
4.6	Effect of light wavelength on the photocatalysis of aniline……..	32
4.7	Aniline adsorption onto synthetic TiO_2…….	34
4.8	Effect of alcohol and acid types on the phtocatalytic property of TiO_2	34
4.9	UV-VIS adsorption spectra of the TiO_2 synthesized by using different alcohol and acid types……	35
4.10	Effect of calcinations temperature on the photocatalytic property of TiO_2……...	35
4.11	UV-VIS adsorption spectra of the TiO_2 synthesized at different calcinations temperature……	36
4.12	XRD patterns of the TiO_2 synthesized at different calcinations temperature……	36
4.13	Effect of light position on the photo-catalysis of aniline……..	37
4.14	Effect of light power on the photo-catalysis of aniline…….	38
4.15	Effect of light distance on the photo-catalysis of aniline……..	39
4.16	Point of zero charge determination using the mass titration method…	40
4.17	Point of zero charge determination using the zeta potential method…	40
4.18	Adsorption of aniline onto TiO_2 at different pH……...	41
4.19	Effect of pH on the photo-catalysis of aniline……...	41
4.20	Fitting comparison between the linearization and non-linear least squares methods……	43
4.21	Data fitting by various kinetic equations……...	43
4.22	Aniline degradation profiles……..	44

Figure		Page
4.23	Linearized reciprocal kinetic plot for the photocatalytic degradation of aniline……	45
4.24	Half-life profile of observed and estimated on the different initial concentration of aniline…….	46

LIST OF ABBREVIATIONS

AOPs	=	advanced oxidation processes
$OH^{\bullet}$	=	hydroxyl radical
O_3	=	ozone
H_2O_2	=	hydrogen peroxide
TiO_2	=	titanium dioxide
UV	=	ultraviolet
LEDs	=	light emitting diodes
CO_2	=	carbon dioxide
H_2O	=	water
POPs	=	persistent organic pollutants
VB	=	valance band
CB	=	conduction band
$O^{-}_{2}{}^{\bullet}$	=	superoxide radical
h^{+}	=	electron hole
ZnO	=	zinc oxide
Pzc	=	point of zero charge
$C_6H_5NH_3^{+}$	=	anilinenium
r	=	reaction rate
k_r	=	reaction rate constant
K	=	Langmuir constant
C_0	=	initial concentration
°C	=	celsius degree
mol	=	mole
ml	=	milliliter
mg	=	milligram
ppm	=	part per million
mM	=	milli molar
MΩ	=	mega oam
mV	=	milli volt
nm	=	nanometer
L	=	liter
g	=	gram
µL	=	microliter
BET	=	Brunauer-Emmett-Teller
HPLC	=	High Performance Liquid Chromatography
IC	=	Ion Chromatography
XRD	=	X-ray Diffraction
2-CP	=	2-chlorophenol
APAP	=	acetaminophen
OH^{-}	=	hydroxide ion
TNT	=	2,4,6-trinitrotoluene
DDVP	=	organophosphorous pesticide dichlorvos
NO_x	=	nitrogen oxides

CHAPTER I

INTRODUCTION

At the moment, the problem arise from environmental contaminants discharged from factories is one of the major problems affecting the public health of people in the neighborhood. The factories generally release organic compounds into the environment which consists of aquatic, air, and soil systems.

Aniline is one of the organic compounds that are typically used in many factories as a precursor chemical in many processes such as rubber processing, pesticide, and dye manufacturing. Aniline with a benzene ring structure must be treated before being released into the environment because it has been classified in a hazardous group. Aniline could be treated by various techniques including advanced oxidation processes (AOPs) (Karunakaran, Senthilvelan, and Karuthapandian, 2004).

AOPs represent an alternative approach for treatment of hazardous organic compounds. The processes have shown great potential for treating pollutants because they produce the powerful hydroxyl radical ($OH^{\bullet}$). The $OH^{\bullet}$ is almost the most powerful oxidative species. It is a non-selective oxidant which can oxidize many pollutants. AOPs are consisted of many processes such as Fenton processes, ozone with ultraviolet (O_3/UV), hydrogen peroxide with ultraviolet (H_2O_2/UV), semiconductor photocatalysis, etc. This research focused on the semiconductor photocatalysis.

Titanium dioxide (TiO_2) photocatalysis is one of the AOPs which can remove organic pollutants in both aqueous and gas phases. In recent years, semiconductor particulate systems have been employed to degrade several pollutants such as 2,4-dichlorophenol (Chen et al., 2003), and nitrogen oxides (Lin et al., 2006). In most systems, the semiconductor particles are excited by Ultraviolet (UV) light to induce the charge separation. However, the catalysts which can be activated by visible light would be more attractive in terms of the effective utilization of ordinary light and safety concern. Several researches tries to improve the property of TiO_2 which is one of the most widely used photocatalyst in term of light activation within the visible range. This study intended to characterize the behavior of TiO_2 photocatalysis activated by visible light by using aniline as a target compound.

1.1 Objectives

The main objectives of this study are:

-To determine the effect of synthetic conditions including acid and alcohol types and calcine temperature on the visible light absorption property of TiO_2.

-To characterize the degradation of aniline by TiO_2 under visible light irradiation.

1.2 Scopes of the Study

This research consists of two parts. The first part was the synthesis of visible-light-activated titanium dioxide and the second part was treatment of wastewater using synthetic titanium dioxide with visible light irradiation. The scopes of this research are as follows:

-Using aniline as a target compound.
-Using light emitting diodes (LEDs) as a light source.
-Working at room conditions
-Operating in a batch mode
-Using a lab scale reactor

1.3 Obtained Results

This research provides valuable information on the synthesis of TiO_2 which can be activated by visible light. This visible-light activated TiO_2 is a very useful photocatalyst and can be applied in field practice with lower operative cost due to no UV light irradiation. In addition, the Langmuir-Hinshelwood kinetics for aniline oxidation by TiO_2 with visible light process are also purposed which can be applied to treat aniline-contaminated wastewater in the future.

CHAPTER II

THEORIES AND LITERATURE REVIEWS

2.1 Theoretical Backgrounds

2.1.1 Advanced Oxidation Processes (AOPs)

AOPs represent an alternative approach which provides the destructible treatment of hazardous organic compounds. The AOP technologies can refer to two stages of sequential reaction. First is the formation of strong oxidants (i.e., $OH^{\bullet}$) and second is the reaction of these oxidants with organic compounds that contaminate in wastewater. However, the term of AOPs refers specifically to processes in which oxidation of organic contaminant occurs via $OH^{\bullet}$. The $OH^{\bullet}$ is a powerful oxidant, short lived, highly reactive, and a non-selective oxidant which can oxidize many pollutants. These radicals react with pollutants and lead to degradation reaction. The ability of the AOPs technique to complete oxidation of organic contaminants leads to mineralization which consist of carbon dioxide (CO_2) and water (H_2O) and without generating any harmful byproducts. The application of AOPs can cover many fields such as oxidative degradation of organic compounds, bactericidal, and non-biodegradable compounds, detoxification of persistent organic pollutants (POPs), disinfection and purification of contaminated air and wastewater streams. AOPs particularly based on photocatalytic degradation are currently interesting for the effective oxidation of a wide variety of organic and dyes (Jain and Shrivastava, 2008 and Son et al., 2004).

2.1.2 Photolysis

Photochemical technologies are simple, cost effective, and give the benefit for environmental pollutant treatment and disinfection. UV driven AOPs are primarily based on the generation of powerful $OH^{\bullet}$, through the direct photolysis of H_2O_2, or photocatalysis. In UV direct photolysis, the pollutant to be destroyed must absorb the irradiation and the degradation starting from its excited state.

Major reaction pathway in the UV photolysis begins with the electronically excited state RX* generated through the light absorption process which is highly energetic. It can deactivate to ground state of the molecule or transform to other intermediate products. The most common pathways are summarized in equations (2.1) to (2.6). In equation (2.2), the excited state of molecule is broken down into two radicals trapped in the solvent cage. Recombination of the primary radicals in equation (2.3) leading to the parent molecule occurs with high probability. In polar solvents, such as water, heterolytic bond have been observed in equation (2.4). The reactions with oxygen are also possible in equations (2.5) and (2.6) but require a relatively long-live excited-state species.

$$RX + h\nu \longrightarrow RX^* \quad (2.1)$$

$$RX^* \longrightarrow (R^{\bullet} \cdots {}^{\bullet}X)_{cage} \longrightarrow R^{\bullet} + {}^{\bullet}X \quad (2.2)$$

$$(R^{\bullet} \cdots {}^{\bullet}X)_{cage} \longrightarrow RX \quad (2.3)$$

$$RX^* \longrightarrow (R^{+} \cdots X^{-})_{cage} \longrightarrow R^{+} + X^{-} \quad (2.4)$$

$$RX^* + O_2 \longrightarrow RX^{+\bullet} + O_2^{-\bullet} \quad (2.5)$$

$$RX^* + {}^3O_2 \longrightarrow RX + {}^1O_2 \quad (2.6)$$

2.1.3. Photocatalysis

Photocatalysis consists of two words. The first word is “photo” which is light. And the second is “catalysis” which is the process by which the rate of a chemical reaction is increased by means of the addition of a species known as a catalyst to the reaction. Therefore, photocatalysis means the process which requires irradiation to initiate the catalysis reaction, without the radiation, the reaction cannot proceed.

Photocatalytic mechanism occurs when the semiconductor, such as TiO_2, is exposed to energetic light. The semiconductor is consisted of two band gap; the first is valance band (VB), the highest occupied band full of electron, and the second is conduction band (CB), the lowest unoccupied band. The bands are separated by different energy level which is called band gap energy (Parsons, 2004) as shown in Figure 2.1. As the TiO_2 absorbs energy greater than the band gap energy, the electrons from the valence band are excited and will move to the conduction band causing an electron hole in the valence band leading to the oxidation process. These holes can react with water to produce the highly reactive $OH^{\bullet}$ as shown in equation (2.9). At the same moment, the electrons that transferred to the conduction band will cause a reduction reaction to occur, these e^- can react with oxygen to produce superoxide ($O^-_2{}^{\bullet}$). This electron-hole pair can recombine as the electron returns to its original state. Therefore, it should have an electron acceptor, for example O_2, to obstruct the recombination (Peterson et al., 1991; Turchi and Ollis, 1990). Several researches have found that $O^-_2{}^{\bullet}$ is as important as the electron hole (h^+) and $OH^{\bullet}$ in breaking down organic compounds (Fujishima, Hashimoto, and Watanabe, 1999). The responsibility for the oxidation of organic molecules is believed to be due to the $OH^{\bullet}$ being generated.

$$TiO_2 + h\nu \longrightarrow e^- + h^+ \quad (2.7)$$

$$h^+ + OH^- \text{(surface)} \longrightarrow OH^{\bullet} \quad (2.8)$$

$$h^+ + H_2O \longrightarrow OH^{\bullet} \quad (2.9)$$

$$O_2 + e^- \longrightarrow O^-_2{}^{\bullet} \quad (2.10)$$

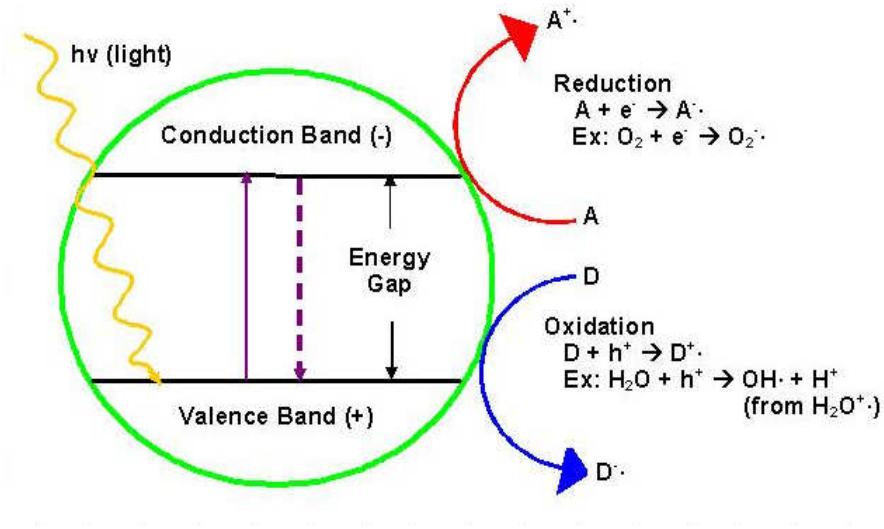

Figure 2.1 The mechanism of heterogeneous photocatalysis.

Thus, the h^+ and $OH^\bullet$ are the primary oxidant species in photocatalysis, while molecular oxygen serves only to scavenge the photo-produced electrons in order to prevent electron-hole recombination. However, TiO_2 has a relatively large band gap of 3.2 eV, relates to wavelengths of shorter than 388 nm. These short wavelengths are in the UV range which are accounted for only 3-4% of the solar energy reaching the earth (Anpo and Takeuchi, 2003; Yamashita and Anpo, 2004). In indoor environment, the amount of UV light in the light source is also low. Thus, it is quite costly to activate TiO_2 with the UV radiation which, consequently, raises the overall treatment cost. In addition, UV radiation can also cause skin cancer in human; hence, caution has to be made when working with UV irradiation. Recently, there are several researches tried to synthesize the TiO_2 with a specific structure that can be activated by lower energy particularly those in the wavelength of 300 to 700 nm (Lin et al., 2006), which are accounted for 50% of the solar energy. One approach of such modifications is to create intra-band gap states that are close to the conduction or valence band edges with the sub-band gap energies of less than 3.2 eV.

In photocatalysis, several semiconductors such as TiO_2, ZnO, metal sulfide, iron oxide, etc., can be used; however, the most popular one that applied in environmental applications is TiO_2 due to the following reasons (Fu et al., 1996):

-It has good adsorption for many pollutants.

-It has high absorption for UV radiation because its band gap energy is 3.2 eV.

-It shows high photocatalytic activity and highly resistant to photocorrosion.

-It is stable, non-hazardous, readily available, and an inexpensive semi-conducting material.

-The oxidation and reduction reaction of its valence and conduction band edges are appropriate for oxidizing organic pollutants.

It is used extensively for air cleansing, water purification, odor control, etc. TiO_2 can be applied in many different fields for example, self-sterilizing photocatalytic tiles, self-cleaning tunnel lighting fixture and photocatalytic air cleaners etc. (Fujishima et al., 1999).

The Degussa P-25 is one of the most used commercial types of photocatalytic titanium dioxide, which is produced under license to the Degussa Company. It was composed mostly of anatase (80% anatase and 20% rutile).

2.1.4. Property of TiO_2

The structure of TiO_2 is consisted of rutile, anatase, and brookite (Smyth, 1997) as shown in Figure 2.2. Rutile will be more stable at high temperatures, anatase will be more stable form at low temperatures, and brookite is usually found only in mineral ores. The structure of TiO_2 will depend largely on the temperature of calcinations. Lin et al., (2006) found that anatase was the main structure at a calcination temperature below 500°C and when the calcination temperature increased more than 600°C, the dominant crystal structure was rutile.

The properties of rutile and anatase are the same or nearly the same such as crystalline form, hardness, gibbs free energy**,** and density. The anatase type of TiO_2 generally shows a higher photoactivity than another type of TiO_2 by comparison of physical properties as shown in Table 2.1. However, the structure between rutile and anatase are different thus makes them differ slightly in crystal habit. The difference of band gap energy between anatase and rutile is 0.2 eV. The VB energies for anatase and rutile are similar and both of them can generate VB hole and sequentially the hydroxyl radicals. On the other hand, the CB energy for rutile is closely than anatase to the potential required to reduce water to hydrogen gas, meaning that anatase has higher reducing power. Therefore, the photogenerated CB electrons and VB holes of rutile can easily recombine with each other before they can do anything useful unlike in the case of anatase. TiO_2 can be used in two forms. The first form is suspended TiO_2 and the second form is immobilized TiO_2 as shown in Table 2.2.

The special property of TiO_2 is the charge. The form of TiO_2 charge depends on its environment. For example, TiO_2 in the acid solution will have positive charge; in contrast, TiO_2 in alkaline solution will be the negative charge.

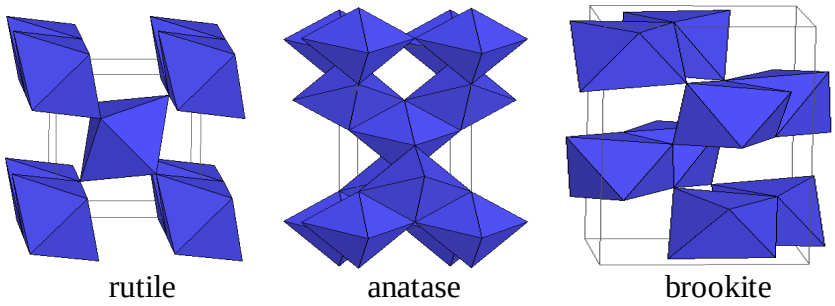

Figure 2.2 Crystalline structures of TiO_2.

Table 2.1 Comparison between rutile and anatase.

Properties	Rutile	Anatase
Crystalline form	Tetragonal system	Tetragonal system
Band gap energy (eV)	3.0	3.2
Gibbs free energy (kcal/mole)	-212.6	-211.4
Melting point (°C)	1858	Change to rutile at high temperature (~800)
Hardness (Mohs)	6.0-7.0	5.5-6.0
Permittivity	114	31
Density (g/cm^3)	4.250	3.894
Lattice constant a (Å)	4.58	3.78
Lattice constant c (Å)	2.95	9.49

Table 2.2 Forms of TiO_2.

Form of TiO_2	Description
Suspended TiO_2	-High surface areas -Turbidity effect -Require the technique for separation of TiO_2 particle from the suspension -Available to buy
Immobilized TiO_2	- Low surface areas -Require the preparation technique -Require the practical for industrial use

2.1.5. Sol-Gel Process

One method for preparing visible-light-activated titanium dioxide photocatalyst is an acid-catalyzed sol-gel process. The sol-gel process is a wet-chemical technique (or chemical solution deposition). This process occurs in liquid solution of organometallic precursors (Titanium (lV) n-butoxide), which undergo hydrolysis and condensation reaction as shown in equations (2.11) to (2.13), lead to the formation of a new phase (sol & gel).

$$\text{Ti-O-R} + H_2O \longrightarrow \text{Ti-OH} + \text{R-OH (hydrolysis)} \quad (2.11)$$

$$\text{Ti-OH} + \text{HO-Ti} \longrightarrow \text{Ti-O-Ti} + H_2O \text{ (water condensation)} \quad (2.12)$$

$$\text{Ti-O-R} + \text{HO-Ti} \longrightarrow \text{Ti-O-Ti} + \text{R-OH (alcohol condensation)} \quad (2.13)$$

A sol is a dispersion of the solid particles of a diameter of few hundred of nanometer suspended in a liquid phase where only the Brownian motions suspend the particles. A gel is a state which a solid macromolecule is immersed in a liquid phase (solvent) causing to a solid network containing liquid components occurs. As shown in Figure 2.3, the sol-gel coating process usually consists of 4 steps as follows:

-Desired colloidal particles disperse in a liquid to form a sol.

-Deposition of sol solution produces the coatings on the substrates by spraying, dipping or spinning.

-Polymerize the particles in sol and produce a gel in a state of a interconnected network.

-Heat treatments of the particle so that the remaining organic or inorganic components form an amorphous or crystalline coating.

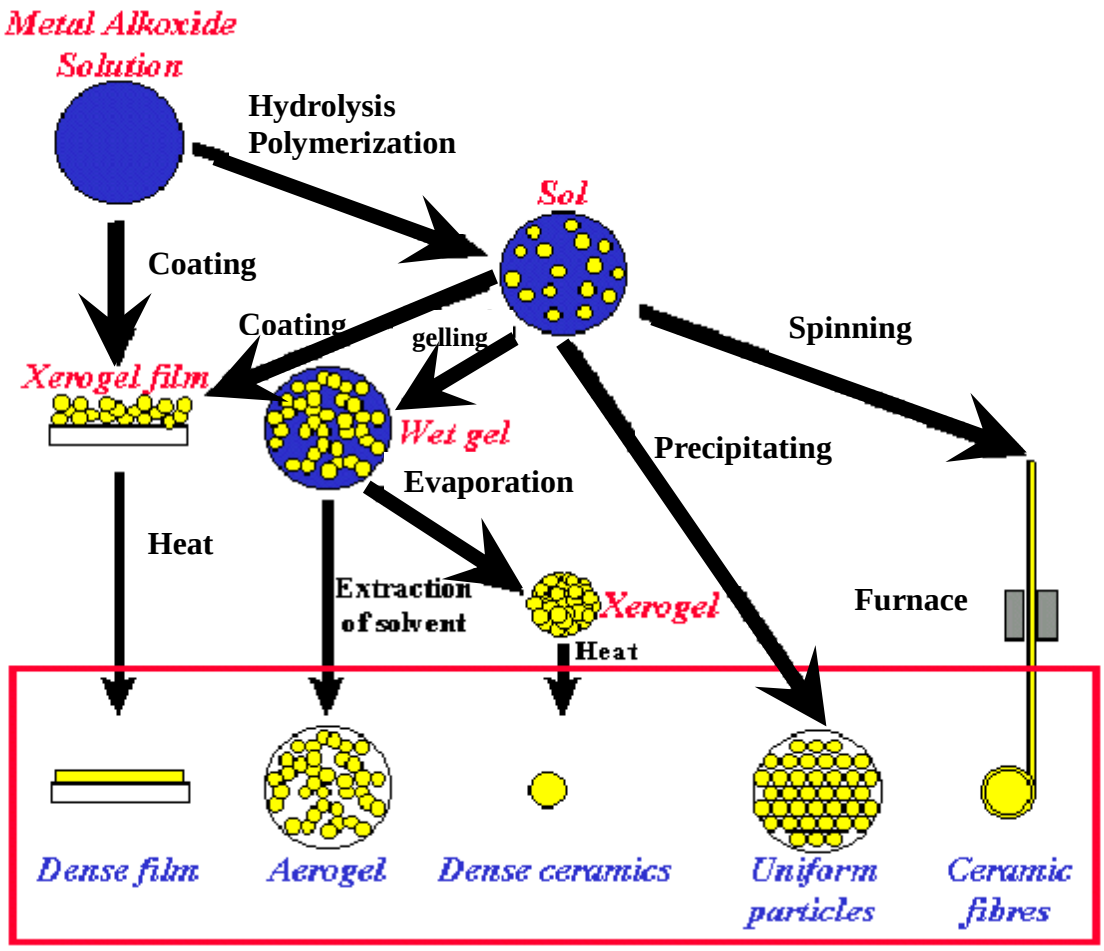

Figure 2.3 Sol-Gel technologies.

2.1.6. Point of Zero Charge

Point of zero charge (pzc) is a surface charge when the electrical charge density on the solid surface is zero. The value of pH is used to describe pzc only for systems in which H^+/OH^- are the potential-determining ions. Generally, pzc is a value of the negative logarithm of the activity in the bulk of the charge-determining ions. For example, the charge on the surface of silver iodide crystals may be determined by the concentration of iodide ions in the solution above the crystals. When the pH is lower than the pzc value, it means that the acidic water donates more protons than hydroxide groups. Therefore, the adsorbent surface is positively charged. On the other hand, the pH is higher than the pzc value, so the surface of adsorbent is negatively charged. The position of the curve differs among the various minerals. Figure 2.4 is the diagram that shown the position of pzc of a mineral.

2.1.7. Property of Aniline (Wikipedia, 2008)

Aniline, phenylamine or aminobenzene is an organic compound which has the formula of C_6H_7N. The chemical structure consists of a benzene ring and an amino group as shown in the Figure 2.5. It's important physical and chemical properties are summarized in Table 2.3. Aniline is one of the most important aromatic compounds in industrial production process. It is widely used as a precursor for several more complex chemicals. Aniline is also used in many other processes such as rubber processing chemicals, pesticides, dyes, fibers, pharmaceuticals, petroleum refining etc. Aniline is colorless, oily liquid and a weak base, it is slowly oxidized in the air.

Two steps for producing aniline from benzene in industry is shown in the Figure 2.6. First step, benzene is nitrated using a concentrated mixture of nitric acid and sulfuric acid, which gives nitrobenzene. In the second step, nitrobenzene is hydrogenated to give aniline. Pathway for aniline mineralization by $OH^{\bullet}$ is shown in Figure 2.7 (Brillas et al., 1998).

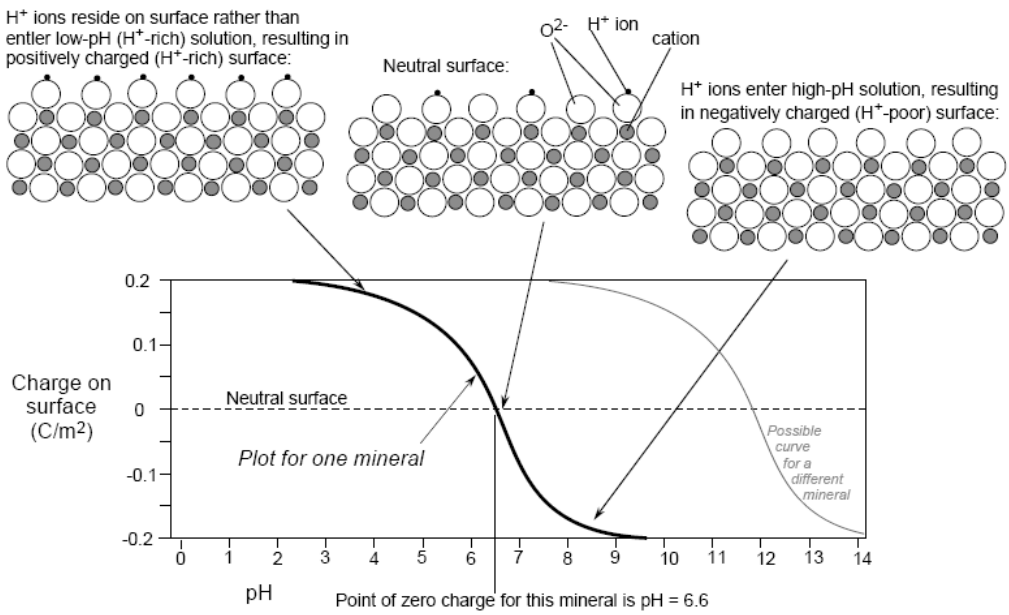

Figure 2.4 Characteristic of surface charge and the point of zero charge.

Human can exposure to aniline through many ways including inhalation (the vapour), ingestion (swallowing), and dermal (absorption through the skin). Most of the exposure ways affected to ability of blood to carry oxygen. Aniline is a blood toxin. It is causing hemoglobin convert to methemoglobin, resulting in cyanosis because it decreases the ability of blood to carry oxygen (Baker, 2008). Symptoms may include bluish discoloration of lips and tongue, severe headache, nausea, mental confusion, shock, respiratory paralysis, death. The effect for eye contact is an eye irritant which may cause tearing and blurred vision. The splashes may cause corneal damage. However, It does not remain in the body due to its breakdown and removal.

Aniline can be released to the environment because of their manufacture, processing, and use. Exposure to aniline can occur in the workplace or in the environment following releases to air, water, land or groundwater. Aniline can evaporate when exposed to air and dissolves when mixed with water. It can break down to other chemicals in water and soil. Aniline in solution adsorbs strongly to organic matter, which effectively increases its solubility and movement into groundwater.

The reaction of aniline with water is shown in equation (2.14). Aniline reacts reversibly with water to give anilinium ($C_6H_5NH_3^+$) and hydroxide ions (Clark, 2004). Aniline is a weak base and its conjugate acid is anilinium ion and the pK_a of anilinium is 9.37 at 25°C (Edwards and Ormsby, 2006).

$$C_6H_5NH_{2(aq)} + H_2O_{(l)} \longleftrightarrow C_6H_5NH_3^+{}_{(aq)} + OH^-{}_{(aq)} \qquad (2.14)$$

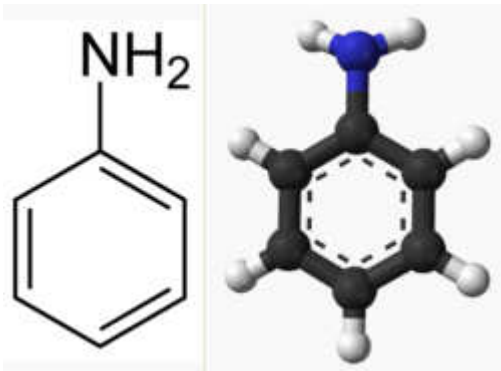

Figure 2.5 Chemical structure of aniline.

Table 2.3 Properties of aniline

Property	Information
Synonyms	Phenylamine, Aminobenzene, Benzenamine, Aminophen, Blue Oil, Cyanol, Benzamine, etc.
Molecular formula	C_6H_7N
Molecular weight	93.12 g/mol
CAS number	62-53-3
Melting point	-6.3 °C
Boiling point	184.13 °C
Vapor density	3.22 at 185 °C
Vapor pressure	0.7 mm Hg at 25 °C
Specific gravity	1.08
Flash point	70 °C
Explosion limits	1.3-11%
Appearance	Colourless to brown, oily liquid
Density	1.0217 g/ml
Water solubility	Moderately (3.6 g/100 ml at 20 °C)
Vapor pressure	0.489 mm Hg at 25 °C
Log Octanol/Water Partition Coefficient	0.90
Henry's Law Constant	0.136 atm-m^3/mole at pH 7.3
Conversion Factor	1 ppm = 3.8 mg/m^3

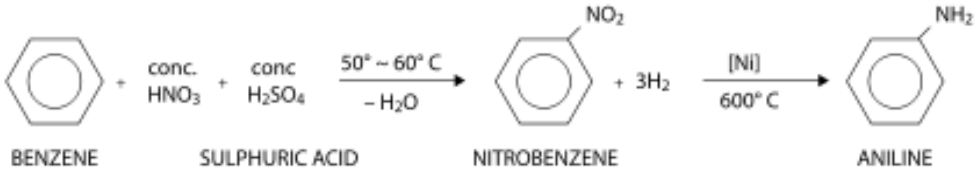

Figure 2.6 Synthesis of aniline.

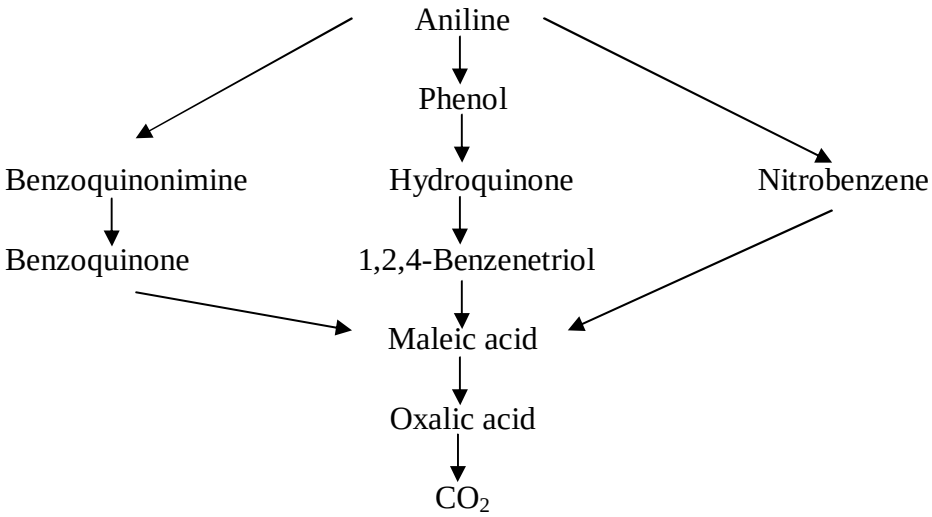

Figure 2.7 Reaction pathways for mineralization of aniline by $OH^{\bullet}$.

2.1.8. Light-Emitting Diodes (Wikipedia, 2008)

A light-emitting diodes (LEDs) is a semiconductor diode that emits light when an electric current passes through its. LEDs must be connected correctly, the electrodes may be labeled “a” or “+” for anode and “k” or “-” for cathode (Hewes, 2008) as shown in Figures 2.8 and 2.9. The color of the emitted light depends on the composition and condition of the semiconducting material used, and can be infrared, visible, or ultraviolet. The colors of LEDs are available in red, orange, amber, yellow, green, blue, and white. Blue and white LEDs are much more expensive than the other colours. The colour of an LED is determined by the semiconductor material, not by the colouring of the 'package' (the plastic body).

The LED materials technology became more advanced i.e., the light output was increased, while maintaining the efficiency and the reliability to an acceptable level, causing LEDs to become bright enough to be used for illumination, in various applications such as lamps and other lighting fixtures.

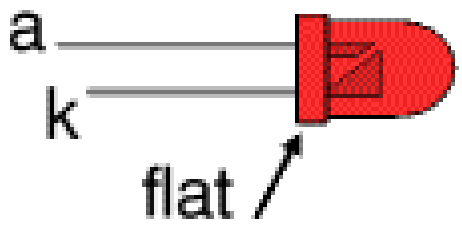

Figure 2.8 Connecting of LEDs.

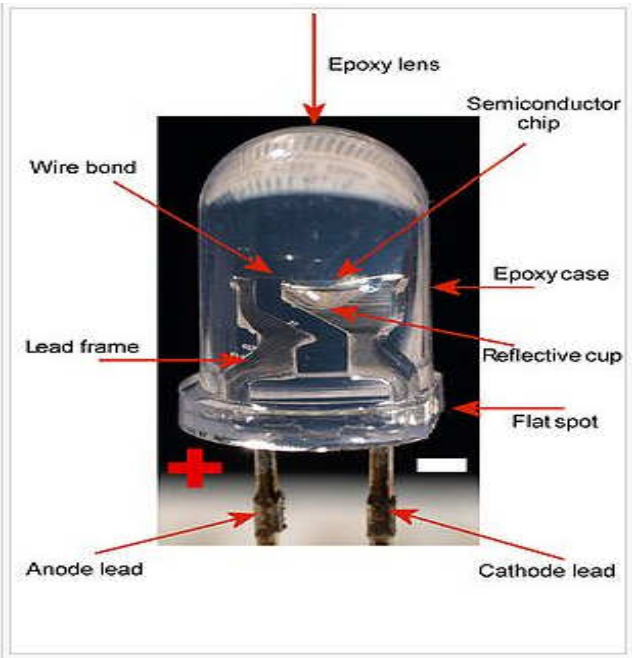

Figure 2.9 Appearance of LEDs.

2.1.9. Langmuir-Hinshelwood Expression

Langmuir-Hinshelwood expression is one of the kinetic models that used to analyze the heterogeneous photocatalytic oxidation (Oancea and Oncescu, 2008; Zhang et al., 2008; Son et al., 2004; Chen et al., 2003; Chan, Chen, and Lu, 2001; Lu et al., 1993). This model was developed base on the assumption of no competition with reaction byproducts. The photocatalytic oxidation of aniline over TiO_2 should comply with the following equation (equation 2.15):

$$r = -\frac{d[AN]}{dt} = \frac{k_r K[AN]_0}{1 + K[AN]_0} \qquad (2.15)$$

Where "r" is the reaction rate for the oxidation of aniline (mM min^{-1}), "k_r" is an reaction rate constant which is related to the adsorption/desorption (mM min^{-1}) , "K" is the Langmuir constant reflecting the adsorption/desorption equilibrium between the reagent and the surface of the photocatalyst (mM^{-1}), and "C_0" is the initial concentration of aniline (mM). This equation can be linearized when plotted between inverse initial rate and initial concentration as shown in equation (2.16). Slope ($1/k_rK$) and interception ($1/k_r$) are positive.

$$\frac{1}{r} = \frac{1}{k_r} + \frac{1}{k_r K}\frac{1}{C_0} \qquad (2.16)$$

The constants, "k_r" and "K", can be obtained from the intercept and slope of the line formed when "1/rate" is plotted against "1/C". The integrated form of equation (2.15) is shown in equation (2.17).

$$t = \frac{1}{k_r K}\ln\left(\frac{C}{C_0}\right) + \frac{1}{k_r}(C_0 - C) \qquad (2.17)$$

Plotting between "$t_{1/2}^*$" and initial concentration of aniline should yield a linear line as shown in the following equation:

$$t_{1/2}^* = \frac{0.5C_0}{k_r} + \frac{\ln 2}{k_r K} \qquad (2.18)$$

Where "$t_{1/2}^*$" is the half-life estimated based on the initial rate (no effect of intermediate). If the disappearance of aniline can be explained by a pseudo-second order kinetics (as will be discussed in chapter 4), the half-life for second-order reaction could also be calculated by following equation (2.19):

$$t_{1/2} = \frac{1}{k[AN]_0} \qquad (2.19)$$

where "$t_{1/2}$" is the observed half-life and "k" is the apparent rate constant for the oxidation of aniline at different initial concentration (mM^{-1} min^{-1}).

2.1.10. Application of TiO_2 in Fields Practices

2.1.10.1 Self-Sterilizing Photocatalytic Tiles

The TiO_2 can decompose viruses and bacteria on the tile surface due to the strong oxidizing properties. If the floor, ceiling and walls are covered with photocatalytic tile, viruses and bacteria that drifting in the air in an operating room will be inactivated as they come in contact with the surface.

2.1.10.2 Self-Cleaning Tunnel Lighting Fixtures

The glass that covers on the highway tunnel lighting fixtures is darken because of the automobile exhaust. Therefore, TiO_2-coated lamp covers are used for protectant. It can make the glass surface remains clean longer and the number of required cleanings is greatly reduced.

2.1.10.3 Anti-Fogging Glass

When small water droplets come to contract with glass, it becomes fogged. Therefore, on TiO_2-coated glass, the water forms a continuous flat sheet, so that there is no fogging effect which occurs on the glass. This property is called "Super-hydrophilicity".

2.2 Literature Reviews

2.2.1 Oxidative Degradation of Pollutant by AOPs

Sanchez, Peral, and Domenech (1998) degraded aniline in aqueous solution using the combination of ozonation and photocatalysis with TiO_2. The experimental results observed that using ozonation pretreatment followed by photocatalysis significantly increased the yield of TOC removal in comparison to either ozonation or photocatalysis acting separately. This enhanced efficiency was not observed for photocatalysis pretreatment followed by ozonation. It was proposed that ozone acted by accepting a photogenerated electron of TiO_2 to from an ozonide anion radical, which was an intermediate species in the formation of OH radicals.

Anotai, Lu, and Chewpreecha (2006) studied the aniline degradation by Fenton and electro-Fenton processes. The presence of electric current (electro-Fenton) could improve both aniline removal efficiency and the rate of Fenton reactions due to the rapid electrochemical regeneration of Fe^{2+}. Higher current density significantly decreased the required treatment period. A decrease in the TOC removal efficiency rate was obtained as the solution pH decreased and the optimum pH was 3 for the electro-Fenton process.

Brillas et al. (1998) found that the electrochemical experiment performed in the presence of electro-Fenton and UV irradiation led to a quickly aniline mineralization. Almost complete mineralization of aniline was achieved using photoelectron-Fenton process because of an increase in Fe^{2+} concentration in solution due to UVA irradiation and direct photodecomposition of intermediates.

2.2.2 Oxidative Degradation of Pollutant by TiO_2/UV

Jain and Shrivastava (2008) found that a small amount of dye could be adsorbed onto the TiO_2 surface. Photodegradation of cyanosine increased rapidly when increasing the amount of TiO_2 from 0.01 to 0.08 g/L because it increased the number of active sites on the TiO_2 surface which consequently increased the number of $OH^{\bullet}$ and $O_2^{-\bullet}$. As the concentration of contaminant increased, it was found that the photocatalytic degradation decreased because the active sites on TiO_2 remained the same but the number of substrate ions accommodated in the inter-layer space increased. The pH was also an important parameter for reaction on the particulate surface. The pH range between 3.7 and 10.2 was studied in this study. It was observed that the degradation rate increased with an increase in pH because of more

efficient generation of $OH^{\bullet}$ by TiO_2 when increasing concentration of hydroxide ion (OH^-). H_2O_2 is a key factor that can significantly influence the degradation of cyanosine because it is directly related to $OH^{\bullet}$ generation. The degradation rate increased as the H_2O_2 increased until a critical H_2O_2 concentration was achieved. It was observed that photocatalytic degradation by TiO_2 was an effective, economic and faster method for removing cyanosine from aqueous solution.

Karunakaran et al. (2005) investigated the TiO_2 photocatalyzed oxidation of aniline using a multilamp photoreactor with mercury UV lamps at wavelength of 365 nm. The function of light intensity was examined for photooxidation. The reaction did not happen in the dark so the experiments were carried out with eight, four, and two lamps. The results showed that high energy radiation was more effective than low energy radiation in the photocatalysis.

Chen et al. (2003) investigated photocatalytic degradation of 2,4-dichlorophenol in aqueous TiO_2 suspensions under UV light and found that the degradation rates of 2,4-dichlorophenol increased when TiO_2 dosages increased up to 1 g/L and then decreased with increase of TiO_2 dosages because of the obstruction of light source. Furthermore, higher 2,4-dichlorophenol degradation rates were obtained at lower 2,4-dichlorophenol concentrations and they followed the Langmuir-Hinshelwood equation. Increase of pH, also meaning increase of OH^- concentration which leading to the increase of $OH^{\bullet}$ formation, increased the removal of 2,4-dichlorophenol

Son et al. (2004) investigated the photocatalytic degradation of TNT (2,4,6-trinitrotoluene) using a UV lamp as a light source. The initial pH of the solution was adjusted to pH 7.0 ($\pm$0.4). TNT was more effectively degraded than with either UV or TiO_2 alone. The pollutant concentration was found to be a very important parameter for treatment. It showed that the degradation rate decreased as the initial TNT concentration increased and TNT degradation kinetics was not a simple first-order but pseudo first-order reaction. TNT degradation is least effective at acidic pH (3) but higher effective at neutral (7) and basic pH (11). Higher degradation rate at neutral pH could be explained by the point of zero charge (pzc) of the TiO_2. The pzc value was 6.25 (TiO_2 used as the photocatalyst was commercially available Degussa P-25) (Poulios and Tsachpinis, 1999). From the control experiment, they found that only 10% of the initial TNT was adsorbed onto the TiO_2 particles under the condition of darkness. Furthermore, the color did not change during the adsorption reaction but the solution turned pink when the UV irradiation was started. The effect of adsorption by NO_3^- which is a major nitrogen anionic by-product on the TiO_2 surface was also examined. The result indicated that the effect of NO_3^- adsorption on TiO_2 surface was minimal and did not affect on the TNT degradation in photocatalysis. Formate, acetate, NO_3^-, NO_2^-, and NH_4^+ were identified as the intermediates from TNT oxidation.

Zhang et al. (2008) investigated the degradation of acetaminophen (APAP) in TiO_2 suspended solution by photocatalytic under a metal halide lamp. TiO_2 dosage and initial APAP concentration had effects on the efficiency of APAP degradation which increased with increasing TiO_2 dosage, and decreased with increasing initial APAP concentration. The effect of photocatalytic degradation at different initial pH was also studied. The result showed that the removal efficiency of APAP increased slightly as the pH changed from 3 (acidic) to 9 (weakly alkaline). However, when the solution became more alkaline (pH 11), the efficiency of APAP degradation was lower than in acidic solution. In this work, the photodegradation efficiency of APAP

increased when increased the TiO_2 dosage up to 1 g/L. The data were fitted to the Langmuir-Hinshelwood kinetics model. It was concluded that this TiO_2/UV method was a highly effective way to remove APAP from wastewater and drinking water without any generation of more toxic product.

Tanaka et al. (1997) studied the photocatalytic degradation of three mononitrophenol compounds (2-, 3- and 4-nitrophenol), 2,4-dinitrophenol, and picric acid (2,4,6-trinitrophenol) in aqueous TiO_2 suspension. It was found that photocatalytic degradation rate of aromatic compound was affected by functional groups attached to the aromatic ring, and particularly nitro-substituent suppressed the degradation. The difference in the rates between organic disappearance and TOC elimination indicated the formation of photocatalytically less degradable intermediate compounds than starting material. Intermediates of organic acid were identified besides aromatic compounds, formic and acetic acids were formed at the highest concentrations. Therefore, it could be expected that a large part of CO_2 was formed via mineralization of both acids.

Chan et al. (2001) used Langmuir-Hinshelwood kinetic expression to develop a basic mathematical model, which could describe the inhibition of intermediates on the photocatalysis of 2-chlorophenol (2-CP) in aqueous TiO_2 suspension. This model could be used successfully to explain the observed reaction rate at different initial concentrations. The modification model was developed based on the combination of pseudo-first-order and Langmuir-Hinshelwood model.

2.2.3 Oxidative Degradation of Pollutant by TiO_2/Solar Light

Karunakaran et al. (2005) studied on the influence of different aniline concentrations on the solar photocatalysis and found that the reaction rate increased depending on the concentration of aniline and could be explained by the Langmuir-Hinshelwood model. The TiO_2 could be reused again because the photocatalytic activity did not lose. Increasing of the surface area of catalyst enriched the solar photocatalysis and made it comparable with using UV light that carried out in a continuously stirred reactor.

Oancea and Oncescu (2008) investigated the photocatalytic degradation of the organophoshorous pesticide dichlorvos (DDVP) in suspended TiO_2 under solar irradiation. The degradation followed pseudo first order kinetic. In this work, the Langmuir-Hinshelwood equation was tested at different initial concentrations of DDVP. The values of the initial rate of DDVP degradation were independently obtained by linear fit that using only the experimental data during the first period of illumination and the half-life ($t_{1/2}$*) was calculated. The linearity obtained proved that the reaction occurred at the TiO_2 surface. Then, they compared the $t_{1/2}$ (half-life of pseudo first-order kinetics) to $t_{1/2}^*$ and found that $t_{1/2}^*$ is higher than $t_{1/2}$ which suggests that the oxidation of DDVP occurred faster than predicted by Langmuir-Hinshelwood theory. In contrast, when $t_{1/2}^*$ was less than $t_{1/2}$, it means the competition prevailed and the inhibitor effect occurred. The half-life profiles of observed and predicted versus the initial concentration of DDVP showed that increasing in DDVP concentration lessen the difference between $t_{1/2}^*$ and $t_{1/2}$ because the same amount of $OH^\bullet$ was used to oxidize higher quantities of the pollutant and its by-products. The presence of H_2O_2 at low concentration enhanced the degradation of DDVP because H_2O_2 is a good electron acceptor which generating $OH^\bullet$. However, at

higher H_2O_2 concentration, the degradation rate of DDVP decreases because H_2O_2 acted as a scavenger of $OH^{\bullet}$.

2.2.4 Oxidative Degradation of Pollutant by TiO_2/Visible Light

Lin et al. (2006) investigated the photocatalytic degradation of nitrogen oxides (NO_x) with titania-based photocatalysts radiated by ultraviolet and visible lights. The TiO_2 was synthesized in a sol-gel process using titanium butoxide as the precursor. After calcination between 150 and 300°C, the synthesized TiO_2 replied strongly to visible light and could photocatalytically degrade NO_x. This is probably because of the existence of carbonaceous species that act as sensitizers. At higher calcination temperature, carbonaceous species were burnt out so the ability to absorb visible light was eliminated. In contrary, as the calcination temperature was below 200°C, the carbonaceous species did not act as sensitizers which induced the visible light absorption. Therefore, an optimum calcinations temperature of 200°C was applied in the preparation of a TiO_2. If the calcination temperature was above 300 °C, the visible light absorbance disappeared and absorbance profile was similar to that of conventional TiO_2. The removal rates of NO_x were measured under blue, green, and red light from LED sources. The efficiency of commercial photocatalysts in the visible light (λ = 435-546) were much lower than the synthesized photocatalysts. Moreover, degradation of NO_x was not occurred by commercial catalysts when irradiated at wavelength of 500 and 546 nm. The TiO_2 which prepared by sol-gel process exhibited stronger activity than conventional TiO_2 when radiated under fluorescent lamp (simulate indoor radiation condition). The photocatalyst that responds to visible light, which provides almost the same reactivity under indoor and outdoor conditions, may extend the application for removal of NO_x from outdoor condition to indoor condition.

2.2.5 Adsorption of Pollutant onto TiO_2 Surface

Lu et al. (1996) studied on the adsorption of dichlorvos onto hydrous TiO_2. Decreased adsorption of dichlorvos was observed at an initial pH of 4. The inhibitory adsorption was attributed to the blockade of surface site by electrolytes. At pH less than pH_{pzc}, the adsorption of dichlorvos was inhibited because electrolytes competed with dichlorvos for surface site. At pH higher than pH_{pzc}, the adsorption density of dichlorvos decreased with increasing solution pH because of decrease of surface group (TiOH) on the surface of TiO_2. It was found that the dichlorvos adsorption increased with increasing temperature because the adsorption is mostly controlled by enthalpy.

Lu, Chen, and Chang (1998) studied the treatment technology using TiO_2 coated on the support for the degradation of propoxur (an insecticide). The supports that used in this study consisted of activated carbon, zeolite, brick, quartz and glass beads. The results showed that GAC/TiO_2 was the best complexing agent for oxidizing propozur because of its adsorption properties. For other support agents, the efficiency were as follows: plain TiO_2 > glass beads > zeolite > brick > quartz sequentially.

CHAPTER III

METHODOLOGY

3.1 Materials and Chemicals

3.1.1 Chemicals

-Titanium (lV) n-butoxide (98+%) was purchased from Alfa Aesar.

-Anhydrous ethanol (99.5+%, MERCK) was used as a co-solvent to dissolve titanium (lV) n-butoxide.

-Nitric acid (65%, MERCK) was used to catalyze the hydrolysis and condensation reactions.

-Aniline (99.5+%, MERCK) was used for preparing the synthesis wastewater.

-Commercial TiO_2 (Degussa P-25) was used to compare with synthetic TiO_2. P-25 was composed mostly of anatase and had a BET surface area of 59.1 m^2/g and an average particle diameter of 27 nm.

-$HClO_4$ and NaOH aqueous solutions were used to adjust pH.

-All other chemicals were reagent grade.

-Deionized water from a Millipore system (18.2 MΩ.cm) was used for all reagent preparation.

3.1.2 Reactor

-250 ml beaker was used as a reactor in this research (Figures 3.1 and 3.2).

-The light-emitting diodes (LEDs) at various wavelength were installed above and/or beside the reactor as the radiation source.

3.2 Experimental Procedures

3.2.1 Photocatalyst Synthesis

The visible-light-activated titanium dioxide photocatalyst was prepared following the procedures of Lin, Tseng, and chen, (2006). The TiO_2 powders were synthesized by titanium (IV) n-butoxide ($Ti(OC_4H_9)_4$) using an acid-catalyzed sol-gel process. TiO_2 synthesis and analytical steps for point of zero charge are described in Figures 3.3 and 3.4, respectively. Figure 3.5 shows the visible-light-activated titanium dioxide. Identification of crystalline structure, BET surface area, average particle size, point of zero charge (pzc), and spectrum analysis were also determined.

3.2.2 Photoreactivity Investigation

All photocatalytic degradation experiments were performed in a batch photoreactor system and the TiO_2 reactivity was evaluated by observing the decomposition of aniline under visible light irradiation. The reactor was set up and operated in a closed box to prevent sunlight interference. A 250 ml beaker was used to conduct the degradation of aniline, a mini fan was attached inside the box to control the temperature, if necessary, the light-emitting diodes (LEDs) of 3 watt was used as the light source. The wavelength of light was between 400–700 nm; i.e., 475 (blue), 510 (green), 570 (yellow), and 650 nm (red).

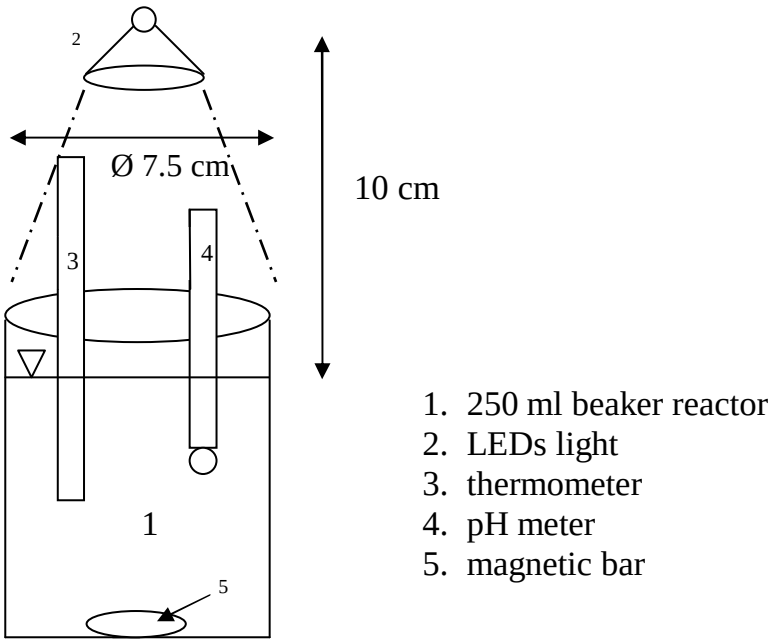

Figure 3.1 Schematic batch reactor for photocatalytic study.

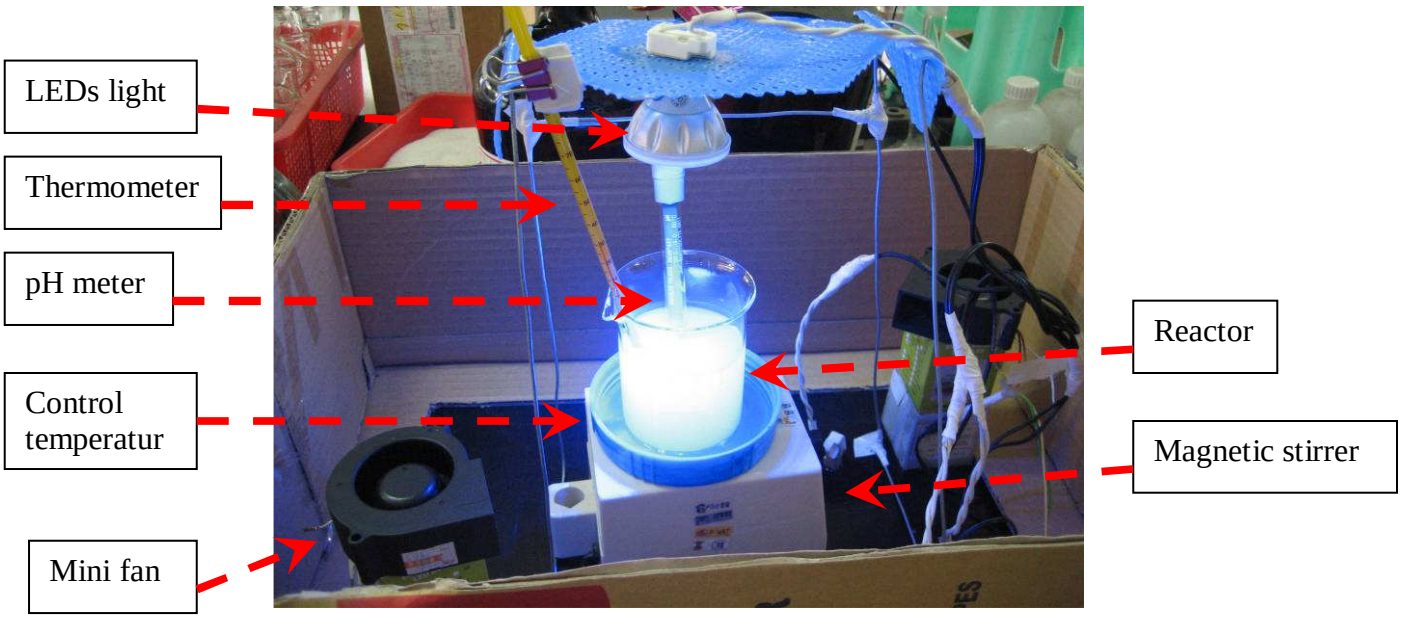

Figure 3.2 Reactor setup.

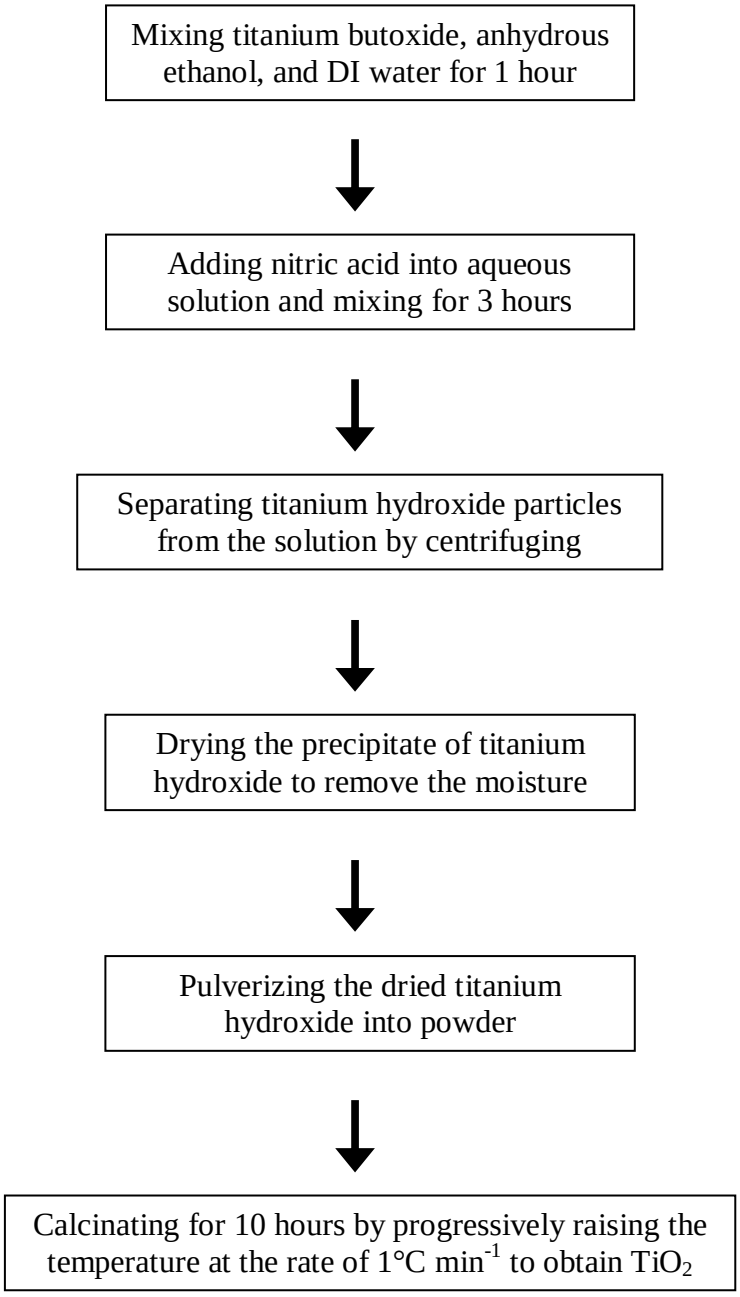

Figure 3.3 TiO_2 synthetic scheme.

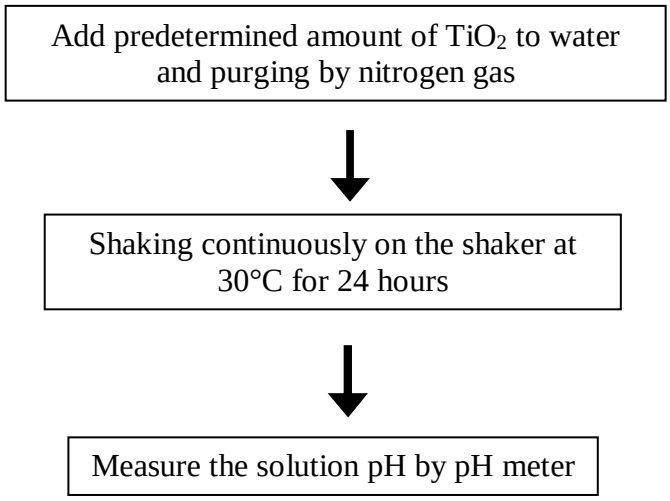

Figure 3.4 Analytical scheme for point of zero charge.

Figure 3.5 Visible-light-activated titanium dioxide photocatalyst.

The solutions were mixed by a magnetic stirrer to homogenize the solution. The reaction solutions were prepared using reagent-grade aniline diluted with deionized water to the desire concentration of 1 mM and 1 g/L of the catalyst. The pH of reaction solution was adjusted to pH 7.0±0.1 with $HClO_4$ and NaOH. Sampling time was 0, 5, 35, 65, 95, 125, 155, 185 minutes. All the experiments were carried out at room temperature (30±0.5°C). The steps of photoreactivity investigation are described in Figure 3.6.

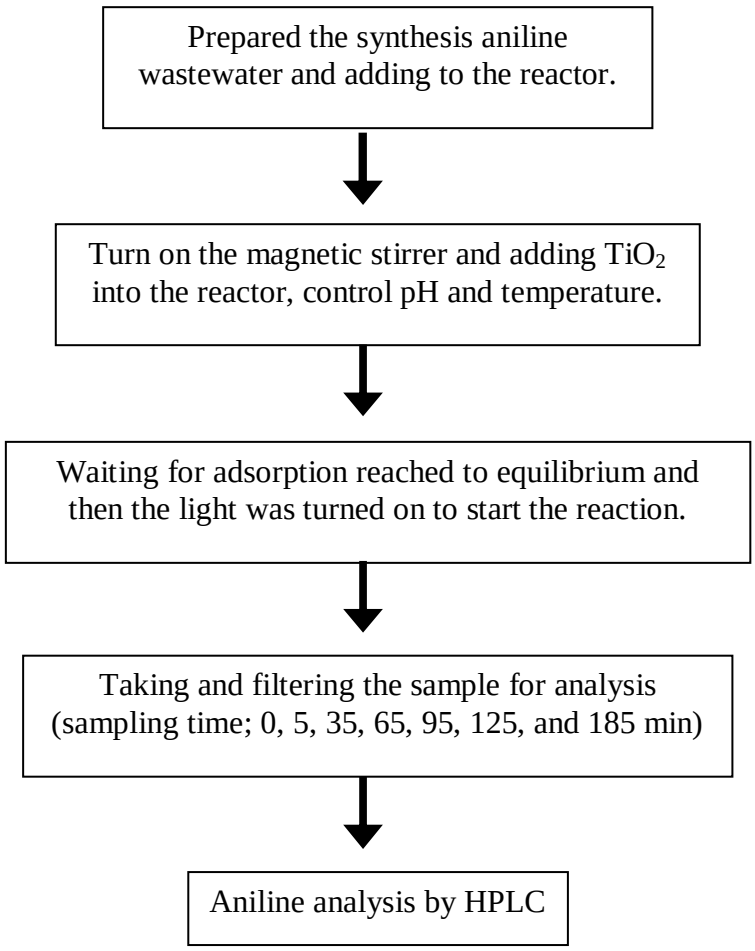

Figure 3.6 Experiment scheme for photoreactivity investigation.

3.3 Experimental Scenarios

3.3.1 Scenarios for Preliminary Study

Several screening tests were performed to obtain basic information as shown in the following tables.

Table 3.1 Scenario for the effect of light wavelength.

Aniline (mM)	TiO_2 (g/L)	pH	Temp. (°C)	Light power (lamp)	Light wavelength (nm)
1	1	7.0±0.1	30.0±0.5	1	Blue light (475)
					Green light (510)
					Yellow light (570)
					Red light (650)

Table 3.2 Scenario for the comparison of commercial TiO_2 and synthetic TiO_2.

Aniline (mM)	TiO_2 (g/L)	pH	Temp. (°C)	Light power (lamp)	Type of TiO_2
1	1	7.0±0.1	30.0±0.5	1	Synthetic TiO_2
					Commercial P-25

Table 3.3 Scenario for aniline adsorption characterization.

Aniline (mM)	TiO_2 (g/L)	pH	Temp. (°C)	Light power (lamp)	Control parameter
1	1	7.0±0.1	30.0±0.5	1	Aniline + light
					Aniline + TiO_2
					Aniline + light + TiO_2

3.3.2 Scenarios for Modification of TiO_2 Synthesis

To Investigate the effects of alcohol type, acid type, and calcination temperature on the TiO_2 property regarding on visible light absorption, various scenarios were established as shown in Tables 3.4 and 3.5. Optimum conditions for visible-light activated TiO_2 were obtained by comparing the reactivity under visible light using aniline as a target compound.

3.3.3 Photo-Reactivity Investigation

Photoreactivity of synthetic TiO_2 was investigated under several conditions including light wavelength, light power, light distance, and light position. The experimental scenarios were shown in Tables 3.6 to 3.8.

Table 3.4 Scenario for the effect of alcohol and acid types.

Aniline (mM)	TiO_2 (g/L)	pH	Temp. (°C)	Light power (lamp)	Acid type	Alcohol type
1	1	7.0±0.1	30.0±0.5	1	Nitric	Ethanol
					Acetic	Methanol

Table 3.5 Scenario for the effect of calcinations temperature.

Aniline (mM)	TiO_2 (g/L)	pH	Temp. (°C)	Light power (lamp)	Acid type & Alcohol type	Calcine temp. (°C)
1	1	7.0±0.1	30.0±0.5	1	Nitric & Ethanol	150
						200
						300

Table 3.6 Scenario for the effect of light distance.

Aniline (mM)	TiO_2 (g/L)	pH	Temp. (°C)	Light power (lamp)	Light distance (cm)
1	1	7.0±0.1	30.0±0.5	1	5
					10

Table 3.7 Scenario for the effect of light power.

Aniline (mM)	TiO_2 (g/L)	pH	Temp. (°C)	Light power (lamp)
1	1	7.0±0.1	30.0±0.5	1
				2
				3
				4

Table 3.8 Scenario for the effect of light position.

Aniline (mM)	TiO_2 (g/L)	pH	Temp. (°C)	Light power (lamp)	Light position
1	1	7.0±0.1	30.0±0.5	4	above the reactor
					Around the reactor

3.3.4 Photo-Catalytic Study

The effect of pH and kinetics determination were studied in order to characterize the photoreactivity of synthetic TiO_2. The experimental scenarios were shown in Tables 3.9 to 3.10.

Table 3.9 Scenario for the effect of pH.

Aniline (mM)	TiO_2 (g/L)	Temp. (°C)	Light power (lamp)	pH
0.05	1	30.0±0.5	1	4
				7
				10

Table 3.10 Scenario for the effect of aniline concentration.

TiO_2 (g/L)	Temp. (°C)	pH	Light power (lamp)	Aniline (mM)
1	30.0±0.5	7.0±0.1	1	0.047
				0.067
				0.32
				0.54
				0.80

3.4 Analytical Methods

3.4.1 Measurement of Aniline

The aniline decomposition was determined by measuring aniline concentration remaining in the sample. The liquid samples were filtered through mixed cellulose ester membrane with 0.2 µm pore size to remove the TiO_2 particles before analysis. The residual aniline concentrations were measured by high performance liquid chromatography (HPLC) using 60% acetonitrile and 40% distilled water as a mobile phase. The column was operated between 18 and 22°C. The pump was a SpectraSYSTEM model SN4000 with the operating flow rate of 1.0 ml/min through Asahi pak ODP-50 6D column (150mm×6mm×5µm). The 254 nm outputs from UV1000 detector were measured. The injection volume was 20 µL.

3.4.2 Identification Crystalline Structure

The powder TiO_2 samples were determined by the X-ray diffraction (XRD) (D8 Discovered, Bruker AXS). The patterns were recorded over the angular range 20-80° (2θ).

3.4.3 Point of Zero Charge (pzc) Analysis

Point of zero charge of TiO_2 samples were analyzed in two ways. The first way followed mass titration method (Reymond and Kolenda, 1999) as shown in Figure 3.5 and the second way was determined by zeta potential method using dynamic light seattering (Malvern ZS90).

3.4.4 Spectrum Analysis

The powder TiO_2 samples were determined by using a diffuse-reflectance scanning spectrophotometer (Perkin Elmer, Lambda 35 UV-vis Spectrometer) to obtain the UV-visible absorption spectra of the powders.

3.4.5 Surface Area Analysis

The surface area of TiO_2 powder was obtained from nitrogen adsorption isotherm by the Brunauer-Emmett-Teller (BET) method (Autosorb-1, Quantachrome) following the ASTM standard.

3.4.6 Particle Size Analysis

The powder TiO_2 samples were determined for their size distribution by using laser particle size analyzer (Mastersizer-2000, Malvern).

3.4.7 Soluble Ion Analysis

Most of intermediate product anions from photocatalytic degradation of aniline were analyzed by Ion Chromatography (IC). The samples were filtered through mixed cellulose ester membrane with 0.2 µm pore size to remove the TiO_2 particles before analysis. The IC consisted of Dionex DX-120 Ion Chromatograph with the operating flow rate of 1.0 ml/min, Reagent-Free™ Controller with RFIC™ EGC II KOH, Autosampler Thermo Finnigan SpectraSYSTEM model AS1000 with 20 µl injection volume, Guard column IonPac® AG-11 (4Í50 mm), column IonPac® AS-11 (4Í250 mm), column temperature stabilizer model CTS-10 control at 30 ˚C, suppressor ASRS®-ULTRA II 4-mm with conductivity detector with gradient 0.1 mM KOH 0-4 min, 0.1 – 18 mM KOH time 4-22 min, 18 mM KOH 22-26 min, 0.1 mM KOH 26-30 min.

CHAPTER IV

RESULTS AND DISCUSSION

The experimental works, under the visible-light irradiation by using aniline as a target compound, consisted of four parts: preliminary study, modification of TiO_2 synthesis, photo-reactivity investigation, and photo-catalytic Study. The results are summarized below:

4.1 Preliminary Study

4.1.1 Comparison between Commercial P-25 and Synthetic TiO_2

This experimental part aimed to confirm the reactivity under visible light of the synthetic TiO_2 prepared following the procedures of Lin (Lin et al., 2006) and compared with the P-25 which is one of the most widely used commercial TiO_2. The results are shown in Figures 4.1 and 4.2 for the synthetic TiO_2 and P-25, respectively. It can be seen that aniline was not transformed under direct photolysis and its volatilization could be neglected within the experimental period (less than 5% reduction in 3 hours). Aniline seemed to adsorb onto the P-25 better than the synthetic TiO_2, i.e., approximately 17 and 12%, respectively, and the equilibrium was obtained in less than 30 minutes for both cases. Their properties are shown in Tables 4.1. and 4.2. It can be inferred that the surface area of synthetic TiO_2 is higher than commercial P-25 but the particle size of synthetic TiO_2 is larger than commercial P-25 because of non-porous property of the commercial P-25 (Lettmann et.al, 2001). However, under the illumination of the blue light, aniline was degraded in the presence of synthetic TiO_2, i.e., 20% more reduction as compared to adsorption alone, whereas no reaction other than adsorption occurred in the case of P-25. Figure 4.3 compares the reactivity of the synthetic TiO_2 with the P-25 which significantly demonstrated that the synthetic TiO_2 was able to be activated by the blue light to generate the $OH^{\bullet}$ which further reacted with aniline. On the other hand, the P-25 could not; hence, no $OH^{\bullet}$ was generated. This is not surprising because it is well known that typical P-25 will be activated only by the UV light with the wavelength shorter than 400 nm.

The optical absorption spectra of the synthetic TiO_2 and the P-25 were examined to verify this hypothesis and the outcomes are shown in Figure 4.4. It can be seen that the P-25 almost did not absorb any light at the wavelength longer than 400 nm whereas the synthetic TiO_2 was able to absorb some lights within the visible range. However, in the UV range (wavelength lower than 400 nm), the absorption spectra of the synthetic TiO_2 and the P-25 were almost the same. This can be implied that the efficiency for aniline degradation under the UV irradiation between these two TiO_2 should not have any significant difference. Different physical appearance between these two TiO_2 also supported the spectral scan. The synthetic TiO_2 was yellowish red (absorbed most blue and some green light) whereas the P-25 was white (reflected all blue, green, yellow and red light; hence, no absorption) as shown in the Appendix A.4. These spectral analyses supported the observation of aniline oxidation by the synthetic TiO_2 under the blue light.

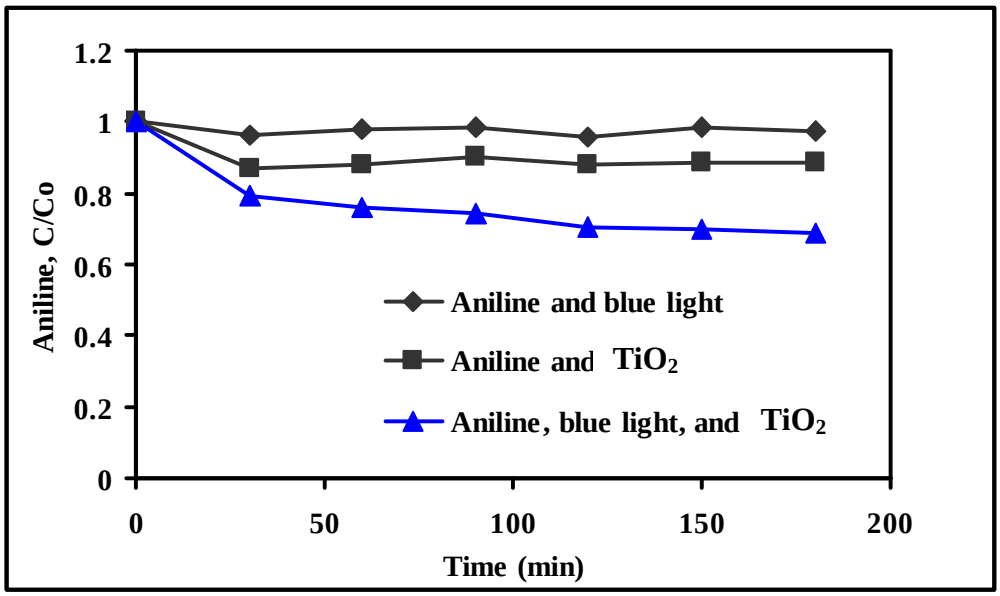

Figure 4.1 Effect of light and synthetic TiO_2 on the removal of aniline (initial conditions were as follows: 1 mM aniline, 1g/l TiO_2, 3 W of light, pH at 7.0±0.1, and temperature at 30.0±0.5 °C).

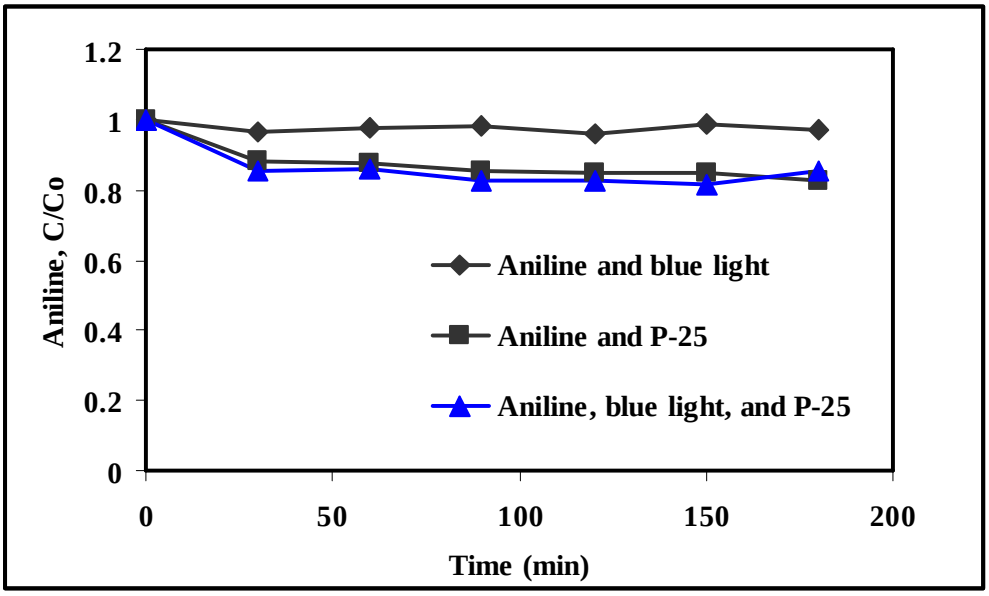

Figure 4.2 Effect of light and commercial P-25 on the removal of aniline (initial conditions were as follows: 1 mM aniline, 1g/l TiO_2, 3 W of light, pH at 7.0±0.1, and temperature at 30.0±0.5 °C).

Table 4.1 Comparison between synthetic TiO_2 and commercial TiO_2.

Properties	Synthetic TiO_2	Commercial P-25
Crystalline Structure	Anatase	Anatase and Rutile
Absorption spectra	Visible light	UV light
Surface area (m^2/g)	139.60	43.00

Table 4.2 Comparison the particle size distribution between synthetic TiO_2 and commercial TiO_2 in differential phase.

Particle size distribution	Synthetic TiO_2		Commercial P-25	
	Wet measurement	Dry measurement	Wet measurement	Dry measurement
d(0.1) (µm)	19.95	9.00	0.16	0.88
d(0.5) (µm)	52.08	36.99	0.25	3.46
d(0.9) (µm)	121.16	114.23	2.38	8.52

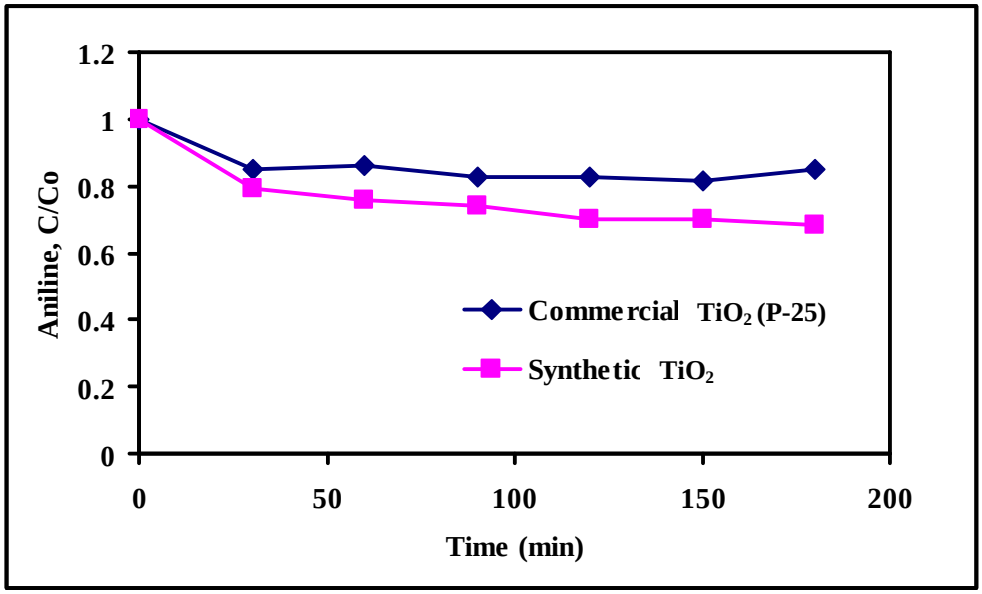

Figure 4.3 Comparison between synthetic TiO_2 and Commercial P-25 on the photocatalysis of aniline (initial conditions were as follows: 1 mM aniline, 1g/l TiO_2, 3 W of light, pH at 7.0±0.1, and temperature at 30.0±0.5 °C).

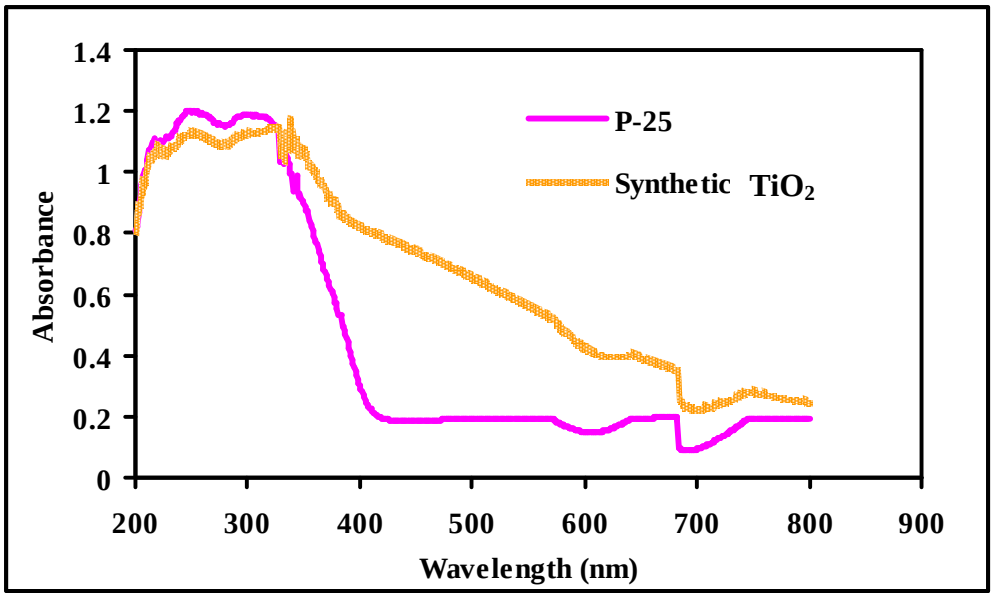

Figure 4.4 UV-vis absorption spectra of synthetic TiO_2 and Commercial P-25.

Further examination on the crystalline structure was conducted and the results are shown in Figure 4.5. The P-25 showed two main peaks for the anatase and rutile crystalline structure. This confirmed with the specification of the P-25 which consisted of 80% anatase and 20% rutile. The synthetic TiO_2; however, had only one peak of anatase implying that the synthetic procedure of Lin et al. (2006) produced mostly anatase structure. It is well known that anatase has relatively large band gap of 3.2 eV which relates to the wavelengths of shorter than 388 nm as already shown in Figure 2.1. Therefore, it implies that this synthetic TiO_2, which could respond to the light at the wavelength longer than 388 nm, consists of some intra-band gap states that are close to the conduction or valence band edges with the sub-band gap energies of less than 3.2 eV.

4.1.2 Effect of Light Wavelength on TiO_2 Photo-Activity

It is interesting to determine the photo-response of the synthetic TiO_2 to the light at other wavelength rather than blue light since its adsorption spectra also showed a superior trend to the P-25. In this part, the green, yellow, and red lights were used and their abilities to degrade aniline were summarized in Figure 4.6. The removal efficiency of the blue light was better than green, yellow, and red lights, sequentially, which was corresponding very well with the adsorption spectra.

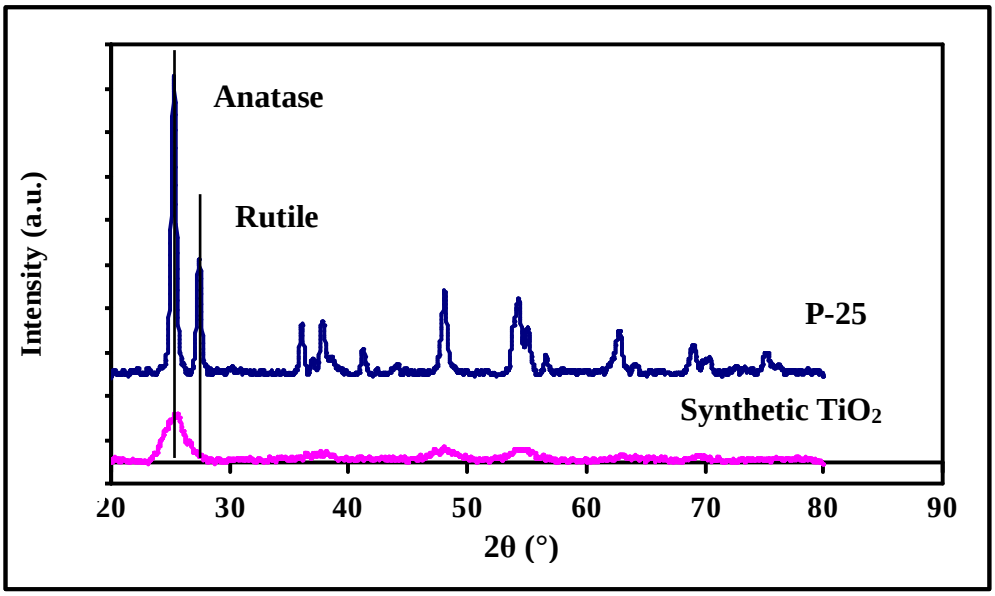

Figure 4.5 XRD patterns of synthetic TiO_2 and Commercial P-25.

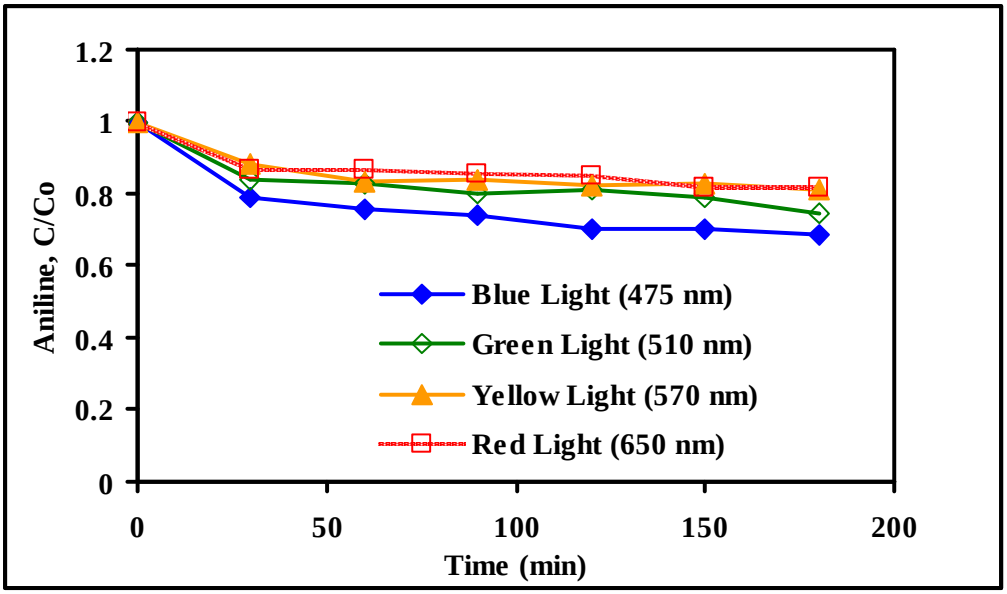

Figure 4.6 Effect of light wavelength on the photocatalysis of aniline (initial conditions were as follows: 1 mM aniline, 1g/l TiO_2, 3 W of light, pH at 7.0±0.1, and temperature at 30.0±0.5 °C).

4.1.3 Aniline Adsorption Equilibrium

For more precise study on the kinetics of the photo-catalysis, adsorption equilibrium time was examined in order to make sure that aniline adsorption reached equilibrium prior to light illumination. It was found that the adsorption of aniline reached equilibrium very rapidly in less than one minute under the study condition as shown in Figure 4.7. Therefore, all the later experiments were conducted by allowing 5 minutes adsorption to ensure the equilibrium and then followed by the light illumination. However, the data during the first 5-minute adsorption were omitted from the figures in order to demonstrate only the aniline reduction due to photo-catalysis process.

4.2 Modification of TiO_2 Synthesis

4.2.1 Effect of Alcohol and Acid Types

In the procedures of Lin et al. (2006), nitric acid and ethanol were used in the synthetic process. However, from literature surveys, there were some other researchers used different acids and alcohols. Therefore, this experimental part aimed to investigate the possibility to improve theTiO_2 property of Lin et al., (2006). Acetic acid and methanol were used together with nitric acid and ethanol to generate 4 combinations and their abilities in aniline degradation were shown in Figure 4.8. It was found that TiO_2 synthesized by using nitric acid/ethanol performed slightly better than acetic acid/ethanol, nitric acid/methanol, and acetic acid/methanol, chronologically. These performances agreed very well with the visible adsorption spectra as shown in Figure 4.9 in which the TiO_2 from nitric acid/ethanol absorbed better than from acetic acid/ethanol and acetic acid/methanol, respectively. As a result, the TiO_2 synthesized by using nitric acid/ethanol as suggested by Lin et al., (2006) was used for further investigation through out this study. Although its performance regarding on aniline oxidation was not really superior to other combination, its visible absorption spectra seems to be more promising than the others.

4.2.2 Effect of Calcinations Temperature

According to Lin et al. (2006), the calcinations temperature was maintained at 200°C. This study tried to improve the TiO_2 property by varying the calcinations temperature to 150 and 300°C and the results on aniline photo-oxidation were shown in Figure 4.10. From the figure, no precise conclusion could be drawn since the reductions of aniline were quite similar for all temperature, though the 200°C seemed to be just a little better. Nonetheless, the spectra of the TiO_2 calcined at 200°C clearly showed the strongest absorption among the three temperatures as shown in Figure 4.11. This was corresponding very well with the visible appearance in which the TiO_2 calcined at 200°C had the darkest color (see Appendix A.3). It also implied that the temperature suggested by Lin et al. (2006) was already the optimum value for this synthetic procedure.

The results from XRD analysis of TiO_2 showed that the TiO_2 calcined at 150 and 200°C contained only anatase crystalline structure whereas rutile peak was also observed together with anatase peak when the calcinations temperature increased to 300°C as illustrated in Figure 4.12.

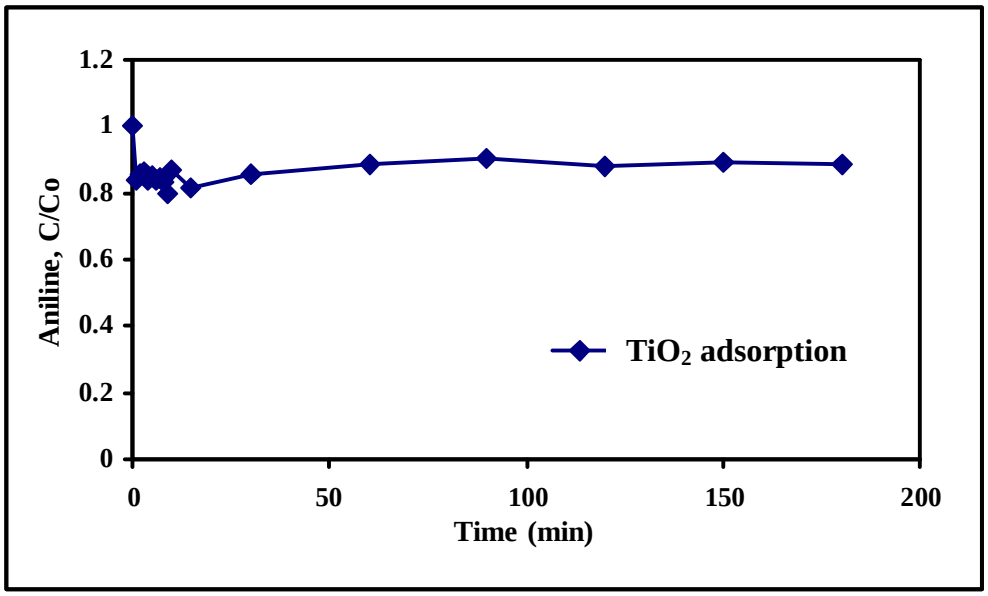

Figure 4.7 Aniline adsorption onto synthetic TiO_2 (initial conditions were as follows: 1 mM aniline, 1g/l TiO_2, 3 W of light, pH at 7.0±0.1, and temperature at 30.0±0.5 °C).

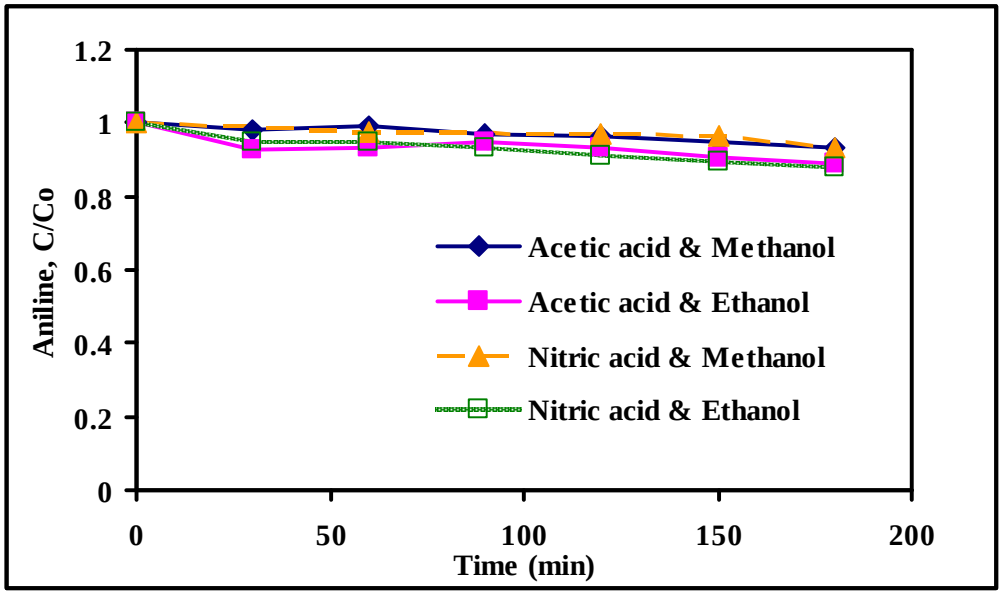

Figure 4.8 Effect of alcohol and acid types on the phtocatalytic property of TiO_2 (initial conditions were as follows: 1 mM aniline, 1 g/l TiO_2, 3 W of light, pH at 7.0±0.1, and temperature at 30.0±0.5 °C).

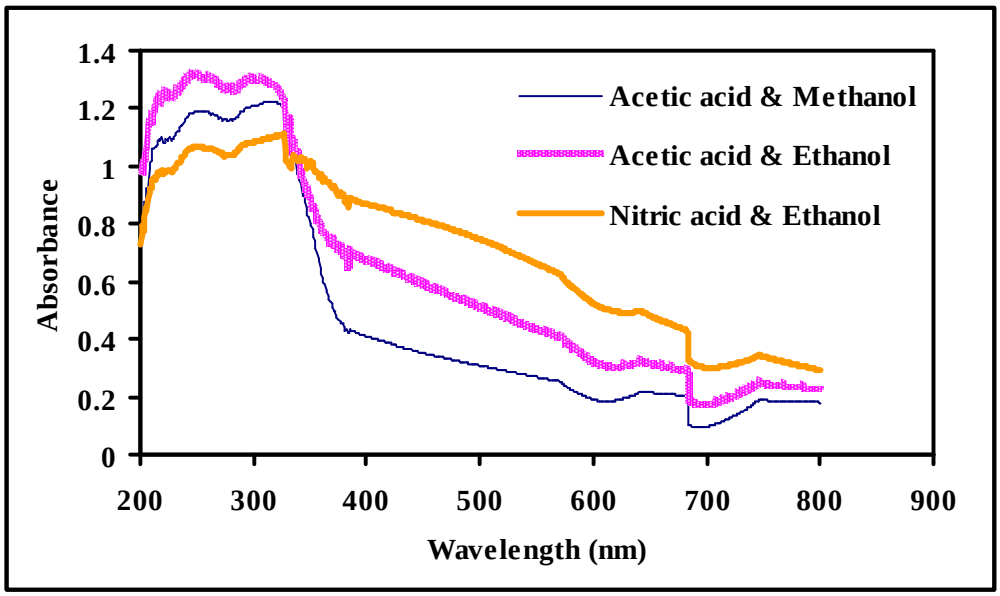

Figure 4.9 UV-vis absorption spectra of the TiO_2 synthesized by using different alcohol and acid types.

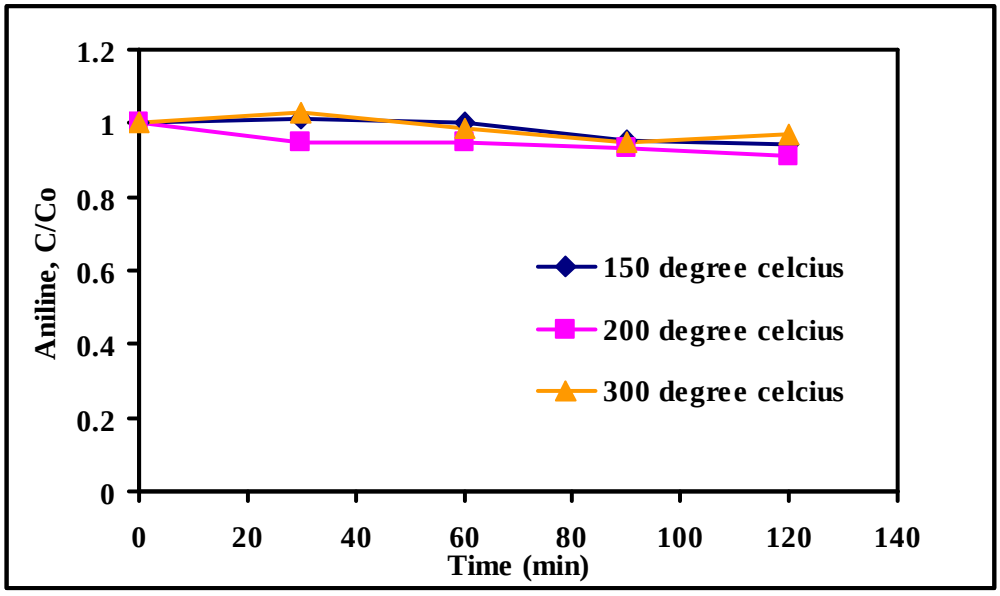

Figure 4.10 Effect of calcinations temperature on the photocatalytic property of TiO_2 (initial conditions were as follows: 1 mM aniline, 1g/l TiO_2, 3 W of light, pH at 7.0±0.1, and temperature at 30.0±0.5 °C).

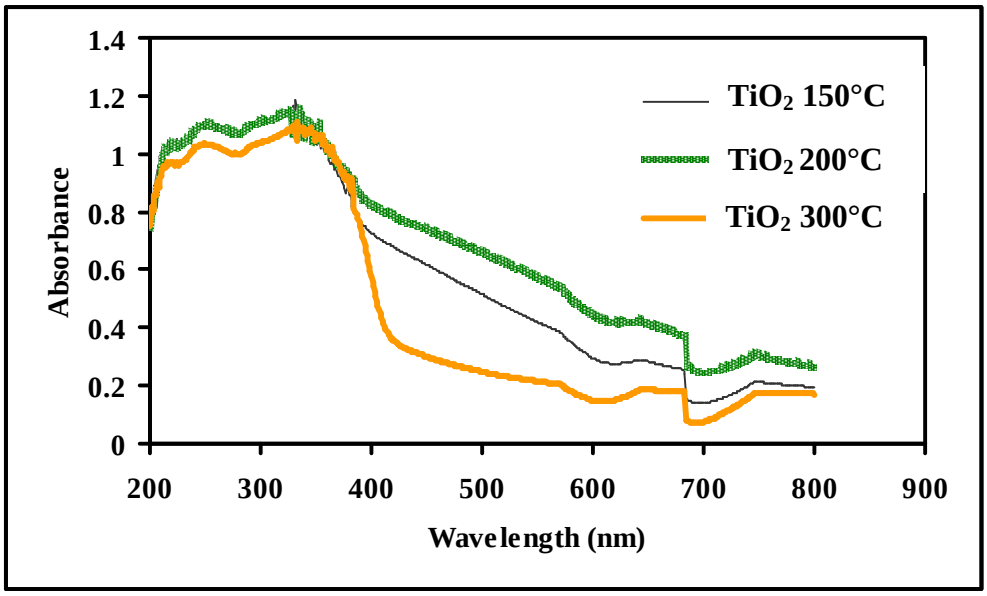

Figure 4.11 UV-vis absorption spectra of the TiO_2 synthesized at different calcinations temperature.

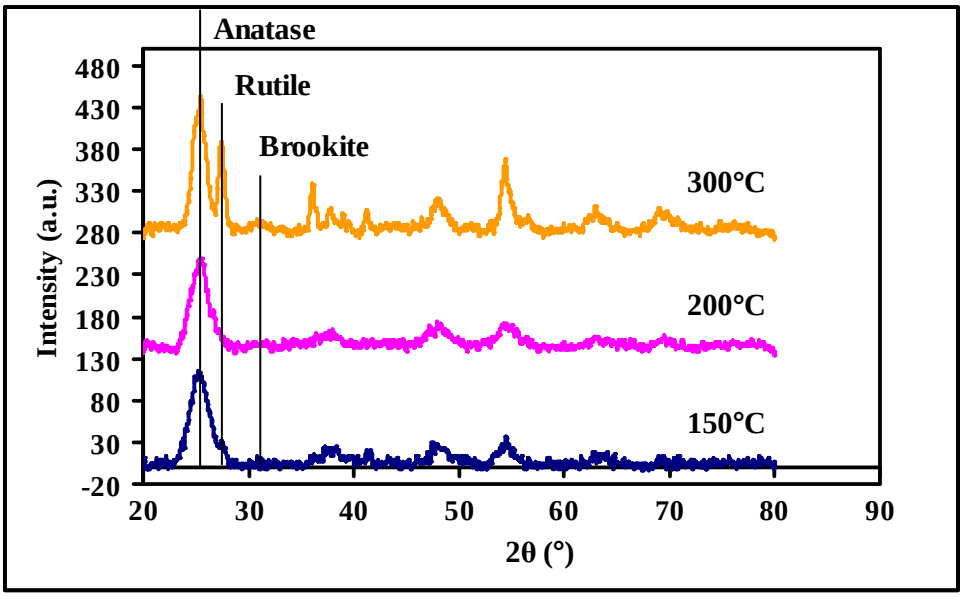

Figure 4.12 XRD patterns of the TiO_2 synthesized at different calcinations temperature.

4.3 Photo-Reactivity Investigation

4.3.1 Determination of Optimum Light Configuration

This experimental part aimed to determine the optimum configuration of the light source which mainly used LEDs at the wavelength of 475 nm. Light intensity is one of the important factors affecting the performance of the photo-catalysis process. The photo-degradation of aniline was examined under different lighting conditions including distance, position, and power of the light source.

4.3.1.1 Effect of Light Position

To determine the best position for installing the light source regarding on lighting efficiency and experimental convenience, four LED lamps were placed around the photo-reactor in two manners, i.e., positioned above the reactor and around the reactor (one on the top and three along the side) (see Appendice A.1 and A.2). These two different placements caused two different effects. The light from the lamps which placed above the reactor only passed through the air before reaching the solution whereas those placing along the side of the reactor would have to pass the air and the pyrex glass before reaching the solution. As a result, the latter case would lead to some losses due to adsorption by the pyrex glass. However, the latter setup would provide more illumination area which could lead to better photo-catalytic activity. The results are shown in Figure 4.13 indicating that placing the light around the reactor provided only slightly better performance on aniline degradation than placing on the top of the reactor. Therefore, this study mainly placed the LED lamp on the top of the reactor due to its more convenience in the experimental operation.

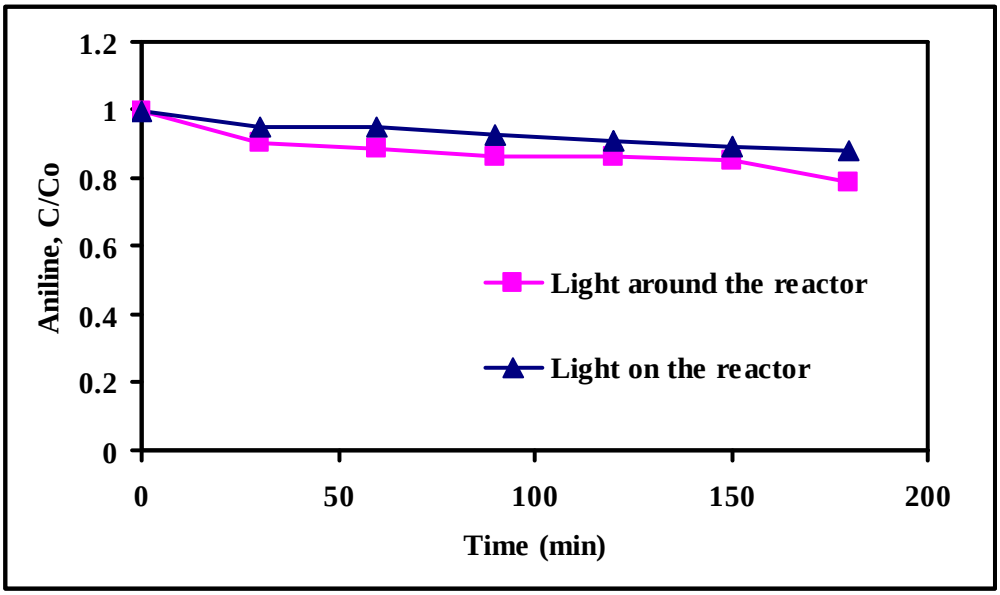

Figure 4.13 Effect of light position on the photo-catalysis of aniline (initial conditions were: 1 mM aniline, 1g/L TiO_2, pH at 7.0±0.1, and temperature at 30±0.5 °C).

4.3.1.2 Effect of Light Power

The LED lamps used in this study had the output power of 3 watt each. More light power would have a potential to accelerate the photo-activity as well as to increase the temperature. Figure 4.14 shows the degradation of aniline under one, two, three, and four LED lamps placing above the reactor. It was found that one lamp provided a little slower degradation rate than the others which had comparable performance. This implies that the cloudy manner of TiO_2 suspension prevented the light to penetrate deeper into the solution; hence, did not provide any significant improvement on the photo-catalytic reaction. In addition, it was difficult to control the temperature at the set point of 30±0.5°C as the number of LED lamps greater than one. Therefore, one LED lamp was used through out the photo-catalytic experiments.

4.3.1.3 Effect of Light Distance

As the light travels through a medium, certain energy will be lost. Hence, placing the light source near the reactor as much as possible should provide the most efficient configuration for a photo-reactor. However, this might cause some difficulties in the operation. To determine the effect of light distance on the aniline degradation, the LED lamp was placed either 5 or 10 cm above the reactor and the results are demonstrated in Figure 4.15. There was no significance in aniline degradation between these two placements; however, placing the light source too close to the solution caused some difficulties in temperature control. Therefore, the LED will be placed 10 cm above the surface of the solution through out this work.

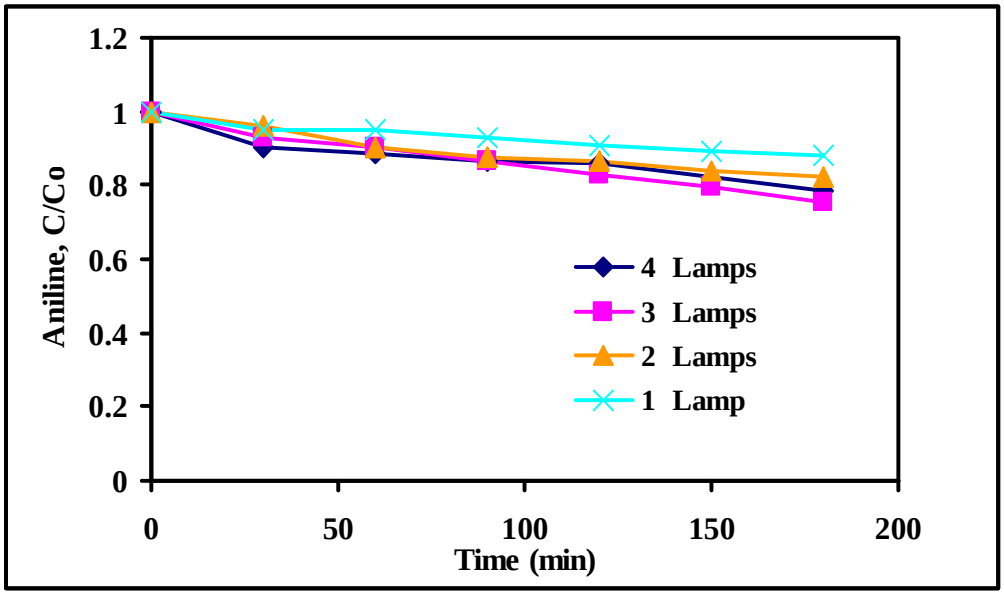

Figure 4.14 Effect of light power on the photo-catalysis of aniline (initial conditions were: 1 mM aniline, 1 g/L TiO_2, pH at 7.0±0.1, and temperature at 30±0.5 °C).

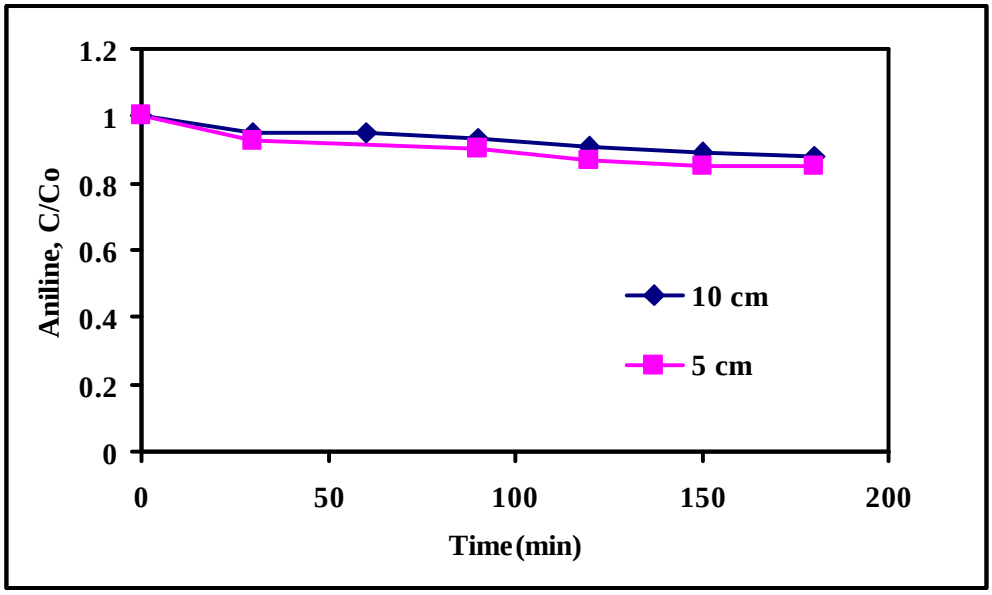

Figure 4.15 Effect of light distance on the photo-catalysis of aniline (initial conditions were: 1 mM aniline, 1 g/L TiO_2, pH at 7.0±0.1, and temperature at 30±0.5 °C).

4.4 Photo-Catalytic Study

4.4.1 Effect of pH

pH is the master variable controlling behavior of TiO_2 and reaction in aqueous solution. The point of zero charge (pzc) of the synthetic TiO_2 was 3.5 and 3.2 according to the mass titration method and zeta potential method as shown in Figures 4.16 and 4.17, respectively. According to pzc definition, the TiO_2 surface will exhibit a positive charge when pH is lower than 3.5 or 3.2 and becomes negative as the pH is higher than these values. Aniline is a weak base and its conjugate acid is anilinium ion ($C_6H_5NH_3^+$) as shown previously in equation (4.1).

$$C_6H_5NH_3^+{}_{(aq)} \longleftrightarrow C_6H_5NH_{2(aq)} + H^+; \qquad pK_a = 9.37 \qquad (4.1)$$

At pH of 4, 7, and 10 used in this study, the anilinium ion was accounted for approximately 1.0, 0.994, and 0.2007 of total aniline species in the solution, respectively. This suggests that the adsorption of aniline species should occur the most at pH 7 which corresponded very well with the adsorption data as shown in Figure 4.18. Aniline adsorption at pH 10 was almost similar to pH 7 even though the anilinium ion at pH 10 was accounted for only 20.07% compared to 100% at pH 7 indicating that higher negative potential on the TiO_2 surface (-35 mV at pH 10 versus -25 mV at pH 7) might be able to compensate for lower concentration of positive anilinium ion. The photo-catalytic oxidation of aniline; nonetheless, did not followed the trend of aniline adsorption, i.e., pH 7 > pH 4 > pH 10, as shown in Figure 4.19.

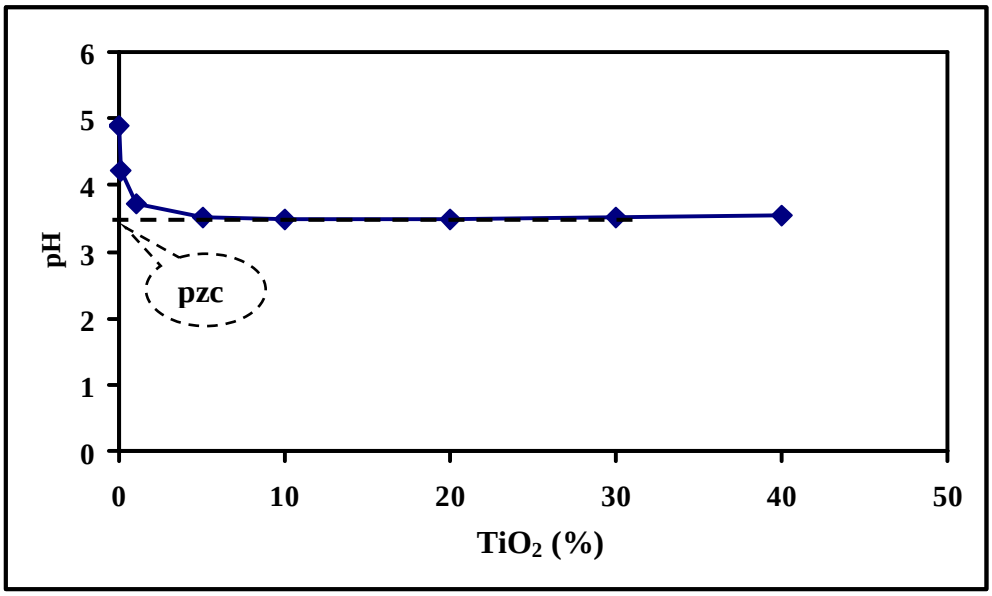

Figure 4.16 Point of zero charge determination using the mass titration method.

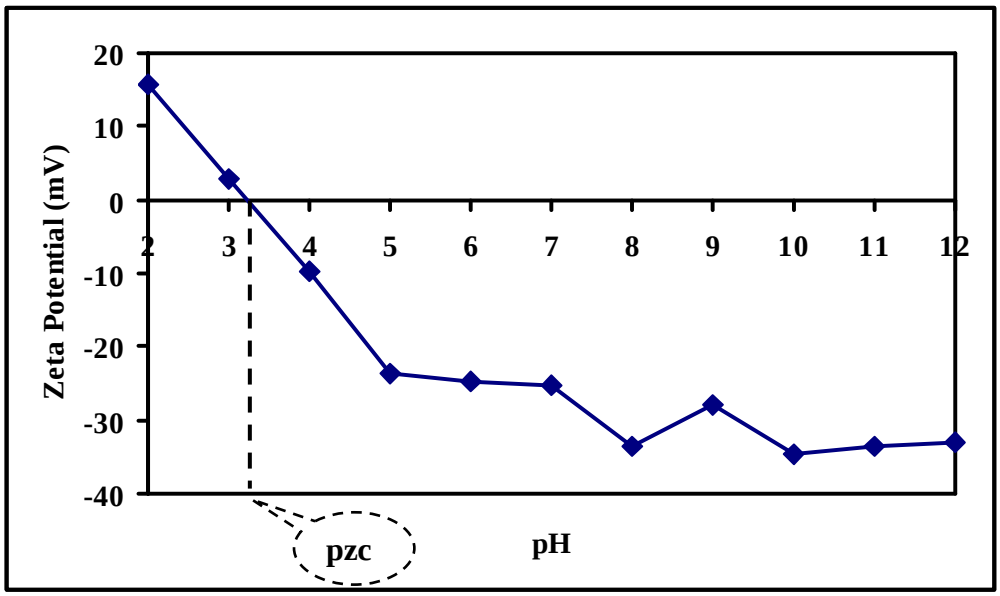

Figure 4.17 Point of zero charge determination using the zeta potential method.

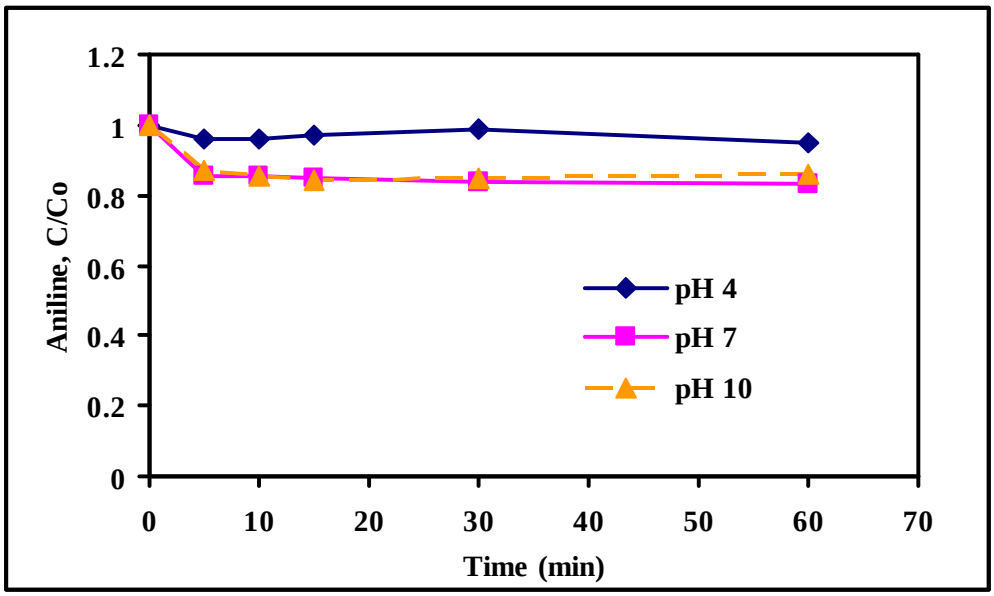

Figure 4.18 Adsorption of aniline onto TiO_2 at different pH (initial conditions were: 0.05 mM aniline, 1 g/L TiO_2, 3 W of light, and temperature at 30.0±0.5 °C).

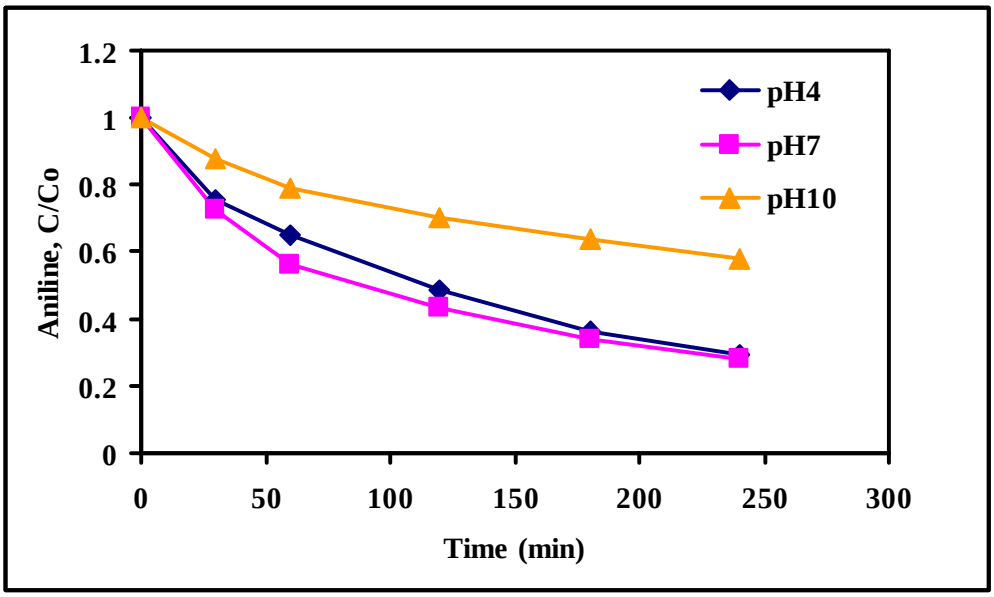

Figure 4.19 Effect of pH on the photo-catalysis of aniline (initial conditions were: 0.05 mM aniline, 1 g/L TiO_2, 3 W of light, and temperature 30.0±0.5 °C).

According to Thounaojam et al. (2001) and Solar et al. (1986), the second-order rate constants with $OH^{\bullet}$ for anilinium ion and aniline were 5.0×10^{9} and 1.5×10^{10} $M^{-1}sec^{-1}$, respectively, implying that aniline (predominant species at pH > 9.37) will react with $OH^{\bullet}$ approximately 3 times faster than anilinium ion (predominant at pH < 9.37). There is no clear explanation for these observations at this point. It might involve the scavenging effect of carbonate ion which was predominant at high pH and direct oxidation of anilinium ion at the electron hole (h^{+}). Nevertheless, these data suggested that the adsorption was not the rate-limiting step in aniline oxidation by photo-catalytic process. In order to obtain significant reduction of aniline, the pH will be controlled at 7 for the kinetics study.

4.4.2 Kinetics Determination

The kinetics of aniline oxidation by the photo-catalytic reaction by TiO_2 under visible light was determined by using the Langmuir-Hinshelwood kinetic expression as mentioned earlier in Section 2.1.9. The linearized form of the Langmuir-Hinshelwood expression is illustrated in equation (4.2).

$$\frac{1}{\left(\frac{d[AN]}{dt}\right)_0} = \frac{1}{r_0} = \frac{1}{k_r} + \frac{1}{k_r K}\frac{1}{[AN]_0} \qquad (4.2)$$

The plot between inverse initial rate and inverse initial aniline concentration will show a linear line with the y-intercept equals to “1/kr” and the slope equals to “$1/(k_r K)$”. The initial disappearance rate was determined by fitting the observed data with either zero-, first-, or second-order kinetics of which provided the best fit. Two methods were employed to correlate the data to the kinetics equation, i.e., R^2 and non-linear least squares methods. According to the observed data, it was found that the non-linear least squares method provided a better fit than the R^2 method as shown in Figure 4.20. Hence, the non-linear least square method was used intensively in the kinetics determination. Figure 4.21 shows the results from data fitting by using zero-, first-, and second-order kinetics. It shows that the second-order kinetics was able to explain the obtained data better than the other two models; hence, second-order kinetics was used to determine the initial degradation rate of aniline.

To estimate the “k_r” and “K” of the Langmuir-Hinshelwood kinetics, several experiments were conducted using different aniline concentrations. The aniline time-profiles and rates were summarized in Figure 4.22 and Table 4.3, respectively. The removal efficiency decreased as the initial aniline concentration increased from 0.047 mM to 0.067, 0.32, 0.54, and 0.80 mM, respectively. This is understandable since the amount of $OH^{\bullet}$ generation in each system was the same; therefore, the portion of aniline being removed was the highest at the lowest concentration and lessened as the concentration increased. However, the initial degradation rate of aniline was in the opposite direction, i.e., increased from 0.00043 to 0.0011 mM min^{-1} as the initial aniline increased from 0.047 to 0.80 mM. The plot between “1/r” and “1/[AN]” yielded a linear line with the R^2 of 0.96 as shown in Figure 4.23.

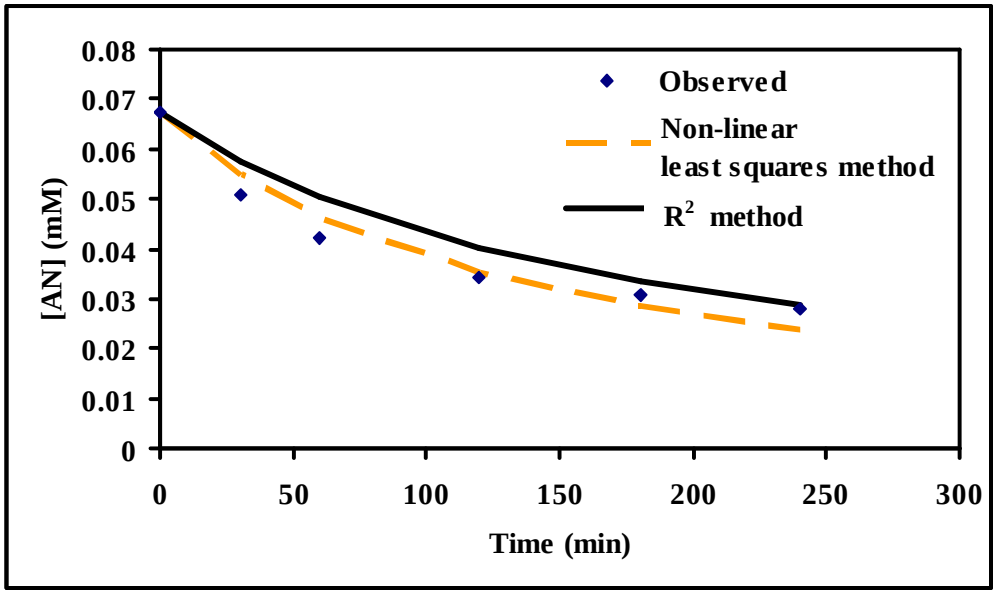

Figure 4.20 Fitting comparison between the linearization and non-linear least squares methods.

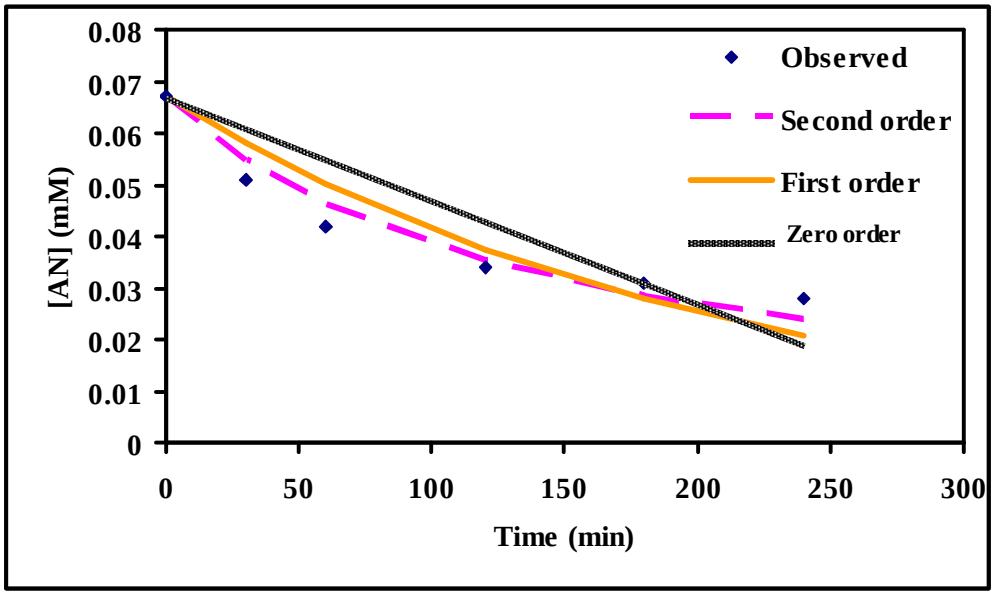

Figure 4.21 Data fitting by various kinetic equations.

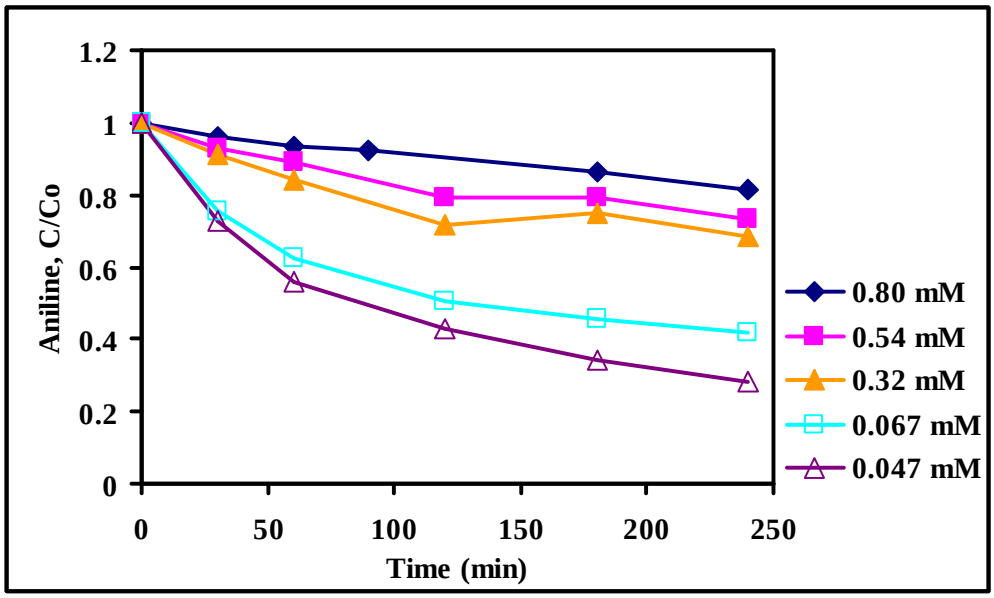

Figure 4.22 Aniline degradation profiles (initial conditions were: 1 g/L TiO_2, 3 W of light, pH at 7.0±0.1, and temperature at 30.0±0.5 °C).

Table 4.3 Apparent second-order rate constants (k_{app}) of the photodegradation of aniline at different initial concentration.

Initial concentration (mM)	k_{app} (mM^{-1} min^{-1})	Rate (mM min^{-1})	$t_{1/2}$ (min)	$t_{1/2}^{*}$ (min)
0.047	0.195	0.000425	109.7	67.24
0.067	0.114	0.000519	129.8	77.61
0.32	0.00725	0.000720	437.9	202.0
0.54	0.00309	0.000909	597.1	316.1
0.80	0.00167	0.00106	749.8	444.2

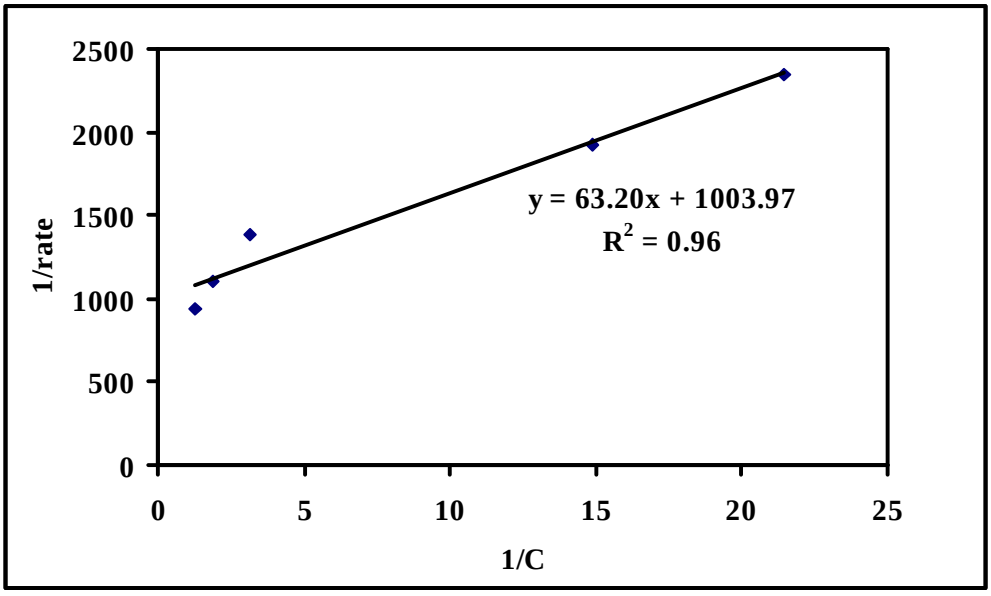

Figure 4.23 Linearized reciprocal kinetic plot for the photocatalytic degradation of aniline (Initial conditions were follows: TiO_2 1 g/L, control pH 7±0.1, and control temperature 30±0.5 °C).

The "k_r" and "K" were estimated to be 9.96×10^{-4} mM min^{-1} and 15.89 mM^{-1}, respectively as shown previously in Equation (2.15).

$$-\frac{d[AN]}{dt} = \frac{k_r K [AN]_0}{1+K[AN]_0} = \frac{\left(9.96\times10^{-4}\right)(15.89)\,[AN]_0}{1+15.89\,[AN]_0} \qquad (2.15)$$

The true half-life ($t_{1/2}^*$) was estimated following Equation (2.18). The plot of $t_{1/2}^*$ versus the initial concentration of aniline would be linear because of no competition of with reaction by-products. On the other hand, the observed half-life for second-order reaction could be calculated by Equation (2.19).

$$t_{1/2}^* = \frac{0.5[AN]_0}{k_r} + \frac{\ln 2}{k_r K} \qquad (2.18)$$

$$t_{1/2} = \frac{1}{k[AN]_0} \qquad (2.19)$$

Figure 4.24 shows the dependence of $t_{1/2}^*$ and $t_{1/2}$ on the initial concentration of aniline. It can be seen that $t_{1/2}^*$ and $t_{1/2}$ are almost the same at low initial concentrations but the $t_{1/2}^*$ became longer than $t_{1/2}$ as of the initial aniline increased. It is expected that the reaction by-products (such as acetic acid, formic acid, oxalic acid, and butyric acid) might compete with aniline for $OH^{\bullet}$; hence, inducing the delay in aniline degradation. Table 4.3 also summarizes the apparent rate constant and half-lives of the photodegradation of aniline as a function of initial concentration.

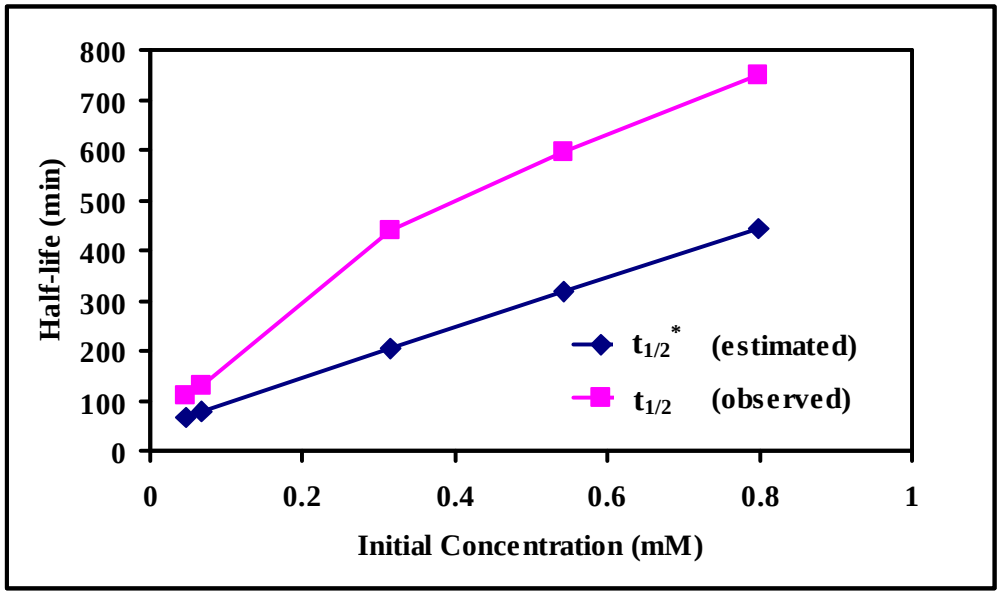

Figure 4.24 Half-life profile of observed and estimated on the different initial concentration of aniline.

4.5 Application of TiO_2/Visible Light in Water Treatment

This research could successfully remove aniline in aqueous phase by using the photocatalytic technology with TiO_2 radiated with visible light. This result also implies that this technique should be able to apply to treat other organic pollutants as well. The use of visible light could significantly reduce the treatment cost as compared to UV irradiation. However, it was found that the decomposition rate under the visible light irradiation was much lower than those of UV light. As a result, longer retention period is needed for visible light irradiation to achieve a comparable treatment level as in the case of UV irradiation. Economic consideration and comparison between these two light sources should be included in the decision step when applying in practice. One very promising application is to coat the visible light activated TiO_2 onto the surface of the open channel carrying raw water from natural water resource to the water treatment plant. By doing this, the micropollutants contaminated in the raw water such as humic acids and other trace organics will be removed when the sun light reaches the TiO_2-coated open channel walls serving as a pretreatment unit for the water treatment plant.

CHAPTER V

CONCLUSIONS

5.1 Conclusions

The present thesis brings new details regarding the aniline degradation in aqueous suspended TiO_2 under visible light irradiation and the following conclusions could be drawn from the results of this study:

- Synthetic TiO_2 crystal structure was dominated by anatase**.** The point of zero charge (pzc) of the synthetic TiO_2 was 3.5 and 3.2 according to the mass titration method and zeta potential method, respectively.

-Aniline was not transformed under direct photolysis and its volatilization could be neglected within the experimental period.

-The synthetic TiO_2 was able to be activated by the visible light (blue light was better than green, yellow, and red lights, sequentially) to generate the $OH^{\bullet}$ which further reacted with aniline whereas the commercial P-25 could not.

-The kinetics of aniline oxidation by the photo-catalytic reaction by TiO_2 under the blue light could be sufficiently explained by the Langmuir-Hinshelwood kinetic expression as follows:

$$-\frac{d[AN]}{dt} = \frac{k_r\, K\,[AN]_0}{1+K[AN]_0} = \frac{\left(9.96\times10^{-4}\right)(15.89)\,[AN]_0}{1+15.89\,[AN]_0}$$

5.2 Recommendations for Further Studies

-Investigation of photodegradation process behavior under a continuous operation.

-Identification of oxidation intermediates from aniline degradation by photodegradation process.

REFERENCE

Anotai, J., Lu, M.C., and Chewpreecha, P. 2006. Kinetics of aniline degradation by Fenton and electro-Fenton processes. Water Research. 40: 1841-1847.

Anpo, M., and Takeuchi, M. 2003. The design and development of highly reactive titanium oxide photocatalysts operating under visible light irradiation. Journal of Catalysis. 216: 505-516.

Brillas, E., Mur, E., Sauleda, R., Sanchez, L., Peral, J., Domenech, X., Casadi, J. 1998. Aniline mineralization by AOP's: anodic oxidation, photocatalysis, electro-Fenton and photoelectron-Fenton processes. Applied Catalysis B: Environmental. 16: 31-42

Baker, J.T. 2008. Aniline[online]. U.S.A.: Environmental Health & Safety. Available from: http://www.jtbaker.com/msds/englishhtml/a6660.htm[2008,-September 12]

Chan, Y.C., Chen, J.N., and Lu, M.C. 2001. Intermediate inhibition in the heterogeneous UV-catalysis using a TiO_2 suspension system. Chemosphere. 45: 29-35.

Chen, C.W., Dong, C.D., and Liao, Y.L. 2003. Photocatalytic degradation of 2,4-dichlorophenol in aqueous TiO_2 suspensions. Asian-Pacific Regional Conference on Practical Environmental Technologies. A2-55-A2-61.

Clark, J. 2004. Phenylamine as a primary amine[online]. Available from: http://www.chemguide.co.uk/organicprops/aniline/amine.html[2008, August 20]

Edwards, J., and Ormsby, D. 2006. Dissociation constants of organic bases in aqueous solution[online]. Available from: http://ifs.massey.ac.nz/resources/chemistry/dissociation/orgbases.htm#A [2008,-September 12]

Fujishima, A., Hashimoto, K., and Watanabe, T. 1999. TiO_2 Photocatalysis Fundamentals and Applications. Japan: BKC, Inc.

Fu, X., Zeltner, W A., and Anderson, M.A. 1996. Applications in photocatalytic purification of air. Stud. Surf. Sci. Catal. 103: 445-461.

Hewes, J. 2008. Light emitting diodes (LEDs)[online]. Available from: http://www.kpsec.freeuk.com/components/led.htm [2008, May 25]

Jain, R., and Shrivastava. M., 2008. Photocatalytic removal of hazardous dye cyanosine from industrial waste using titanium dioxide. Journal of Hazardous Materials.152: 216-220.

Karunakaran, C., Senthilvelan, S., and Karuthapandian, S. 2005. TiO_2-photocatalyzed oxidation of aniline. Journal of Photochemistry and Photobiology A: Chemistry. 172: 207-213.

Lettmann, C., Hildenbrand, K., Kisch, H., Macyk, W., and Maier, W.F. 2001. Visible light photodegradation of 4-chlorophenol with a coke-containing titanium dioxide photocatalyst. Applied Catalysis B: Environmental. 32: 215-227.

Lin Y.M., Tseng, Y.H., and Chen, C.C. 2006. USA patent. US0034752 A1.

Lin, Y.M., Tseng, Y.H., Huang, J.H., Chao, C.C., Chen, C.C., and Wang, I. 2006. Photocatalytic activity for degradation of nitrogen oxides over visible light responsive titania-based photocatalysts. Environmental Science & Technology. 40: 1616-1621.

Lu, M.C., Roam, G.D., Chen, J.N., and Huang, C.P. 1996. Adsorption characteristics of dichlorvos onto hydrous titanium dioxide surface. Water Research. 30: 1670-1676.

Lu, M.C., Roam, G.D., Chen, J.N., and Huang, C.P. 1993. Factors affecting the photocatalytic degradation of dichlorvos over titanium dioxide supported on glass. Journal of Photochemistry and Photobiology A: Chemistry. 76: 103-110.

Lu, M.C., Chen, J.N., and Chang, K.T. 1998. Effect of adsorbents coated with titanium dioxide on the photocatalytic degradation of propoxur. Chemosphere. 38: 617-627.

Oancea, P.,and Oncescu, T. 2008. The photocatalytic degradation of dichlorvos under solar irradiation. Journal of Photochemistry and Photobiology A: Chemistry. 199: 8-13.

Parsons, S. 2004. Advanced Oxidation Processes for Water and Wastewater Treatment. London: IWA Publishing.

Peterson, M. W., Turner, J.A., and Nozik, A.J. 1991. Mechanistic studies of the photocatalytic behavior of TiO_2 particles in a photoelectrochemical slurry and the relevance to photodetoxification reactions. Journal of Physical Chemistry. 95: 221.

Reymond, J.P., and Kolenda, F. 1999. Estimantion of the point of zero charge of simple and mixed oxides by mass titration. Powder Technology. 103: 30-36.

Sanchez, L., Peral, J., and Domenech, X. 1998. Aniline degradation by combined photocatalysis and ozonation. Applied Catalysis B: Environmental. 19: 59-65.

Smyth, J.,R. 1997. Mineral structure and property data TiO_2 group[Online]. University of Colorado. Available from: http://ruby.colorado.edu/~smyth/min/tio2.html[2008, August 12]

Solar, S., Solar, W., and Getoff, N. 1986. Resolved multisite OH-attack on aqueous aniline studied by pulse radiolysis. International Journal of Radiation Applications and Instrumentation. 28: 229-234.

Son, H.S., Lee, S.J., Cho, I.H., and Zoh, K.D. 2004. Kinetic and mechanism of TNT degradation in TiO_2 photocatalysis. Chemosphere. 57: 309-317.

Tanaka, K., Luesaiwong, W., and Hisanaga, T. 1997. Photocatalytic degradation of mono-, di- and trinitrophenol in aqueous TiO_2 suspension. Journal of Molecular Catalysis A: Chemical. 122: 67-74.

Thounaojam, S.S., Shridhar, P.G., Madhava, R., Hari, M., and Jai, P.M. 2001. Radiation chemical oxidation of aniline derivatives. Journal of the Chemical Society, Perkin. Transactions 2: 1205-1211.

Turchi, C.S., and Ollis, D.F. 1990. Photocatalytic degradation of organic water contaminants: mechanisms involving hydroxyl radical attack. Journal of Catalysis. 122: 178.

Wikipedia. 2008. Aniline[Online]. Available from: http://en.wikipedia.org/wiki/Aniline[2008, September 15]

Wikipedia. 2008. LED lamp[Online]. Available from: http://en.wikipedia.org/wiki/LED_lamp[2008, May 25]

Yamashita, H., and Anpo, M. 2004. Application of an ion beam technique for the design of visible light-sensitive, highly efficient and highly selective photocatalysts: ion-implantation and ionized cluster beam methods. Catalysis Survey from Asia. 8: 35-45.

Zhang, X., Wu, F., Wu, X.W., Chen, P., and Deng, N. 2008. Photodegradation of acetaminophen in TiO_2 suspended solution. Journal of Hazardous Materials 157: 300-307.

APPENDICES

APPENDIX A

Experimental Setup

Figure A.1 Reactor Setup (one lamp).

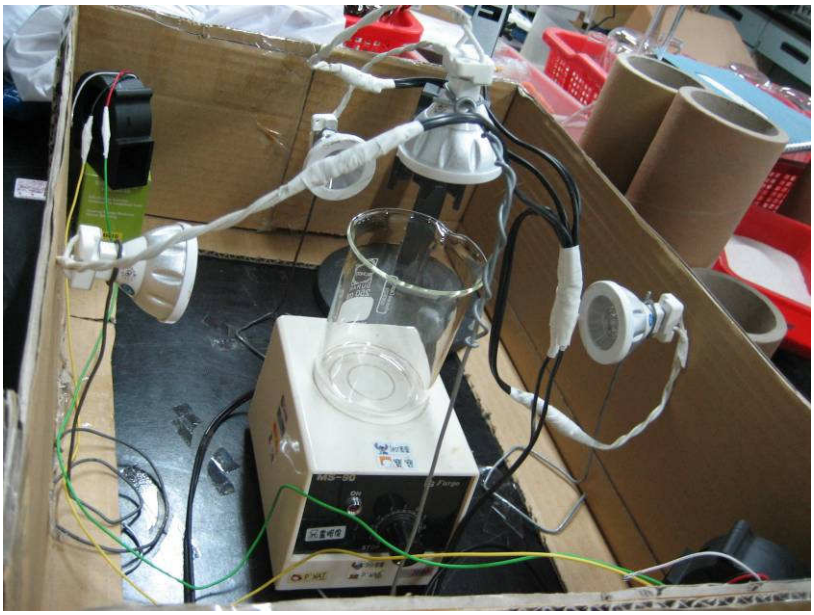

Figure A.2 Reactor Setup (four lamps).

Figure A.3 The color of synthetic TiO_2 at different temperature.

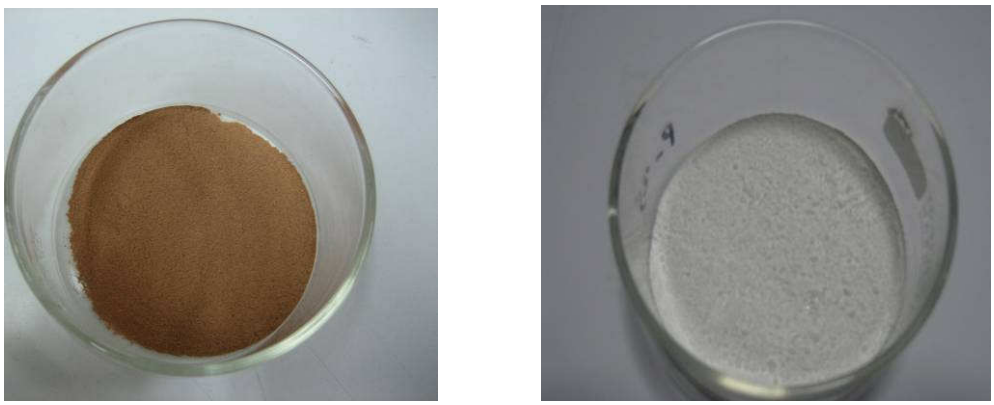

Figure A.4 Color comparison between synthetic TiO_2 and Commercial P-25.

APPENDIX B

Experimental Data

Table B.1 Aniline photocatalysis by the synthetic and commercial TiO_2.

Time (min)	Aniline Remaining			
	Synthetic TiO_2		Commercial P-25	
	mM	C/C_0	mM	C/C_0
0	1.257	1.000	1.090	1.000
30	0.9927	0.7900	0.9290	0.8520
60	0.9529	0.7583	0.9368	0.8591
90	0.9318	0.7415	0.9022	0.8274
120	0.8838	0.7033	0.8992	0.8246
150	0.8796	0.7000	0.8911	0.8172
180	0.8613	0.6855	0.9283	0.8514

Note: 1 mM of aniline, TiO_2 1 g L^{-1}, pH 7±0.1, temperature at 30±0.5 °C, blue light 3 watt, using nitric acid and ethanol for TiO_2 synthesis.

Table B.2 Direct photolysis of aniline under various light wavelength.

Time (min)	Aniline Remaining (photolysis)							
	Blue Light		Green Light		Yellow Light		Red Light	
	mM	C/C_0	mM	C/C_0	mM	C/C_0	mM	C/C_0
0	0.8885	1.000	1.077	1.000	1.219	1.000	1.084	1.000
30	0.8568	0.9644	1.073	0.8362	1.217	0.8837	1.077	0.8668
60	0.8694	0.9785	1.045	0.8292	1.177	0.8353	1.093	0.8636
90	0.8740	0.9837	1.055	0.7999	1.231	0.8404	1.067	0.8552
120	0.8514	0.9582	1.062	0.8103	1.233	0.8235	1.036	0.8490
150	0.8761	0.9860	1.066	0.7874	1.205	0.8282	1.061	0.8176
180	0.8641	0.9725	1.055	0.7449	1.183	0.8099	1.088	0.8168

Note: 1 mM of aniline, pH 7±0.1, temperature at 30±0.5 °C, no TiO_2.

Table B.3 Photocatalysis of aniline with synthetic TiO_2 under various light wavelengths.

Time (min)	Aniline Remaining							
	Blue Light		Green Light		Yellow Light		Red Light	
	mM	C/C_0	mM	C/C_0	mM	C/C_0	mM	C/C_0
0	1.257	1.000	0.8034	1.000	1.228	1.000	0.9269	1.000
30	0.9927	0.7900	0.6718	0.8362	1.085	0.8837	0.8035	0.8668
60	0.9529	0.7583	0.6662	0.8292	1.025	0.8353	0.8005	0.8636
90	0.9318	0.7415	0.6426	0.7999	1.032	0.8404	0.7927	0.8552
120	0.8838	0.7033	0.6509	0.8103	1.011	0.8235	0.7870	0.8490
150	0.8796	0.7000	0.6325	0.7874	1.017	0.8282	0.7578	0.8176
180	0.8613	0.6855	0.5984	0.7449	0.9941	0.8099	0.7571	0.8168

Note: 1 mM of aniline, TiO_2 1 g L^{-1}, pH 7±0.1, temperature at 30±0.5 °C, using nitric acid and ethanol for TiO_2 synthesis.

Table B.4 Aniline adsorption onto the synthetic TiO_2.

Time (min)	Aniline Remaining	
	mM	**C/C_0**
0	0.9593	1.000
1	0.8070	0.8413
2	0.8238	0.8587
3	0.8286	0.8637
4	0.8067	0.8409
5	0.8157	0.8503
6	0.8070	0.8412
7	0.8087	0.8430
8	0.8007	0.8346
9	0.7638	0.7962
10	0.8345	0.8699
15	0.7845	0.8148
30	0.8216	0.8565
60	0.8469	0.8828
90	0.8642	0.9009
120	0.8423	0.8780
150	0.8523	0.8884
180	0.8477	0.8837

Note: 1 mM of aniline, TiO_2 1 g L^{-1}, pH 7±0.1, temperature at 30±0.5 °C, no light, using nitric acid and ethanol for TiO_2 synthesis.

Table B.5 Effect of alcohol and acid types on aniline oxidation by TiO_2 photocatalysis.

Time (min)	Aniline Remaining							
	Acetic acid & Methanol		Acetic acid & Ethanol		Nitric acid & Methanol		Nitric acid & Ethanol	
	mM	C/C_0	mM	C/C_0	mM	C/C_0	mM	C/C_0
0	0.7580	1.000	0.7514	1.000	0.6880	1.000	0.7956	1.000
30	0.7414	0.9781	0.6954	0.9255	fail	fail	0.7558	0.9500
60	0.7523	0.9925	0.7024	0.9347	0.6707	0.9749	0.7507	0.9435
90	0.7364	0.9714	0.7122	0.9479	fail	fail	0.7396	0.9296
120	0.7324	0.9662	0.6990	0.9303	0.6653	0.9670	0.7236	0.9095
150	0.7198	0.9496	0.6783	0.9027	0.6644	0.9657	0.7114	0.8941
180	0.7047	0.9297	0.6686	0.8898	0.6399	0.9301	0.7011	0.8812

Note: 1 mM of aniline, TiO_2 1 g L^{-1}, pH 7±0.1, temperature at 30±0.5 °C, blue light 3 watt.

Table B.6 Effect of calcinations temperature on aniline oxidation by TiO_2 photocatalysis.

Time (min)	Aniline Remaining					
	150°C		200°C		300°C	
	mM	C/C_0	mM	C/C_0	mM	C/C_0
0	0.6955	1.000	0.7956	1.000	0.7130	1.000
30	0.7037	1.0118	0.7558	0.9499	0.7330	1.0281
60	0.6985	1.0042	0.7507	0.9435	0.7036	0.9868
90	0.6623	0.9522	0.7396	0.9296	0.6771	0.9497
120	0.6544	0.9408	0.7236	0.9095	0.6927	0.9716

Note: 1 mM of aniline, TiO_2 1 g L^{-1}, pH 7±0.1, temperature at 30±0.5 °C, blue light 3 watt, using nitric acid and ethanol for TiO_2 synthesis.

Table B.7 Effect of light position on aniline oxidation by TiO_2 photocatalysis.

Time (min)	Aniline Remaining			
	Light around the reactor		Light on the reactor	
	mM	C/C_0	mM	C/C_0
0	0.8270	1.000	0.7956	1.000
30	0.7468	0.9031	0.7558	0.9499
60	0.7355	0.8893	0.7507	0.9435
90	0.7145	0.8640	0.7396	0.9296
120	0.7133	0.8625	0.7236	0.9095
150	0.7034	0.8505	0.7114	0.8941
180	0.6508	0.7869	0.7011	0.8812

Note: 1 mM of aniline, TiO_2 1 g L^{-1}, pH 7±0.1, temperature at 30±0.5 °C, blue light 3 watt, using nitric acid and ethanol for TiO_2 synthesis.

Table B.8 Effect of light power on aniline oxidation by TiO_2 photocatalysis.

Time (min)	Aniline Remaining							
	1 lamp		2 lamps		3 lamps		4 lamps	
	mM	C/C_0	mM	C/C_0	mM	C/C_0	mM	C/C_0
0	0.7956	1.000	0.7612	1.000	0.7851	1.000	0.8270	1.000
30	0.7558	0.9499	0.7333	0.9634	0.7315	0.9318	0.7468	0.9031
60	0.7507	0.9435	0.6866	0.9020	0.7100	0.9044	0.7355	0.8893
90	0.7396	0.9296	0.6654	0.8741	0.6808	0.8671	0.7145	0.8640
120	0.7236	0.9095	0.6605	0.8677	0.6509	0.8290	0.7133	0.8625
150	0.7114	0.8941	0.6406	0.8415	0.6245	0.7954	fail	fail
180	0.7011	0.8812	0.6285	0.8256	0.5928	0.7551	0.6508	0.7869

Note: 1 mM of aniline, TiO_2 1 g L^{-1}, pH 7±0.1, temperature at 30±0.5 °C, blue light 3 watt, using nitric acid and ethanol for TiO_2 synthesis.

Table B.9 Effect of light distance on aniline oxidation by TiO_2 photocatalysis.

Time (min)	Aniline Remaining			
	5 cm		10 cm	
	mM	C/C_0	mM	C/C_0
0	0.8093	1.000	0.7956	1.000
30	0.7490	0.9254	0.7558	0.9499
60	fail	fail	0.7507	0.9435
90	0.7295	0.9013	0.7396	0.9296
120	0.7019	0.8672	0.7236	0.9095
150	0.6880	0.8501	0.7114	0.8941
180	0.6868	0.8486	0.7011	0.8812

Note: 1 mM of aniline, TiO_2 1 g L^{-1}, pH 7±0.1, temperature at 30±0.5 °C, blue light 3 watt, using nitric acid and ethanol for TiO_2 synthesis.

Table B.10 Point of zero charge determination using the mass titration method.

Mass Titration Method	
TiO_2 (%)	**pH**
0.01	4.885
0.1	4.225
1	3.715
5	3.515
10	3.485
20	3.490
30	3.515
40	3.545

Note: Temperature at 30±0.5 °C, 100 rpm, using nitric acid and ethanol for TiO_2 synthesis.

Table B.11 Point of zero charge determination using the zeta potential method.

Zeta Potential Method	
pH	**pzc**
12	-32.9667
11	-33.6667
10	-34.5333
9	-27.8667
8	-33.6333
7	-25.1667
6	-24.6667
5	-23.5667
4	-9.67667
3	2.96333
2	15.7667

Note: Using nitric acid and ethanol for TiO_2 synthesis.

Table B.12 Effect of pH on aniline adsorption by TiO_2.

Time (min)	Aniline Remaining (adsorption Aniline & TiO_2)					
	pH 4		pH 7		pH 10	
	mM	C/C_0	mM	C/C_0	mM	C/C_0
0	0.05391	1.000	0.04606	1.000	0.04579	1.000
5	0.05185	0.9619	0.03928	0.8528	0.03992	0.8719
10	0.05172	0.9594	0.03926	0.8523	0.03913	0.8547
15	0.05245	0.9729	0.03917	0.8503	0.03866	0.8442
30	0.05332	0.9891	0.03861	0.8382	0.03896	0.8508
60	0.05110	0.9479	0.03831	0.8318	0.03929	0.8581

Note: 0.05 mM of aniline, TiO_2 1 g L^{-1}, temperature at 30±0.5 °C, no light, using nitric acid and ethanol for TiO_2 synthesis.

Table B.13 Effect of pH on aniline oxidation by TiO_2 photocatalysis.

Time (min)	Aniline Remaining					
	pH 4		pH 7		pH 10	
	mM	C/C_0	mM	C/C_0	mM	C/C_0
0	0.04772	1.000	0.04668	1.000	0.04270	1.000
30	0.03590	0.7523	0.03879	0.8309	0.03760	0.8807
60	0.03105	0.6507	0.02803	0.6005	0.03370	0.7893
120	0.02329	0.4880	0.02315	0.4960	0.03011	0.7052
180	0.01735	0.3635	0.01757	0.3764	0.02716	0.6362
240	0.01387	0.2907	0.01439	0.3082	0.02484	0.5819

Note: 0.05 mM of aniline, TiO_2 1 g L^{-1}, temperature at 30±0.5 °C, blue light 3 watt, using nitric acid and ethanol for TiO_2 synthesis.

Table B.14 Effect of aniline initial concentration on aniline oxidation by TiO_2 photocatalysis.

Time (min)	Aniline Remaining									
	0.047 mM		0.067 mM		0.32 mM		0.54 mM		0.80 mM	
	mM	C/C_0	mM	C/C_0	mM	C/C_0	mM	C/C_0	mM	C/C_0
0	0.04668	1.000	0.06733	1.000	0.3152	1.000	0.5425	1.000	0.7976	1.000
30	0.03879	0.8309	0.05098	0.7572	0.2871	0.9109	0.5032	0.9276	0.7705	0.9660
60	0.02803	0.6005	0.04205	0.6245	0.2648	0.8402	0.4835	0.8912	0.7445	0.9334
120	0.02315	0.4960	0.03411	0.5066	0.2264	0.7184	0.4290	0.7908	0.6373	0.7990
180	0.01757	0.3764	0.03087	0.4585	0.2360	0.7487	0.4293	0.7913	0.6705	0.8406
240	0.01439	0.3082	0.02802	0.4162	0.2155	0.6837	0.3985	0.7345	0.6107	0.7656

Note: TiO_2 1 g L^{-1}, pH 7±0.1, temperature at 30±0.5 °C, blue light 3 watt, using nitric acid and ethanol for TiO_2 synthesis.

Table B.15 R^2 values for kinetic determination using various reaction orders.

Aniline	R^2		
	Zero order	First order	Second order
0.047	0.8923	0.9670	0.9928
0.067	0.8084	0.8917	0.8602
0.32	0.8399	0.8572	0.8704
0.54	0.9129	0.9278	0.9397
0.80	0.8625	0.8620	0.8602

Table B.16 Particle size distribution of synthetic TiO_2 (wet measurement).

Size (µm)	Volume (%)	Size (µm)	Volume (%)	Size (µm)	Volume (%)	Size (µm)	Volume (%)
0.010	0.00	0.316	0.01	10.000	0.29	316.228	0.14
0.011	0.00	0.363	0.08	11.482	0.49	363.078	0.02
0.013	0.00	0.417	0.16	13.183	0.79	416.869	0.00
0.015	0.00	0.479	0.22	15.136	1.23	478.630	0.00
0.017	0.00	0.550	0.26	17.378	1.78	549.541	0.00
0.020	0.00	0.631	0.28	19.953	2.48	630.957	0.00
0.023	0.00	0.724	0.27	22.909	3.29	724.436	0.00
0.026	0.00	0.832	0.25	26.303	4.18	831.764	0.00
0.030	0.00	0.955	0.21	30.200	5.09	954.993	0.00
0.035	0.00	1.096	0.16	34.674	5.98	1096.478	0.00
0.040	0.00	1.259	0.11	39.811	6.77	1258.925	0.00
0.046	0.00	1.445	0.08	45.709	7.38	1445.440	0.00
0.052	0.00	1.660	0.05	52.481	7.35	1659.587	0.00
0.060	0.00	1.905	0.00	60.256	7.85	1905.461	0.00
0.069	0.00	2.188	0.00	69.183	7.66	2187.762	0.00
0.079	0.00	2.512	0.06	79.433	7.19	2511.886	0.00
0.091	0.00	2.884	0.07	91.201	6.47	2884.032	0.00
0.105	0.00	3.311	0.07	104.713	5.58	3311.311	0.00
0.120	0.00	3.802	0.07	120.226	4.58	3801.894	0.00
0.138	0.00	4.365	0.07	138.038	3.75	4365.158	0.00
0.158	0.00	5.012	0.07	158.489	2.62	5011.872	0.00
0.182	0.00	5.754	0.07	181.970	1.79	5754.399	0.00
0.209	0.00	6.607	0.08	208.930	1.13	6606.934	0.00
0.240	0.00	7.586	0.10	239.883	0.64	7585.776	0.00
0.275	0.00	8.710	0.17	275.423	0.32	8709.636	0.00
						10000.00	0.00

Note: Dispersion medium: water, Stirrer 2975 rpm, using nitric acid and ethanol for TiO_2 synthesis.

Table B.17 Particle size distribution of Commercial P-25 (wet measurement).

Size (µm)	Volume (%)	Size (µm)	Volume (%)	Size (µm)	Volume (%)	Size (µm)	Volume (%)
0.010	0.00	0.316	7.78	10.000	0.55	316.228	0.00
0.011	0.00	0.363	5.49	11.482	0.44	363.078	0.00
0.013	0.00	0.417	3.50	13.183	0.32	416.869	0.00
0.015	0.00	0.479	1.84	15.136	0.22	478.630	0.00
0.017	0.00	0.550	0.60	17.378	0.13	549.541	0.00
0.020	0.00	0.631	0.03	19.953	0.08	630.957	0.00
0.023	0.00	0.724	0.00	22.909	0.02	724.436	0.00
0.026	0.00	0.832	0.21	26.303	0.00	831.764	0.00
0.030	0.00	0.955	0.86	30.200	0.00	954.993	0.00
0.035	0.00	1.096	1.53	34.674	0.00	1096.478	0.00
0.040	0.00	1.259	2.08	39.811	0.00	1258.925	0.00
0.046	0.00	1.445	2.40	45.709	0.00	1445.440	0.00
0.052	0.00	1.660	2.46	52.481	0.00	1659.587	0.00
0.060	0.00	1.905	2.33	60.256	0.00	1905.461	0.00
0.069	0.00	2.188	2.08	69.183	0.00	2187.762	0.00
0.079	0.00	2.512	1.76	79.433	0.00	2511.886	0.00
0.091	0.00	2.884	1.43	91.201	0.00	2884.032	0.00
0.105	0.00	3.311	1.13	104.713	0.00	3311.311	0.00
0.120	0.00	3.802	0.90	120.226	0.00	3801.894	0.00
0.138	2.55	4.365	0.76	138.038	0.00	4365.158	0.00
0.158	7.85	5.012	0.69	158.489	0.00	5011.872	0.00
0.182	11.00	5.754	0.68	181.970	0.00	5754.399	0.00
0.209	12.37	6.607	0.69	208.930	0.00	6606.934	0.00
0.240	11.84	7.586	0.68	239.883	0.00	7585.776	0.00
0.275	10.08	8.710	0.64	275.423	0.00	8709.636	0.00
						10000.00	0.00

Note: Dispersion medium: water, Stirrer 2975 rpm**.**

Table B.18 Particle size distribution of synthetic TiO_2 (dry measurement).

Size (µm)	Volume (%)	Size (µm)	Volume (%)	Size (µm)	Volume (%)	Size (µm)	Volume (%)
0.010	0.00	0.316	0.00	10.000	1.61	316.228	0.00
0.011	0.00	0.363	0.00	11.482	1.94	363.078	0.00
0.013	0.00	0.417	0.00	13.183	2.23	416.869	0.00
0.015	0.00	0.479	0.00	15.136	2.80	478.630	0.00
0.017	0.00	0.550	0.00	17.378	3.33	549.541	0.02
0.020	0.00	0.631	0.00	19.953	3.92	630.957	0.10
0.023	0.00	0.724	0.07	22.909	4.53	724.436	0.31
0.026	0.00	0.832	0.16	26.303	5.13	831.764	0.66
0.030	0.00	0.955	0.24	30.200	5.67	954.993	1.03
0.035	0.00	1.096	0.29	34.674	6.12	1096.478	1.25
0.040	0.00	1.259	0.32	39.811	6.40	1258.925	1.17
0.046	0.00	1.445	0.33	45.709	6.49	1445.440	0.83
0.052	0.00	1.660	0.34	52.481	6.34	1659.587	0.44
0.060	0.00	1.905	0.34	60.256	5.95	1905.461	0.10
0.069	0.00	2.188	0.34	69.183	5.33	2187.762	0.02
0.079	0.00	2.512	0.35	79.433	4.55	2511.886	0.00
0.091	0.00	2.884	0.38	91.201	3.69	2884.032	0.00
0.105	0.00	3.311	0.43	104.713	2.84	3311.311	0.00
0.120	0.00	3.802	0.50	120.226	2.08	3801.894	0.00
0.138	0.00	4.365	0.58	138.038	1.44	4365.158	0.00
0.158	0.00	5.012	0.69	158.489	0.95	5011.872	0.00
0.182	0.00	5.754	0.82	181.970	0.58	5754.399	0.00
0.209	0.00	6.607	0.97	208.930	0.31	6606.934	0.00
0.240	0.00	7.586	1.14	239.883	0.11	7585.776	0.00
0.275	0.00	8.710	1.36	275.423	0.00	8709.636	0.00
						10000.00	0.00

Note: Dispersive air pressure 4 bar, using nitric acid and ethanol for TiO_2 synthesis.

Table B.19 Particle size distribution of Commercial P-25 (dry measurement).

Size (µm)	Volume (%)	Size (µm)	Volume (%)	Size (µm)	Volume (%)	Size (µm)	Volume (%)
0.010	0.00	0.316	0.29	10.000	4.00	316.228	0.00
0.011	0.00	0.363	0.42	11.482	2.85	363.078	0.00
0.013	0.00	0.417	0.62	13.183	1.76	416.869	0.00
0.015	0.00	0.479	0.86	15.136	0.64	478.630	0.00
0.017	0.00	0.550	1.13	17.378	0.03	549.541	0.00
0.020	0.00	0.631	1.45	19.953	0.00	630.957	0.00
0.023	0.00	0.724	1.78	22.909	0.00	724.436	0.00
0.026	0.00	0.832	2.14	26.303	0.00	831.764	0.00
0.030	0.00	0.955	2.49	30.200	0.00	954.993	0.00
0.035	0.00	1.096	2.83	34.674	0.00	1096.478	0.00
0.040	0.00	1.259	3.15	39.811	0.00	1258.925	0.00
0.046	0.00	1.445	3.45	45.709	0.00	1445.440	0.00
0.052	0.00	1.660	3.74	52.481	0.00	1659.587	0.00
0.060	0.00	1.905	4.02	60.256	0.00	1905.461	0.00
0.069	0.00	2.188	4.33	69.183	0.00	2187.762	0.00
0.079	0.00	2.512	4.66	79.433	0.00	2511.886	0.00
0.091	0.00	2.884	5.04	91.201	0.00	2884.032	0.00
0.105	0.00	3.311	5.46	104.713	0.00	3311.311	0.00
0.120	0.00	3.802	5.90	120.226	0.00	3801.894	0.00
0.138	0.00	4.365	6.28	138.038	0.00	4365.158	0.00
0.158	0.00	5.012	6.55	158.489	0.00	5011.872	0.00
0.182	0.00	5.754	6.61	181.970	0.00	5754.399	0.00
0.209	0.00	6.607	6.39	208.930	0.00	6606.934	0.00
0.240	0.07	7.586	5.86	239.883	0.00	7585.776	0.00
0.275	0.19	8.710	5.03	275.423	0.00	8709.636	0.00
						10000.00	0.00

Note: Dispersive air pressure 4 bar.

APPENDIX C

Experimental Figures

C.1 Aniline removal by adsorption, direct photolysis, and photocatalysis.

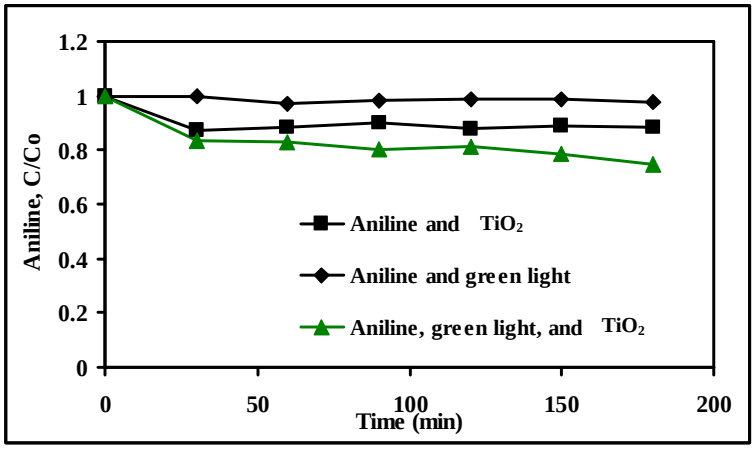

(a) Green light.

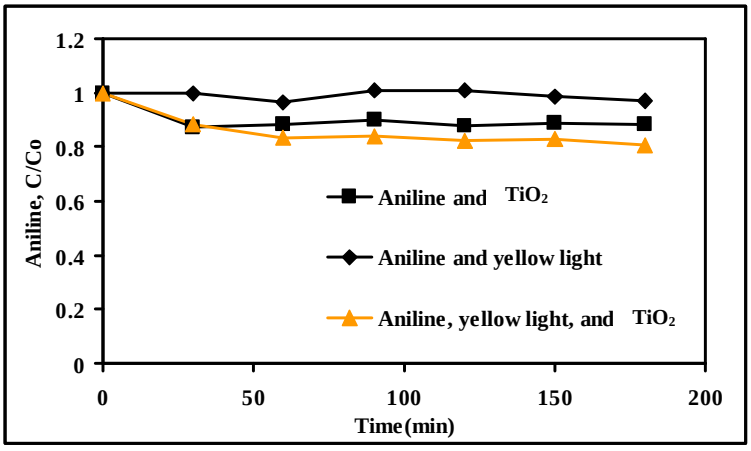

(b) Yellow light.

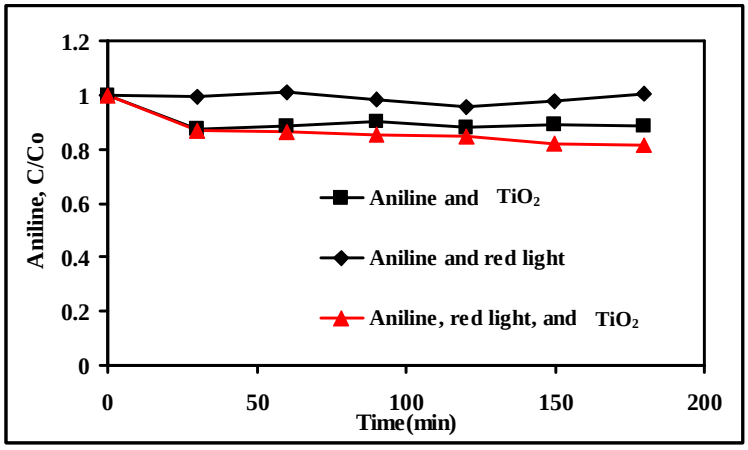

(c) Red light.

Note: 1 mM of aniline TiO_2 1 g L^{-1}, pH 7±0.1, temperature at 30±0.5 °C, blue light 3 watt, using nitric acid and ethanol for TiO_2 synthesis**.**

C.2 Kinetics Determination of effect of aniline concentration.

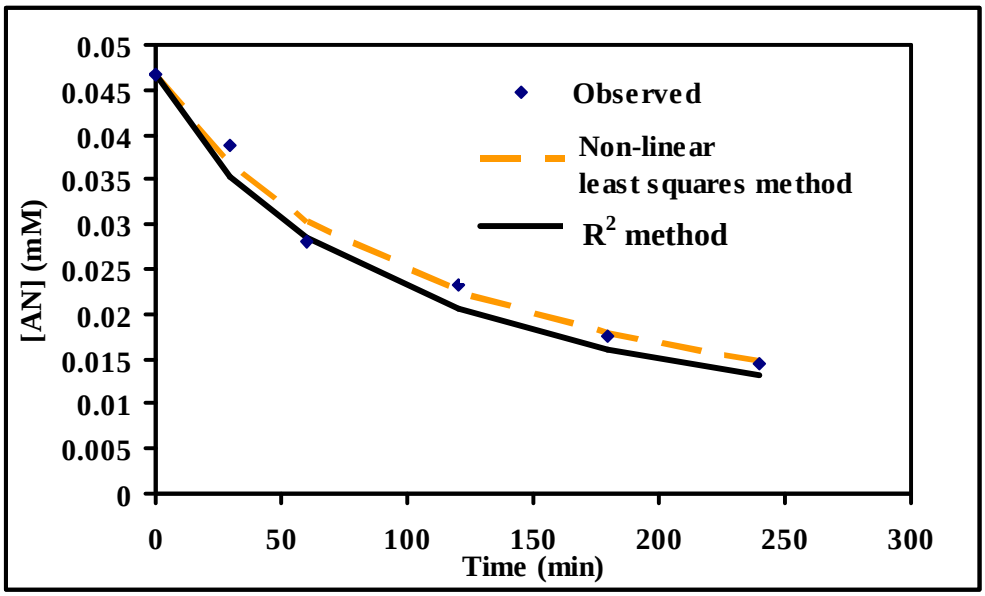

Figure C.4 Data fitting using non-linear least squares and linearized methods for the experiment with initial aniline of 0.047 mM (experimental condition: TiO_2 1 g L^{-1}, pH 7±0.1, temperature at 30±0.5 °C, blue light 3 watt, using nitric acid and ethanol for TiO_2 synthesis)**.**

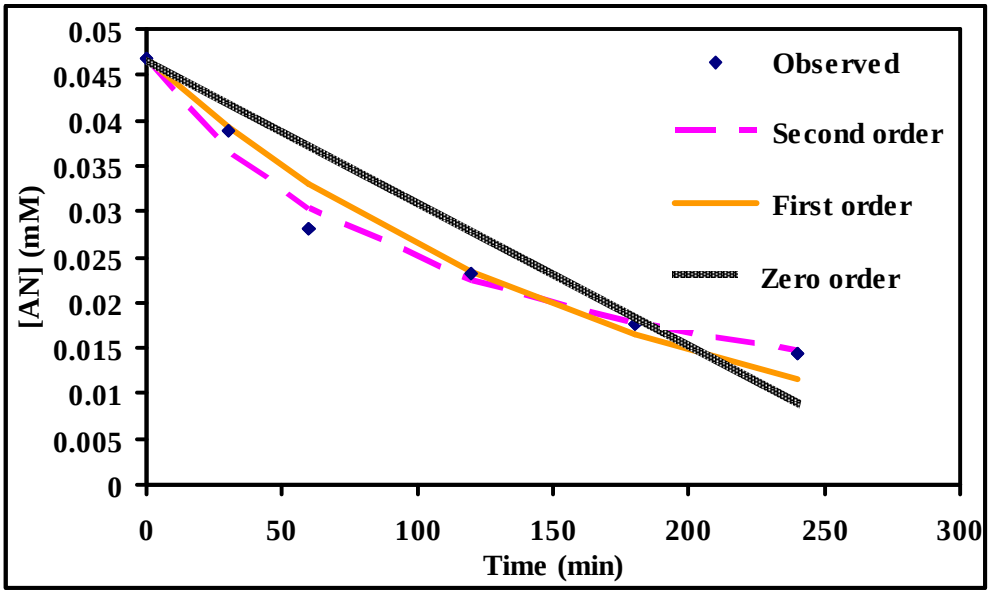

Figure C.5 Data fitting using zero, first, and second order for the experiment with initial aniline of 0.047 mM (experimental condition: TiO_2 1 g L^{-1}, pH 7±0.1, temperature at 30±0.5 °C, blue light 3 watt, using nitric acid and ethanol for TiO_2 synthesis)**.**

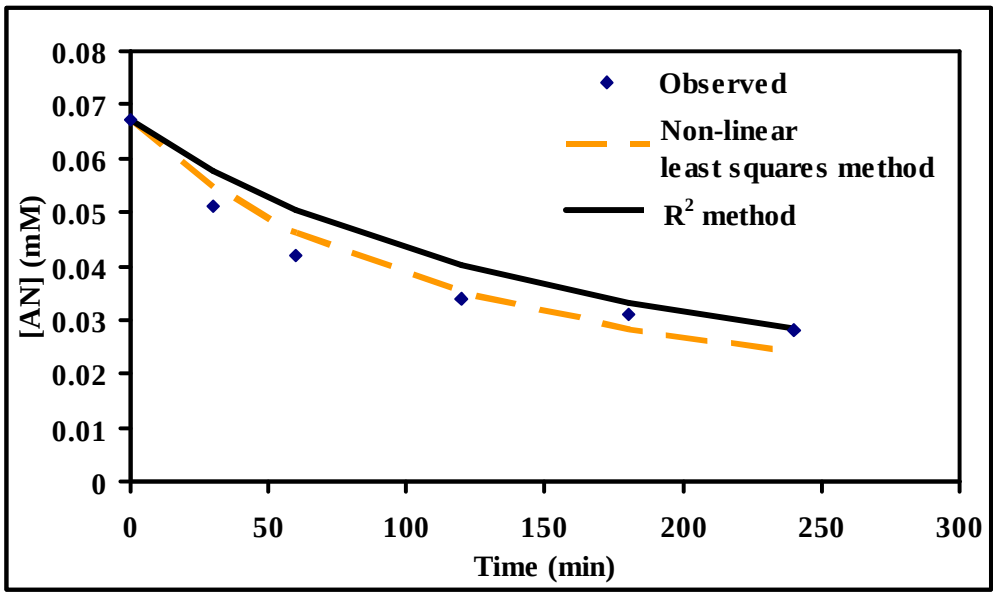

Figure C.6 Data fitting using non-linear least squares and linearized methods for the experiment with initial aniline of 0.067 mM (experimental condition: TiO_2 1 g L^{-1}, pH 7±0.1, temperature at 30±0.5 °C, blue light 3 watt, using nitric acid and ethanol for TiO_2 synthesis)**.**

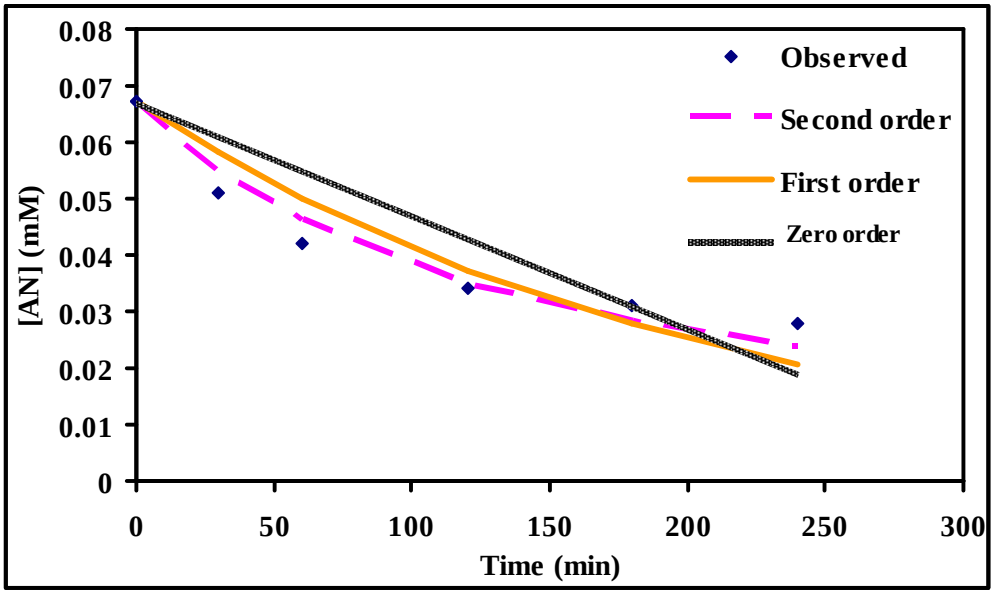

Figure C.7 Data fitting using zero, first, and second order for the experiment with initial aniline of 0.067 mM (experimental condition: TiO_2 1 g L^{-1}, pH 7±0.1, temperature at 30±0.5 °C, blue light 3 watt, using nitric acid and ethanol for TiO_2 synthesis)**.**

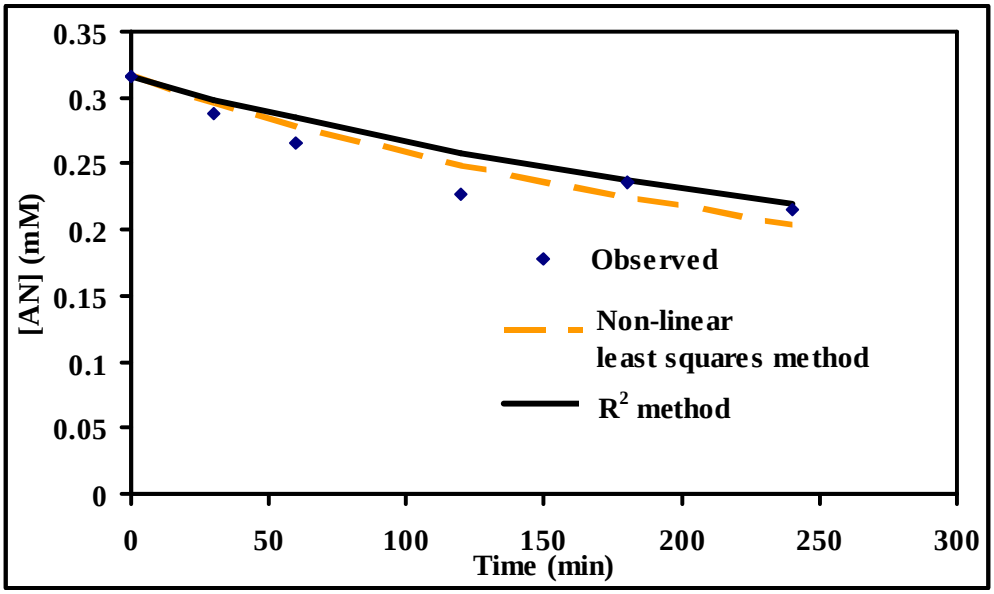

Figure C.8 Data fitting using non-linear least squares and linearized methods for the experiment with initial aniline of 0.32 mM (experimental condition: TiO_2 1 g L^{-1}, pH 7±0.1, temperature at 30±0.5 °C, blue light 3 watt, using nitric acid and ethanol for TiO_2 synthesis)**.**

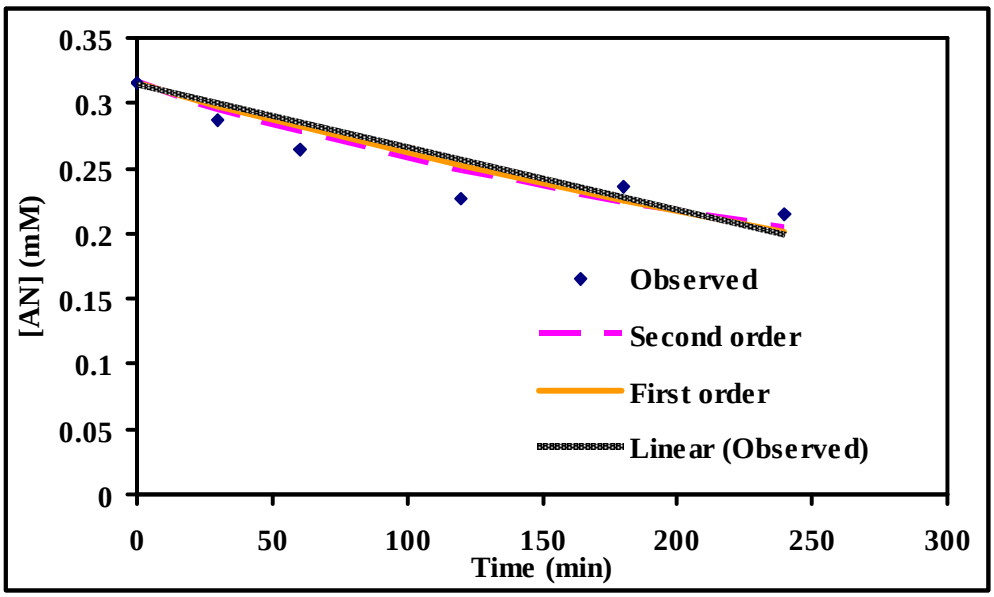

Figure C.9 Data fitting using zero, first, and second order for the experiment with initial aniline of 0.32 mM (experimental condition: TiO_2 1 g L^{-1}, pH 7±0.1, temperature at 30±0.5 °C, blue light 3 watt, using nitric acid and ethanol for TiO_2 synthesis)**.**

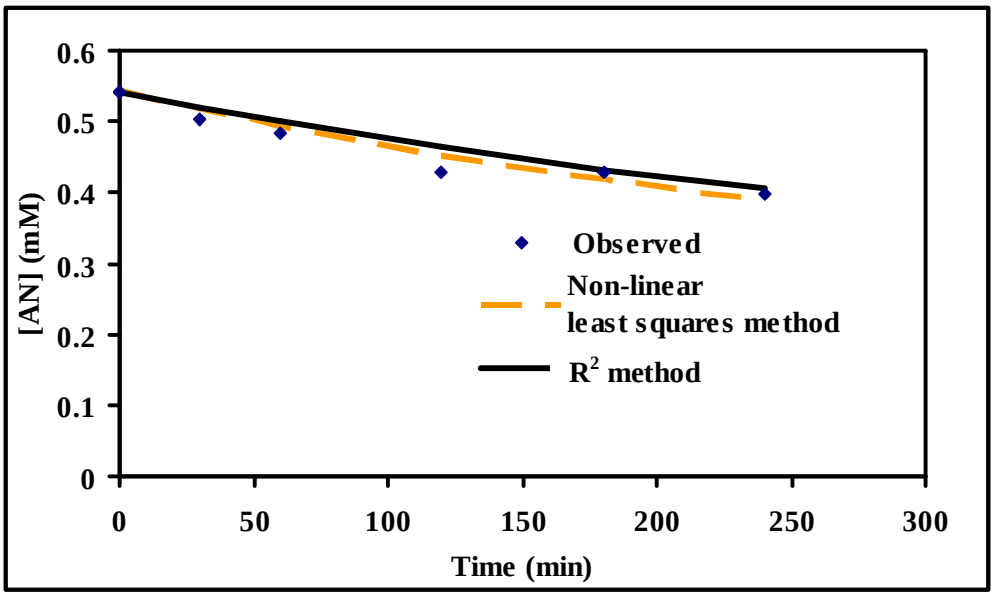

Figure C.10 Data fitting using non-linear least squares and linearized methods for the experiment with initial aniline of 0.54 mM (experimental condition: TiO_2 1 g L^{-1}, pH 7±0.1, temperature at 30±0.5 °C, blue light 3 watt, using nitric acid and ethanol for TiO_2 synthesis)**.**

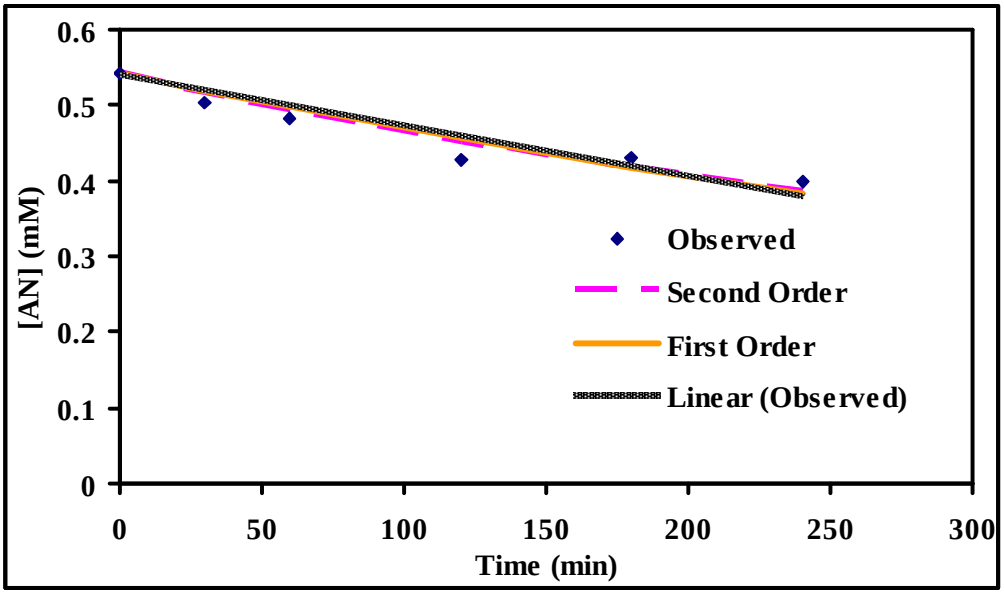

Figure C.11 Data fitting using zero, first, and second order for the experiment with initial aniline of 0.54 mM (experimental condition: TiO_2 1 g L^{-1}, pH 7±0.1, temperature at 30±0.5 °C, blue light 3 watt, using nitric acid and ethanol for TiO_2 synthesis)**.**

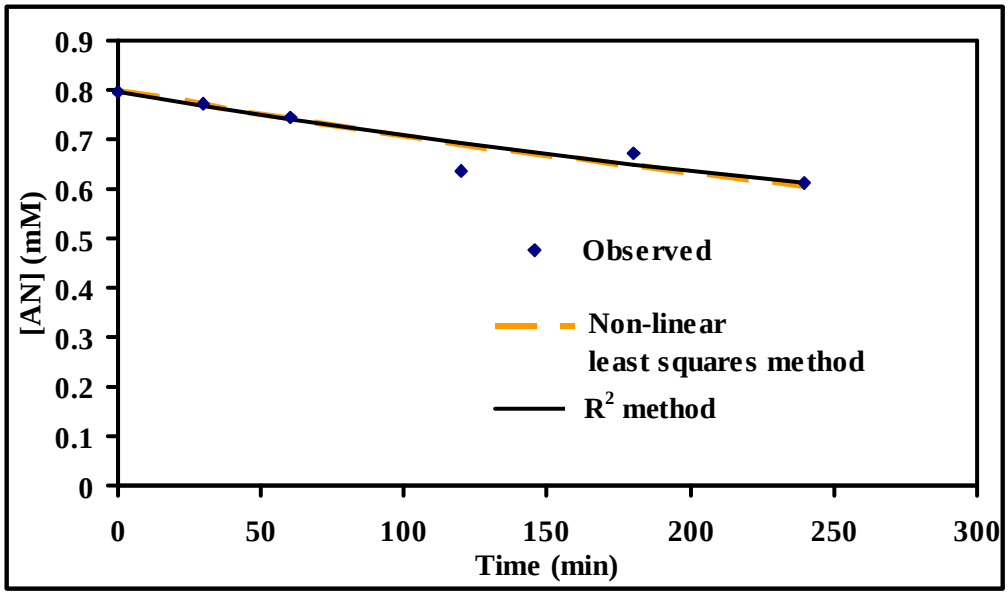

Figure C.12 Data fitting using non-linear least squares and linearized methods for the experiment with initial aniline of 0.80 mM (experimental condition: TiO_2 1 g L^{-1}, pH 7±0.1, temperature at 30±0.5 °C, blue light 3 watt, using nitric acid and ethanol for TiO_2 synthesis)**.**

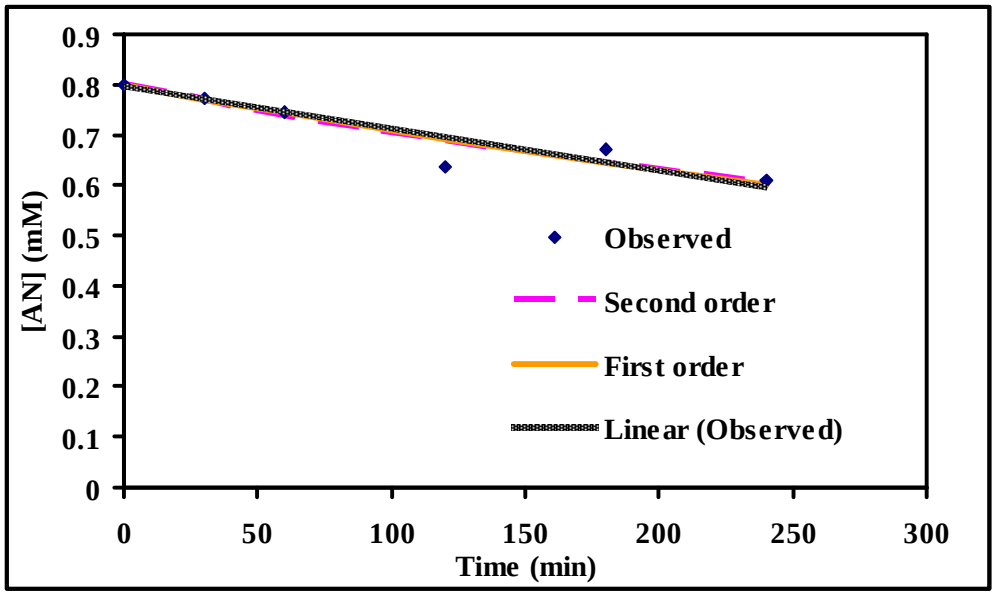

Figure C.13 Data fitting using zero, first, and second order for the experiment with initial aniline of 0.80 mM (experimental condition: TiO_2 1 g L^{-1}, pH 7±0.1, temperature at 30±0.5 °C, blue light 3 watt, using nitric acid and ethanol for TiO_2 synthesis)**.**

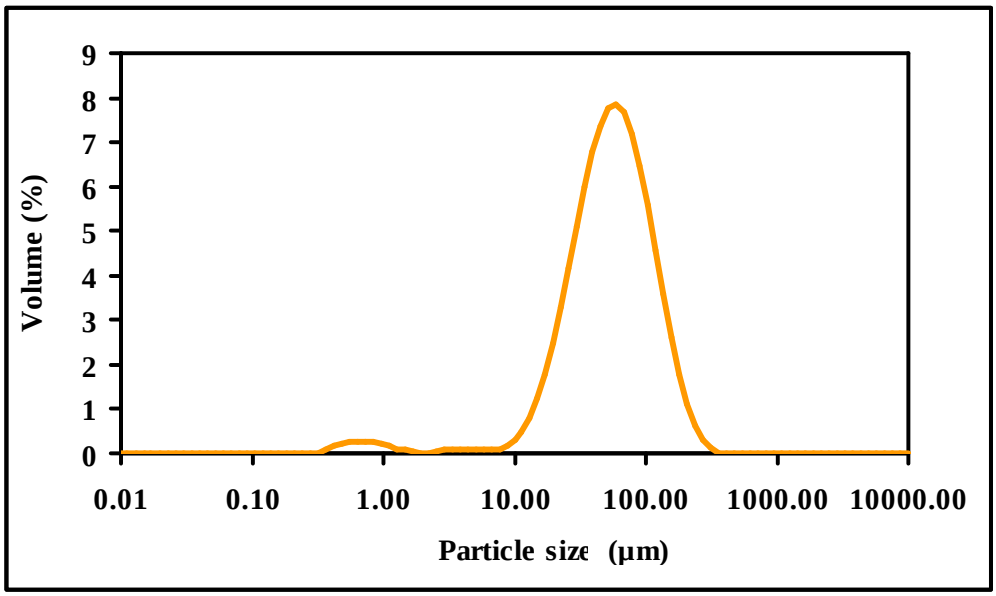

Figure C.14 Particle size distribution of the synthetic TiO_2 (wet measurement) (experimental condition: dispersion medium: water, Stirrer 2975 rpm, using nitric acid and ethanol for TiO_2 synthesis)**.**

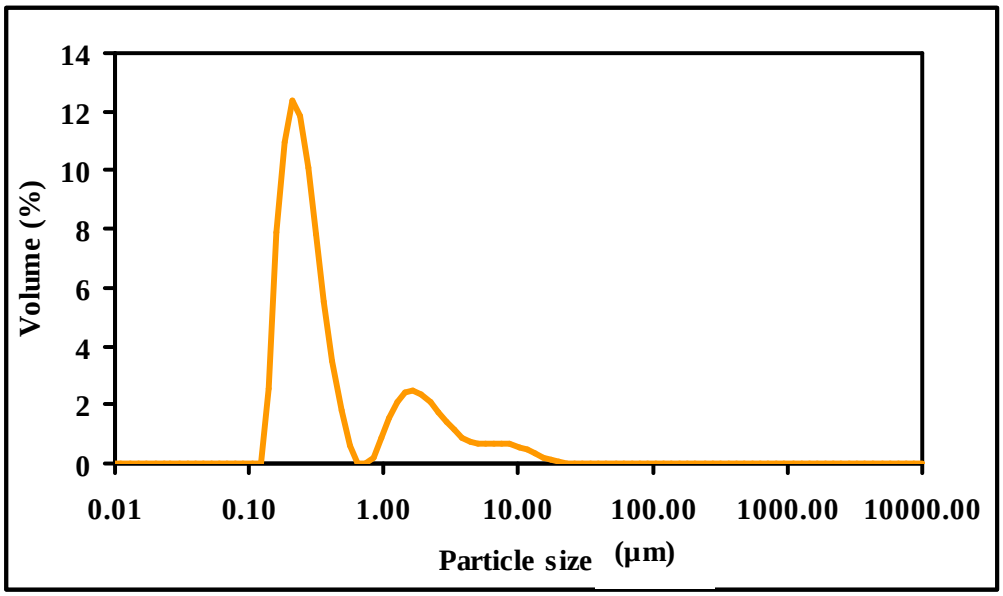

Figure C.15 Particle size distribution of the commercial P-25 (wet measurement) (experimental condition: dispersion medium: water, Stirrer 2975 rpm)**.**

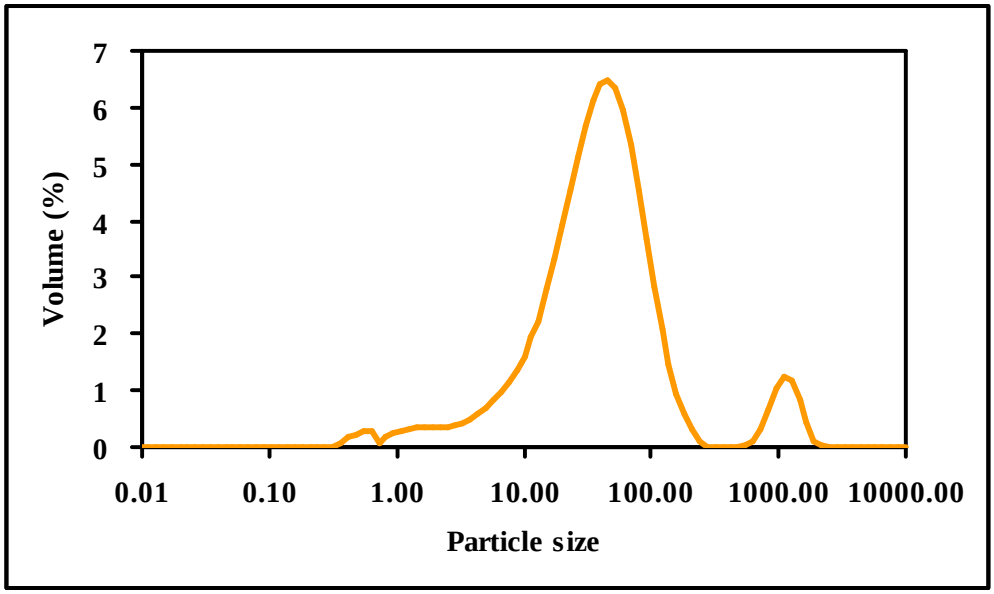

Figure C.16 Particle size distribution of the synthetic TiO_2 (dry measurement) (experimental condition: dispersive air pressure 4 bar, using nitric acid and ethanol for TiO_2 synthesis)**.**

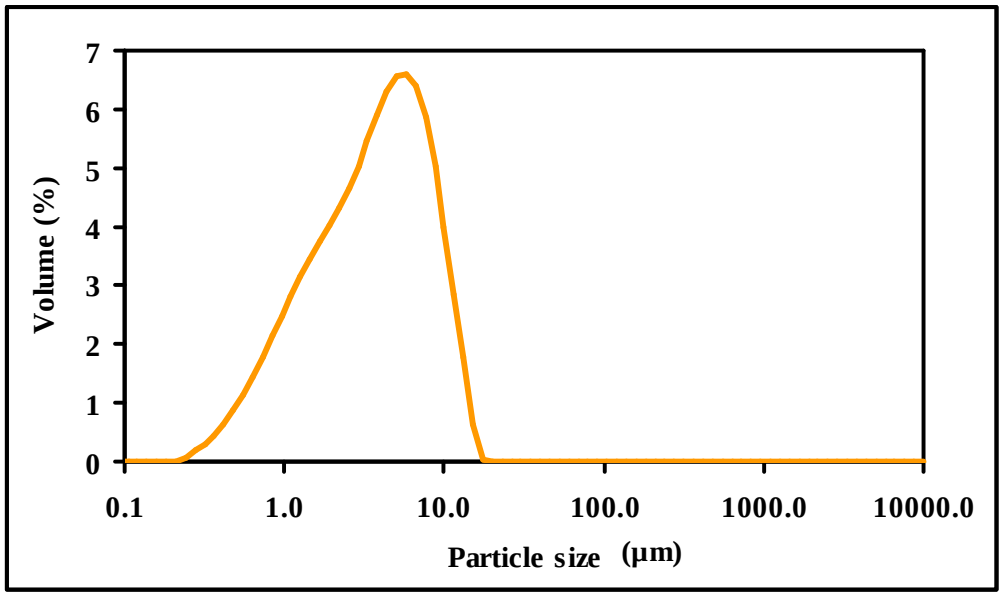

Figure C.17 Particle size distribution of the commercial P-25 (dry measurement) (experimental condition: dispersive air pressure 4 bar)**.**

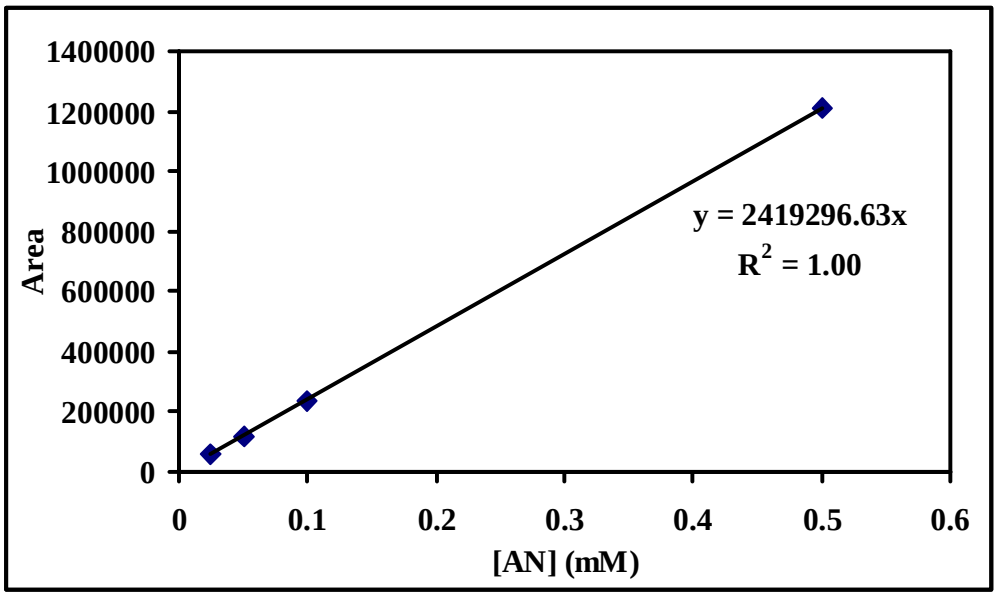

Figure C.18 Standard Curve for Aniline Determination Measurement by HPLC.

BIOGRAPHY

Miss Amornrat Jevprasesphant was born on December 12th, 1984 in Bangkok, Thailand. She received her Bachelor's degree in Environmental Science from Faculty of Science, Silpakorn University, Nakhon Pathom, Thailand in 2007. She pursued her Master's degree study in the National Center of Excellence for Environmental and Hazardous Waste Management, Inter-Department of Environmental Management, Graduate School, Chulalongkorn University, Bangkok, Thailand on May, 2007. She finished her Master's degree on March, 2009. she has published part of her works entitled "Photocatalytic Oxidation of Aniline Using Visible-Light-Activated Titanium Dioxide" in the 2008 International Conference on Environmental Quality Concern, Control and Conservation, May 23, Chia Nan University of Pharmacy and Science, Taiwan, pp. IIIA3_119-124.